CONTRIBUTION OF SOIL PORES TO THE PROCESSING AND PROTECTION OF SOIL CARBON AT MICRO-SCALE

By

Michelle Yvonne Quigley

A DISSERTATION

Submitted to
Michigan State University
in partial fulfillment of the requirements
for the degree of

Crop and Soil Sciences – Doctor of Philosophy

2019

ABSTRACT

CONTRIBUTION OF SOIL PORES TO THE PROCESSING AND PROTECTION OF SOIL CARBON AT MICRO-SCALE

By

Michelle Yvonne Quigley

Soil carbon has the potential to increase crop yield and mitigate climate change. As the largest terrestrial carbon stock, gains and losses of soil carbon can have a great impact on atmospheric CO_2 concentrations. Additionally, many beneficial soil properties for agricultural sustainability are tied to soil carbon. This makes understanding the mechanics of soil carbon vital to accurate climate change modeling and management recommendations. However, current soil carbon models, relying on bulk characteristics, can vary widely in their results and current recommendations for improving soil carbon do not work in all circumstances. Micro-scale processes, the scale at which carbon protection occurs, are currently not well understood. Improving the understanding of micro-scale processes would improve both climate models and management recommendations.

Carbon processes at micro-scale are believed to occur in diverse microenvironments. However, it is soil pores that, through transport of gasses, water, nutrients and microorganisms, may ultimately control the formation of these microenvironments. Therefore, understanding the relationship between soil pores and carbon is potentially vital to understanding micro-scale carbon processes. To understand the relationship between soil pores and carbon I employed computed microtomography (μCT) to obtain pore information and stable carbon isotopes to track carbon. I investigated the spatial variability of soil carbon within the soil matrix of different soil managements and how pores of different origin contributed to this variability to explore the effect of management and pore origin on the creation of microenvironments. Then I investigated

the effect of pore size distribution on carbon addition during growth of cereal rye (*Secale cereale* L.) and usage during a subsequent incubation using natural abundance stable carbon isotopes. I investigated the role of management history on the effect of pore size distribution during new carbon addition and usage using enriched stable carbon isotopes.

I found managements that build carbon have higher spatial variability of grayscale values in μCT images than managements that lose carbon. This variability is related to the amount of biological pores, due to their larger range of influence as compared to mechanical pores (123 μm vs. 30 μm), which would impact variability greater. The influence of biological and mechanical pores on adjacent carbon concentrations was found to be independent of management. Pores of 15-40 μm range were associated with carbon protection after incubation, matching previously reported results, indicating a universal mechanism for carbon protection, possibly related to fungi, in these pores. From both natural abundance and enriched stable carbon isotope studies, I found that 40-90 μm pores are associated with large gains of new carbon during rye growth, but large losses of new carbon in the subsequent incubations.

I found important relationships between pore origin, pore sizes, and carbon, specifically, that biological pores exert more influence on the carbon concentrations adjacent to them than mechanical pores. A technique to measure this influence using osmium staining of organic matter and grayscale gradients of images was developed. I found that 40-90 μm pores are important avenues of carbon addition, but also are associated with carbon losses. However, the reasons for these easy gains and losses is yet unclear, requiring further research, but it is believed to be associated with small plant roots.

ACKNOWLEDGEMENTS

It is with the utmost gratitude that I thank my advisor, Dr. Sasha Kravchenko, without whose support and patience this thesis would not be possible, in addition to her amazing research talent. I would also like to thank the members of my committee: Dr. Alvin Smucker for his wisdom and vast literature knowledge, Dr. Phil Robertson for his “big picture” view and expertise, and Dr. Dirk Colbry for his vast knowledge of anything programming and astounding willingness to help. It has been a really pleasure working with all of you. Humbly, I also thank the Department of Plant, Soil, and Microbial Sciences for all their wonderful support and the things they do for us students every day.

I would also like to thank all the lab members that have helped me on this journey: Dr. Moslem Ladoni, Dr. Ehsan Toosi, Dr. Kusay Alani, Dr. Erin Anders, Dr. Turgut Kutlu, Richard Price, Jessica Fry, Jordan Beehler, Kyungmin “Alyssa” Kim, Maxwell Oerther, and the many visiting scholars from Pakistan and China I had the privilege to get to know. Additionally, I would like to thank the friends and acquaintances I meet during my thesis work, whether through teaching, statistical consulting, or were just on the same journey.

Lastly, but certainly not in the least, I would like to thank my family: my husband, Nathanial Quigley, for his unending support and quick wit; my children, Danius, Kai, and Cora, who make everyday an adventure; and our dear friend and roommate Keiran Fallon, who puts up with us.

TABLE OF CONTENTS

LIST OF TABLES

LIST OF FIGURES

KEY TO ABBREVIATIONS

CO_2 – Carbon dioxide

μCT – Computed microtomography

CT – Computed tomography

SOM – Soil organic matter

Os – Osmium

POM – Particulate organic matter

DOM – Dissolved organic matter

APS – Advanced Photon Source

kGy – Kilogray

Si – Silicon

OsO_4 – Osmium tetraoxide

EDPI – Effective distance of pore influence

C – Carbon

N – Nitrogen

VPDB – Vienna PeeDee Belemite

H_2SO_4 – Sulfuric acid

$CaCO_3$ – Calcium carbonate

Chapter 1: Introduction

Comprising three times the amount of CO_2 in the atmosphere and as the largest terrestrial pool of carbon, soil carbon has the potential to be a prominent player in global climate change (Batjes, 1996; Lal, 1999; Swift, 2001; Paustian et al, 2016). Soils are known to loose carbon when land is converted to agriculture (Grandy and Robertson, 2007; Ruan and Robertson, 2013; Abraha et al, 2018). However, through diligent management, some of this loss can be recovered (Senthilkumar et al, 2009; Syswerda et al, 2011; Paustian et al, 2016), resulting in a reduction in atmospheric CO_2. Additionally, it is projected that agricultural production needs to double current production levels by 2050 (Ray et al, 2013). Boosting soil carbon stocks in agricultural soils is known to improve yields (Melsted, 1954; Bauer and Black, 1994; Lal, 2006). Therefore, improving soil carbon stocks in agricultural soils would mitigate global climate change and help to improve global food security.

Current models of soil carbon cycling, while good at predicting long term soil carbon stocks, are inadequate for modeling rapid changes, such as those that may arise due to agricultural management changes (Jenkinson et al, 1991; Parton et al, 1998; Crow and Sierra, 2018). This leads uncertainty when modeling soil carbon and CO_2 emissions, especially if the use of conservation managements becomes more widespread. As both soil carbon and CO_2 emissions are crucial input for climate change models, such as the HadCM3, this uncertainty propagates to those models. One reason for this uncertainty is that many important processes in soil carbon dynamics occur at micro-scale, but very few models take this scale into account (Young and Crawford, 2004; Kravchenko and Guber, 2017). Including micro-scale parameters in models has already been shown to increase model accuracy in CO_2 emission estimates (Falconer et al, 2015) and hydrodynamic soil properties (Smet et al, 2015), demonstrating that a better understanding of micro-scale carbon dynamics can result in more accurate models.

Soil carbon dynamics at micro-scale is believed to take place within microenvironments in the soil. The greater the diversity of these microenvironments, it is hypothesized, the greater soil carbon protection in a soil (Kuzyakov and Blagodatskaya, 2015). This diversity of microenvironments might be able to be estimated through spatial characteristics of the soil matrix with larger variability indicating greater microenvironment diversity. Microenvironments themselves are created through the distributions of microorganisms, water, gases, and nutrients in the soil (Young et al, 2001; Ekschmitt et al, 2005, 2008; Kravchenko and Guber, 2017; Rabot et al, 2018). These distributions, in turn, are controlled by the soil pore network via their control of water, air, and nutrient flow. It is, therefore, soil pores that may ultimately control soil carbon dynamics.

Even though soil pores control soil carbon dynamics, most research on soil carbon involves soil aggregates, specifically microaggregates-within-macroaggregates (Six et al, 1999, 2000). Originally proposed by Tisdall and Oades (1982), aggregates are hypothesized to have a hierarchical structure with small microaggregates combining to form macroaggregates. Six et al (2000) developed methods to isolate both macroaggregates and microaggregates, as well as microaggregates-within-macroaggregates, and has been widely used (Six and Paustian, 2014 and references within) for understanding carbon retention in soils. However, using microaggregates-within-macroaggregates in modeling is problematic for three reasons, 1) aggregate selection is purely based on the amount of energy used to break apart the soil and therefore, can be somewhat arbitrary, 2) the soil pore information, while theoretically, inversely related, is not clear and 3) information on connections between aggregates is lost. Six and Paustian (2014) likened it to “looking at the walls of a house to understand what is happening in the living-room”.

Until the advent of computed tomography (CT) and computed microtomography (μCT) imaging, however, direct nondestructive measurements of soil pores *in situ* was impossible (Dathe and Thullner, 2005; Gibson et al, 2006). Studies utilizing CT and μCT are increasing, but rarely focus on the relationship of pores and carbon, instead focusing on pore creation (De Gryze et al, 2006; Schlüter and Vogel, 2016), connectivity (Jarvis et al, 2017), and flow dynamics (Wildenschild and Sheppard, 2013; Koestel and Larsbo, 2014). Furthermore, CT imaging, currently, is not utilizable for routine and large volume studies, while aggregate separation is. This has led to a gap in connecting aggregate observations to pores and, therefore, mechanisms.

Pores can be created either through mechanical or biological means and are believed to have different effects on soil carbon dynamics (Park et al, 2007; Peng et al, 2007). Mechanical pores are created through (i) the shrinking and swelling of clay minerals, specifically 2:1 clays, during wetting and drying cycles (Peng et al, 2007) and (ii) the expansion of soil pores due to freeze/thaw action (Parker et al, 1982; Jabro et al, 2013). The size of these pores is usually related to the clay content of a soil, with high clay contents being required for the formation of large pores. The creation of new mechanical pores is believed to allow access to previously physically protected carbon, resulting in carbon losses (Sørensen, 1974; Denef et al, 2001; Smucker et al, 2007). This should result in less soil carbon adjacent to mechanical pores, although the extent of this influence is currently unknown.

Biological pores are created primarily through root action, but can also be the result of macrofauna activity within the soil. Unlike mechanical pores, biological pores are regarded as sources of carbon and result in carbon additions. These carbon additions, if from roots, can be in the form of root biomass or root exudates. Root biomass consists primarily of more difficult to decompose materials, such as lignin and tannin (Rasse et al, 2005; Jackson et al, 2017). In

contrast, root exudates tend to be smaller organic compounds, of lower molecular weight, and more easily decomposable, such as small organic acids, carbohydrates, and amino acids (Dungait et al, 2012).

Biological pores also may play a vital role in carbon protection as a large portion of carbon stored in soils is derived from root sources; up to 75% by some estimates (Balesdent and Balabane, 1996; Gale and Cambardella, 2000; Rasse et al, 2005; Clemmensen et al, 2013; Mazzilli et al, 2015). Due to the close contact between mineral surfaces and root materials, protection of soil carbon through occlusion on mineral surfaces is believed to be enhanced (Kiem and Kögel-Knabner, 2002; Six et al, 2002, Dungait et al, 2012). This protection is believed to be due to the electrostatic forces in the organo-mineral complexes being greater than the enzyme binding energy, protecting the carbon from microbial attack (Dungait et al, 2012). This enhanced protection of carbon from biological pores would result in higher soil carbon concentrations adjacent to these pores, but the extent of influence on these soil carbon concentrations is unclear. Isotopic studies have indicated transport of decomposition materials on the order of 5-10 mm, but this transport is not limited to individual pores (Gaillard et al, 1999, 2003; Toosi et al, 2017). NanoSIMS studies have indicated transport of only a few microns adjacent to a carbon source at nanometer resolution, although higher spatial ranges occurring at higher spatial scales was suggested (Mueller et al, 2012).

Agricultural management has been shown to have a profound effect on soil carbon dynamics (Senthilkumar et al, 2009; Syswerda et al, 2011). Management practices such as reducing tillage and increasing residue biomass are known to increase soil carbon (Follett, 2001, De Gryze et al, 2004; Ogle et al, 2012, Poeplau and Don, 2015). However, cover crop management has been shown to increase soil carbon stocks, despite utilization of heavy tillage

and relatively low biomass inputs (Syswerda et al, 2011; Paul et al, 2015). Additionally, some systems with abundant biomass inputs, such as monoculture switchgrass, and no tillage have unexpectedly low soil carbon accrual (Garten and Wullschleger, 1999; Chimento et al, 2016; Sprunger and Robertson, 2018). It is currently unknown what mechanisms account for these observations as management can affect many soil properties (pore size distribution, microorganism activity, and nutrient concentration, for example). Distinguishing between the effects of these different soil properties is difficult as it is often problematic to manipulate one factor without affecting the others. Additionally, measurements of soil carbon additions are routinely are done on microaggregates-within-microaggregates. These microaggregates-within-macroaggregates have proven an excellent indicator of soil carbon preservation under different agricultural managements (Six et al, 1999; Denef et al, 2004; 2007). However, as noted previously, this is inadequate for understanding mechanisms, which are currently unknown.

Agricultural management can have a substantial effect on pore size distributions. Wang et al (2012) found that conventional management had a higher proportion of 37.5–97.5μm pores, while early successional management had a larger proportion of >97.5 and <15μm pores. Kravchenko et al (2014) found that biologically based management had more >188μm pores and fewer 32–58μm pores. These different pore sizes can be equated to different biological processes. Plant roots are typically greater than 40 μm in size and, therefore, only occur in pores larger than 40 μm (Wiersum, 1957; Cannell, 1977). Fungi can push aside silt particles to create 20-30 μm pores, but are typically excluded from pores less than <10 μm (Dorioz et al, 1993; Bearden, 2001; Emerson and McGarry, 2003; Six et al, 2006). Water content of pores and by extension oxygen concentrations is also tied to soil pore size. Larger pores (>100 μm) tend to drain faster, resulting in high oxygen contents, but water limitation at typical field moisture

levels. Pores of 10-100 μm range have different oxygen and water contents depending on soil moisture. Lastly, pores less than 10 μm are water filled and, therefore, anaerobic at typical field conditions (Schurgers et al, 2006). The gradients of oxygen availability and water content affects decomposition, which can be $1/10^{th}$ in anaerobic sites as compared to aerobic sites (Keiluweit et al, 2017).

The effect of pore size on carbon dynamics has been established previously. Ananyeva et al (2013) found increased carbon concentrations in soil aggregates with an increased presence of 15–37.5μm pores, but decreased carbon concentrations with a greater presence of 37.5–97.5μm pores. Bailey et al (2017) discovered that pore water from <6 μm pores contained more carbon than pore water from > 6 μm pores, but more easily decomposable carbon (lipids) preferentially resided in >6 μm pores, while less decomposable carbon (lignin and tannin) was found in <6 μm pores. Decomposition has also been shown to vary depending on pore size. Killham et al (1993) found increased decomposition in pores of 6-30 μm as compared to pores of <6 μm size. Strong et al (2004) found higher decomposition rates in 15-60 μm pores than pores <4 μm and 60-300 μm. Negassa et al (2015) found that decomposition occurs faster in soil with larger pores (up to 2 mm) than smaller pores. These differences in decomposition rates are believed to be driven by increased microbial activity in certain pores, possibly as a function of water availability (Thomsen et al, 1999; Ruamps et al, 2011; Wang et al, 2013). These studies indicate that pores of different sizes play different roles in carbon protection. However, how pore sizes affect distributions of new carbon within soil and the actual utilization of new carbon sources are still nebulous.

My main study objective is to quantify the role that pores of different sizes play in influencing carbon dynamics in soils from different land use and management practices. The specific objectives were:

- To explore the spatial characteristics of soil matrix from different agricultural managements using μCT images and to relate these differences to soil organic matter (SOM) levels of these practices.
- To explore the effect of pore origin (biological or mechanical) on SOM levels adjacent to the pores and relate these changes to spatial characteristics.
- To examine the relationships between newly added carbon and pore size distribution after addition and subsequent incubation of carbon to understand the effect of pore size on carbon addition and usage.

REFERENCES

REFERENCES

Abraha, M., Hamilton, S. K., Chen, J., and Robertson, G. P. (2018). Ecosystem carbon exchange on conversion of Conservation Reserve Program grasslands to annual and perennial cropping systems. *Agric For Meteorol.* 253-254, 151-160. doi: 10.1016/j.agrformet.2018.02.016

Ananyeva, K., Wang, W., Smucker, A. J. M., Rivers, M. L., and Kravchenko, A. N. (2013). Can intra-aggregate pore structures affect the aggregate's effectiveness in protecting carbon? *Soil Biol. Biochem.* 57, 868-875. doi: 10.1016/j.soilbio.2012.10.019

Bailey, V. L., Smith, A. P., Tfaily, M., Fansler, S. J., and Bond-Lamberty, B. (2017). Differences in soluble organic carbon chemistry in pore waters sampled from different pore size domains. *Soil Biol. Biochem.* 107, 133-143. doi: 10.1016/j.soilbio.2016.11.025

Balesdent, J. and Balabane, M. (1996). Major contribution of roots to soil carbon storage inferred from maize cultivated soils. *Soil Biol. Biochem.* 28, 1261-1263. doi: 10.1016/0038-0717(96)00112-5

Batjes, N. H. (1996). Total carbon and nitrogen in soils of the world. *Eur. J. Soil Sci.* 47, 151-163. doi: 10.1111/j.1365-2389.1996.tb01386.x

Bauer, A. and Black, A. L. (1994). Quantification of the effect of soil organic matter content on soil productivity. *Soil Sci. Soc. Am. J.* 58, 185-193. doi: 10.2136/sssaj1994.03615995005800010027x

Bearden, B. N. (2001). Influence of arbuscular mycorrhizal fungi on soil structure and soil water characteristics of vertisols. *Plant Soil* 229, 245– 258. doi: 10.1023/A:1004835328943

Cannell, R. Q. (1977). Soil aeration and compaction in relation to root growth and soil management. *Appl. Biol*. 2, 1-86.

Chimento, C., Almagro, M., and Amaducci, S. (2016). Carbon sequestration potential in perennial bioenergy crops: the importance of organic matter inputs and its physical protection. *GCB Bioenergy* 8, 111-121. doi: 10.1111/gcbb.12232

Clemmensen, K. E., Bahr, A., Ovaskainen, O., Dahlberg, A., Ekblad, A., Wallander, H., et al. (2013). Roots and associated fungi drive long-term carbon sequestration in boreal forest. *Science* 339, 1615-1618. doi: 10.1126/science.1231923

Crow, S. E. and Sierra, C. A. (2018). Dynamic, intermediate soil carbon pools may drive future responsiveness to environmental change. *J. Environ. Qual.* 47, 607-616. doi:10.2134/jeq2017.07.0280

Dathe, A.and Thullner, M. (2005). The relationship between fractal properties of solid matrix and pore space in porous media. *Geoderma* 134, 318-326. doi:10.1016/j.geoderma.2005.01.003

De Gryze, S., Six, J., Paustin, K., Morris, S. J., Paul, E. A., and Merckx, R. (2004). Soil organic carbon pool changes following land-use conversions. *Global Change Biol.* 10, 1120-1132. doi: 10.1111/j.1365-2486.2004.00786.x

De Gryze, S., Jassogne, L., Six, J., Bossuyt, H., Wevers, M., and Merckx, R. (2006). Pore structure changes during decomposition of fresh residue: X-ray tomography analyses. *Geoderma* 134, 82-96. doi: 10.1016/j.geoderma.2005.09.002

Denef, K., Six, J., Bossuyt, H., Frey, S. D., Elliot, T. E., Merckx, R., et al. (2001). Influence of dry-wet cycles on the interrelationship between aggregate, particulate organic matter, and microbial community dynamics. *Soil Biol. Biochem.* 33, 1599-1611. doi: 10.1016/S0038-0717(01)00076-1

Denef, K., Six, J., Merckx, R., and Paustian, K. (2004). Carbon sequestration in micro-aggregates of no-tillage soils with different clay mineralogy. *Soil Sci. Soc. Am. J.* 68, 1935-1944. doi: 10.2136/sssaj2004.1935

Denef, K., Zotarelli, L., Boddey, R. M., and Six, J. (2007). Microaggregate-associated C as a diagnostic fraction for management-induced changes in soil organic carbon in two Oxisols. *Soil Biol. Biochem.* 39, 1165-1172. doi: 10.1016/j.soilbio.2006.12.024

Dorioz, J. M., Robert, M., and Chenu, C. (1993). The role of roots, fungi and bacteria on clay particle organization. An experimental approach. *Geoderma* 56, 179– 194. doi:10.1016/0016-7061(93)90109-X

Dungait, J. A. J., Hopkins, D. W., Gregory, A. S., and Whitmore, A. P. (2012). Soil organic matter turnover is governed by accessibility not recalcitrance. *Global Change Biol.* 18, 1781-1796. doi: 10.1111/j.1365-2486.2012.02665.x

Ekschmitt, K., Kandeler, E., Poll, C., Brune, A., Buscot, F., Friedrich, M., et al. (2008). Soil-carbon preservation through habitat constraints and biological limitations on decomposer activity. *J. Plant Nutr. Soil Sci.* 171, 27-35. doi: 10.1002/jpln.200700051

Ekschmitt, K., Liu, M., Vetter, S., Fox, O., and Wolters, V. (2005). Strategies used by soil biota to overcome soil organic matter stability – why is dead organic matter left over in soil? *Geoderma* 128, 167-176. doi: 10.1016/j.geoderma.2004.12.024

Emerson, W. W. and McGarry, D. (2003). Organic carbon and soil porosity. *Aust. J. Soil Res.* 41, 107–118. doi: 10.1071/SR01064

Falconer, R. E., Battaia, G., Schmidt, S., Baveye, P., Chenu, C., and Otten, W. (2015). Microscale heterogeneity explains experimental variability and non-linearity in soil organic matter mineralization. *PloS One.* 10(5): e0123774. doi: 10.1371/journal.pone.0123774

Follet, R. F. (2001). Soil management concepts and carbon sequestration in cropland soils. *Soil Tillage Res.* 61, 77-92. doi: 10.1016/S0167-1987(01)00180-5

Gaillard, V., Chenu, C., and Recous, S. (2003). Carbon mineralization in soil adjacent to plant residues of contrasting biochemical quality. *Soil Biol. Biochem.* 35, 93-99. doi: 10.1016/S0038-0717(02)00241-9

Gaillard, V., Chenu, C., Recous, S. and Richard, G. (1999). Carbon, nitrogen and microbial gradients induced by plant residues decomposing in soil. *Eur. J. Soil Sci.* 50, 567-578. doi: 10.1046/j.1365-2389.1999.00266.x

Gale, W. J. and Cambardella, C. A. (2000). Carbon dynamics of surface residue- and root-derived organic matter under simulated no-till. *Soil Sci. Soc. Am. J.* 64, 190-195. doi: 10.2136/sssaj2000.641190x

Garten, C. T., and Wullschleger, S. D. (2000). Soil carbon dynamics beneath switchgrass as indicated by stable isotope analysis. *J. Envrion. Qual.* 29, 645-653. doi: 10.2134/jeq2000.00472425002900020036x

Gibson, J. R., Lin, H., and Bruns, M. A. (2006). A comparison of fractal analytical methods on 2- and 3-dimensional computed tomographic scans of soil aggregates. *Geoderma*. 134, 335-348. doi: 10.1016/j.geoderma.2006.03.052

Grandy, A. S. and Robertson, G. P. (2007). Land-use intensity effects on soil organic carbon accumulation rates and mechanisms. *Ecosystems* 10, 58-73. doi: 10.1007/s10021-006-9010-y

Jabro, J. D, Iverson, W. M., Evans, R. G., Allen, B. L., and Stevens, W. B. (2013). Repeated freeze-thaw cycle effects on soil compaction in a clay loam in northeastern Montana. *Soil Sci. Soc. Am. J.* 78:737-744. doi: 10.2136/sssaj2013.07.0280

Jackson, R. B., Lajtha, K., Crow, S. E., Hugelius, G., Kramer, M. G., and Piñeiro, G. (2017). The ecology of soil carbon: pools, vulnerabilities, and biotic and abiotic controls. *Annu Rev Ecol Evol Syst*. 48, 419-445. doi: 10.1146/annurev-ecolsys-112414-054234

Jarvis, N., Koestel, J., and Larsbo, M. (2017). Understanding preferential flow in vadose zone: Recent advances and future prospects. *Vadose Zone* 15 doi: 10.2136/vzj2016.09.0075

Jenkinson, D. S., Adams, D. E., and Wild, A. (1991). Model estimates of CO_2 emissions from soil in response to global warming. *Nature* 351, 304-306. doi:10.1038/351304a0

Keiluweit, M., Wanzek, T., Kleber, M., Nico, P., and Fendorf, S. (2017). Anaerobic microsites have an unaccounted role in soil carbon stabilization. *Nat. Commun.* 8: 1771. doi: 10.1038/s41467-017-01406-6

Kiem, R., and Kögel-Knabner, I. (2002). Refractory organic carbon in particle-size fractions of arable soils II: organic carbon in relation to mineral surface area and iron oxides in fractions <6 µm. *Org. Geochem.* 33, 1699-1713. doi: 10.1016/S0146-6380(02)00112-2

Killham, K., Amato, M., and Ladd, J. N. (1993). Effect of substrate locations in soil and soil pore-water regime on carbon turnover. *Soil Biol. Biochem.* 25, 57-62. doi: 10.1016/0038-0717(93)90241-3

Koestel, J. and Larsbo, M. (2014). Imaging and quantification of preferential solute transport in soil macropores. *Water Resour Res* 50, 4357-4378. doi: 10.1002/2014WR015351

Kravchenko, A. N., and Guber, A. K. (2017). Soil pores and their contributions to soil carbon processes. *Geoderma* 287, 31-39. doi: 10.1016/j.geoderma.2016.06.027

Kravchenko, A. N., Negassa, W. C., Guber, A. K., Hildebrandt, B., Marsh, T. L., and Rivers, M. L. (2014). Intra-aggregate pore structure influences phylogenetic composition of bacterial community in macroaggregates. *Soil Sci. Soc. Am. J.* 78, 1924-1939. doi: 10.2136/sssaj2014.07.0308

Kuzyakov, Y., and Blagodatskaya, E. (2015). Microbial hotspots and hot moments in soil: concept & review. *Soil Biol. Biochem.* 83, 184-199. doi: 10.1016/j.soilbio.2015.01.025

Lal, R. (1999). Soil management and restoration for carbon sequestration to mitigate the accelerated greenhouse effect. *Prog. Env. Sci.* 1, 307-326. doi: 10.1055/s-2008-1072270

Lal, R. (2006). Enhancing crop yields in the developing countries through restoration of the soil organic carbon pool through restoration of the soil organic carbon pool in agricultural lands. *Land Degrad. Develop.* 17, 197-209. doi: 10.1002/ldr.696

Mazzilli, S. R., Kemanian, A. R., Ernst, O. R., Jackson, R. B., and Piñero, G. (2015). Greater humification of belowground than aboveground biomass carbon into particulate soil organic matter in no-till corn and soybean crops. *Soil Bio. Biochem.* 85, 22-30. doi: 10.1016/j.soilbio.2015.02.014

Melsted, S. W. (1954). New concepts of management of corn belt soils. *Adv. Agron.* 6, 121-142. doi: 10.1016/S0065-2113(08)60383-1

Mueller, C. W., Kölbl, A., Hoeschen, C., Hillion, F., Heister, K., Herrmann, A. M., et al. (2012). Submicron scale imaging of soil organic matter dynamics using NanoSIMS-from single particles to intact aggregates. *Org Geochem.* 42, 1476-1488. doi: 10.1016/j.orggeochem.2011.06.003

Negassa, W. C., Guber, A. K., Kravchenko, A. N., Marsh, T. L., Hildebrandt, B., and Rivers, M. L. (2015). Properties of soil pore space regulate pathways of plant residue decomposition and community structure of associated bacteria. *PLoS One* 10(4): e0123999 doi: 10.1371/journal.pone.0123999

Ogle, S. M., Swan, A., and Paustian, K. (2012). No-till management impacts on crop productivity, carbon input and soil carbon sequestration. *Agric Ecosyst Environ.* 149, 37-49. doi: 10.1016/j.agee.2011.12.010

Park, E. J., Sul, W. J., and Smucker, A. J. M. (2007). Glucose additions to aggregates subjected to drying and wetting cycles promote carbon sequestration and aggregate stability. *Soil Biol. Biochem.* 39, 2758-2768. doi: 10.1016/j.soilbio.2007.06.007

Parker, J. C., Amos, D. F., and Zelazny, L. W. (1982). Water adsorption and swelling of clay minerals in soil systems. *Soil Sci. Soc. Am. J.* 46, 450-456. doi: 10.2136/sssaj1982.03615995004600030002x

Parton, W. J., Hartman, M., Ojima, D., and Schimel, D. (1998). DAYCENT and its land surface submodel: description and testing. *Global Planet. Change* 19, 35-48. doi:10.1016/S0921-8181(98)00040-X

Paul, E. A., Kravchenko, A., Grandy, S., and Morris, S. (2015). "Soil organic matter dynamics: controls and management for sustainable ecosystem functioning," in *The ecology of agricultural landscapes: long-term research on the path to sustainability*, eds. S. K. Hamilton, J. E. Doll, and G. P. Robertson, (New York, New York, USA: Oxford University Press), 104-134.

Paustian, K., Lehmann, J., Ogle, S., Reay, D., Robertson, G. P., and Smith, P. (2016). Climate-smart soils. *Nature* 532, 49-57. doi: 10.1038/nature17174

Peng, X., Horn, R., and Smucker, A. J. M. (2007). Pore-shrinkage dependency of inorganic and organic soils on wetting and drying cycles. *Soil Sci. Soc. Am. J.* 71, 1095-1104. doi: 10.2136/sssaj2006.0156

Poeplau, C. and Don, A. (2015). Carbon sequestration in agricultural soils via cultivation of cover crops-a meta-analysis. *Agric Ecosyst Environ.* 200, 33-41. doi: 10.1016/j.agee.2014.10.024

Rabot, E., Wiesmeier, M., Schlüter, S., and Vogel, H.-J. (2018). Soil structure as an indicator of soil functions: a review. *Geoderma* 314, 122-137. doi:10.1016/j.geoderma.2017.11.009

Rasse, D. P., Rumpel, C. and Dignac, M.-F. (2005). Is soil carbon mostly root carbon? Mechanisms for a specific stablization. *Plant Soil* 269, 341-356. doi: 10.1007/s11104-004-0907-y

Ray, D. K., Mueller, N. D., West, P. C., and Foley, J. A. (2013). Yield trends are insufficient to double global crop production. *PLoS One* 8(6):e66428. doi:10.1371/journal.pone.0066428

Ruamps, L. S., Nunan, N., and Chenu, C. (2011). Microbial biogeography at the soil pore scale. *Soil Biol. Biochem.* 43, 280-286. doi: 10.1016/j.soilbio.2010.10.010

Raun, L. and Robertson, G. P. (2013). Initial nitrous oxide, carbon dioxide, and methane costs of converting Conservation Reserve Program grassland to row crops under no-till vs. conventional tillage. *Global Change Biol.* 19, 2478-2489. doi: 10.1111/gcb.12216

Schlüter, S. and Vogel, H.-J. (2016). Analysis of soil structure turnover with garnet particles and X-ray microtomography. *PLoS One* 11.7:pe0159948. doi: 10.1371/journal.pone.0159948

Schurgers, G., Dörsch, P., Bakken, L., Leffelarr, P., and Haugen, L. E. (2006). Modelling soil anaerobiosis from water retention characteristics and soil respiration. *Soil Biol. Biochem.* 38, 2637-2644. doi: 10.1016/j.soilbio.2006.04.016

Senthilkumar, S., Basso, B., Kravchenko, A. N., and Robertson, G. P. (2009). Contemporary evidence of soil carbon loss in the U.S. corn belt. *Soil Sci. Soc. Am. J.* 73, 2078-2086. doi: 10.2136/sssaj2009.0044

Six, J., Conant, R. T., Paul, E. A., Paustian, K. (2002). Stabilization mechanisms of soil organic matter: implications for C-saturation of soils. *Plant Soil.* 241, 155-176. doi: 10.1023/A:1016125726789

Six, J., Elliot, E. T., and Paustian, K. (1999) Aggregate and soil organic matter dynamics under conventional and no-tillage systems. *Soil Sci. Soc. Am. J.* 63, 1350-1358. doi: 10.2136/sssaj1999.6351350x

Six, J., Elliott, E. T., and Paustian, K. (2000). Soil macroaggregate turnover and microaggregate formation: a mechanism for C sequestration under no-tillage agriculture. *Soil Biol. Biochem.* 32, 2099-2103. doi: 10.1016/S0038-0717(00)00179-6

Six, J., Frey, S. D., Thiet, R. K., and Batten, K. M. (2006). Bacterial and fungal contributions to carbon sequestration in agroecosystems. *Soil Sci. Soc. Am. J.* 70, 555-569. doi:10.2136/sssaj2004.0347

Six, J. and Paustian, K. (2014). Aggregate-associated soil organic matter as an ecosystem property and measurement tool. *Soil Biol. Biochem* 68, A4-A9. doi: 10.1016/j.soilbio.2013.06.014

Smet, S., Beckers, E., Plougonven, E., Léonard, A., and Degré, A. (2018). Can the pore scale geometry explain soil sample scale hydrodynamic properties? *Front. Environ. Sci.* 6:20. doi: 10.3389/fenvs.2018.00020

Smucker, A. J. M., Park, E.-J., Dorner, J., and Horn, R. (2007). Soil micropore development and contributions to soluble carbon transport within macroaggregates. *Vadose Zone J.* 6, 282-290. doi: 10.2136/vzj2007.0031

Sørensen, L. H. (1974). Rate of decomposition of organic matter in soil as influenced by repeated air drying-rewetting and repeated additions of organic material. *Soil Biol. Biochem.* 6, 287-292. doi: 10.1016/0038-0717(74)90032-7

Sprunger C. D. and Robertson, G. P. (2018). Early accumulation of active fraction soil carbon in newly established cellulosic biofuel systems. *Geoderma* 318, 42-51. doi: 10.1016/j.geoderma.2017.11.040

Strong, D. T., De Wever, H., Merckx, R., and Recous, S. (2004). Spatial location of carbon decomposition in the soil pore system. *Eur. J. Soil Sci.* 55, 739-750. doi: 10.1111/j.1365-2389.2004.00639.x

Swift, R. S. (2001). Sequestration of carbon by soil. *Soil Sci.* 166, 858-871. doi: 10.1097/00010694-200111000-00010

Syswerda, S. P., Corbin, A. T., Mokma, D. L., Kravchenko, A. N., and Robertson, G. P. (2011). Agricultural management and soil carbon storage in surface vs. deep layers. *Soil Sci. Soc. Am. J.* 75, 92-101. doi: 10.2136/sssaj2009.0414

Thomsen, I. K, Schjønning, P., Jensen, B., Kristensen, K., and Christensen, B. T. (1999). Turnover of organic matter in differently textured soils-II. Microbial activity as influenced by soil water regimes. *Geoderma* 89, 199-218. doi: 10.1016/S0016-7061(98)00084-6

Tisdall, J. M. and Oades, J. M. (1982). Organic matter and water-stable aggregates in soils. *J. Soil Sci.* 62, 141-163. doi: 10.1111/j.1365-2389.1982.tb01755.x

Toosi, E. R., Kravchenko, A. N., Guber, A. K., and Rivers, M. L. (2017). Pore characteristics regulate priming and fate of carbon from plant residue. *Soil Bio. Biochem.* 113, 219-230. doi: 10.1016/j.soilbio.2017.06.014

Wang, W., Kravchenko, A. N., Johnson, T., Srinivasan, S., Ananyeva, K. A., Smucker, A. J. M., et al. (2013). Intra-aggregate pore structures and *Escherichia coli* distribution by water flow within and movement out of soil macroaggregates. *Vadose Zone J.* 12:4. doi: 10.2136/vzj2013.01.0012

Wang, W., Kravchenko, A. N., Smucker, A. J. M., Liang, W., and Rivers, M. L. (2012). Intra-aggregate pore characteristics: X-ray computed microtomography analysis. *Soil Sci. Soc. Am. J.* 76, 1159-1171. doi: 10.2136/sssaj2011.0281

Wiersum, L. K. (1957). The relationship of the size and structural rigidity of pores to their penetration by roots. *Plant Soil* 9, 75-85. doi: 10.1007/BF01343483

Young, I. M., and Crawford, J. W. (2004). Interactions and self-organization in the soil-microbe complex. *Science* 304, 1634-1637. doi: 10.1126/science.1097394

Young, I. M., Crawford, J. W., and Rappoldt, C. (2001). New methods and models for characterizing structural heterogeneity of soil. *Soil Tillage Res.* 61, 33-45. doi: 10.1016/S0167-1987(01)00188-X

Chapter 2: Patterns and Sources of Spatial Heterogeneity in Soil Matrix from Contrasting Long Term Management Practices*

Abstract

With the advent of computed microtomography (μCT), *in situ* 3D visualization of soil at micron scale became easily achievable. However, most μCT-based research has focused on visualization and quantification of soil pores, roots, and particulate organic matter (POM), while little effort has been invested into exploring the soil matrix itself. This study aims to characterize spatial heterogeneity of soil matrix in macroaggregates from three differing long term managements: conventionally managed and biologically based row-crop agricultural systems and early successional unmanaged system, and explore the utility of using grayscale gradients as a proxy of soil organic matter (SOM). To determine spatial characteristics of the soil matrix, I completed a geostatistical analysis of the aggregate matrix. It demonstrated that, while the treatments had the same range of spatial autocorrelation, there was much greater overall variability in soil from the biologically based system. Since soil from both managements have the same mineralogy and texture, I hypothesized that greater variability is due to differences in SOM distributions, driven by spatial distribution patterns of soil pores. To test this hypothesis, I applied osmium (Os) staining to intact micro-cores from the biologically based management, and examined Os staining gradients every 4 μm from 26 to 213 μm from pores of biological or non-biological origin. Biological pores had the highest SOM levels adjacent to the pore, which receded to background levels at distances of 100-130 μm. Non-biological pores had lower SOM levels adjacent to the pores and returned to background levels at distances of 30-50 μm. This indicates that some of the spatial heterogeneity within the soil matrix can be ascribed to SOM

* Originally published as: Quigley, M. Y., Rivers, M. L., and Kravchenko, A. N. (2018b). Patterns and sources of spatial heterogeneity in soil matrix from contrasting long term management practices. Front. Environ. Sci. 6:28 doi: 10.3389/fenvs.2018.00028

distribution patterns as controlled by pore origins and distributions. Lastly, to determine if the grayscale values could be used as a proxy for SOM levels, gradients of grayscale values from biological and non-biological pores were compared with the Os gradients. Grayscale gradients matched Os gradients for biological pores, but not non-biological pores due to an image processing artifact. Grayscale gradients would, therefore, be a good proxy for SOM gradients near biological origin pores, while their use for non-biological pores should be conducted with caution. As the same pattern was seen for root and non-root pores from all managements, this indicates that SOM distribution is controlled by the same mechanism regardless of management.

2.1 Introduction

The use of computed microtomography (μCT) has allowed for the *in situ* characterization of the physical structure of soil, specifically, positions, size distributions, and shapes of soil pores (Gibson et al, 2006; Chun et al, 2008; Peth et al, 2008; Papadopoulos et al, 2009; Kravchenko et al, 2011; Wang et al, 2012). It has also enabled identification of large organic fragments, including particulate organic matter (POM) (Kravchenko et al, 2014a) and intact plant roots (Mooney et al, 2012). These advances have led to quantitative insights into the contribution of pore characteristics to residue decomposition, carbon protection, and spatial patterns of bacterial distributions (De Gryze et al, 2006; Ananyeva et al, 2013; Wang et al, 2013; Kravchenko et al, 2014b; Negassa et al, 2015). However, little attention has been given to μCT information regarding mineral soil matrix, that is, solid material containing no pores or organic fragments visible at the μCT image resolution. Of particular interest is how characteristics of the solid material may relate to soil organic matter (SOM) dynamics, specifically SOM protection.

Solid material is represented in μCT images by a range of grayscale values that are correlated to the attenuation of x-rays, which is controlled by the density and atomic number (Z) of the elements occurring within an image voxel (Ketcham, 2005; Peth, 2010). Voxels that

contain primarily low Z elements, such as nitrogen, carbon, and oxygen, have lower grayscale values (appear darker) on μCT images, while voxels containing higher Z elements, such as iron, silicon, and aluminum, have higher grayscale values (appear brighter). A voxel's overall grayscale value is the average attenuation of the elements occurring within that voxel. Spatial variability in grayscale values of the solid material originates from multiple sources, including variations in mineralogy, presence of pores with sizes below image resolution, and SOM distribution patterns. The first two of these factors are important drivers of SOM protection, while SOM distribution patterns can be an indicator of where such protection has occurred. Mineralogy influences SOM protection by affecting organic matter binding via electrostatic forces. Small pores can contribute to SOM protection by a combination of restricting decomposers' access and, due to anaerobic conditions prevalent in these pores, slowing of decomposition (Bailey et al, 2017; Keiluweit et al, 2017). Thus, overall SOM distribution patterns are likely controlled by a combination of mineralogy and pore architecture, i.e. pore size and connectivity (Dungait et al, 2012; Kravchenko et al, 2015).

Soil pores function as the soil transport network; regulating the flow of nutrients, microorganisms, oxygen, and organic material (De Gryze et al, 2006; Young and Crawford, 2004; Kuzyakov and Blagodatskaya, 2015; Negassa et al, 2015). Soil pores are created through either biological or non-biological means. Biological pores are formed by macrofauna, such as earthworms, or through action of roots (Rasse and Smucker, 1998) and root hairs as they spread and grow. Non-biological pores are primarily produced in a course of wetting/drying and freeze/thaw cycles and are controlled by soil texture, specifically clay content. Biological and non-biological pores also play different roles in the cycling of organic matter within the soil. Biological pores are generally thought of as a source of new carbon inputs, either through direct

organic addition, such as decaying roots, or through ancillary organic matter additions, such as root exudates. Organic matter that then diffuses out from biological pores typically occurs as dissolved organic matter (DOM). DOM can be bound to minerals by electrostatic forces (Kiem and Kögel-Knabner, 2002; Six et al, 2002, Dungait et al, 2012), where, due to the electrostatic force being greater than the enzyme binding energy, it can be protected from microbial attack and results in SOM protection (Dungait et al, 2012). While biological origin pores are sources of organic matter and SOM protection, they also compress adjacent solid material as roots push through the soil resulting in denser material closer to root pores (Bengough et al, 2011; Aravena et al, 2014). Thus, the net effect of biological pores on proximate grayscale densities is uncertain.

Formation of non-biological pores, on the other hand, created through the shrinking and swelling of clay minerals, can expose previously inaccessible carbon to microbial attack, resulting in a net carbon loss (Sorensen, 1974; Denef et al, 2001; Smucker et al, 2007). However, quantitative data on how presence, abundance, and characteristics of pores of different origins influence SOM accrual and protection is currently lacking. Falconer et al (2015) noted that despite identical bulk characteristics, including average porosity, POM turnover rate varied widely due to micro-scale properties. Their results indicated that an understanding of micro-scale pore properties may be vital to achieve more accurate modeling of soil carbon dynamics.

The grayscale values of the solid material in μCT images could potentially provide insights into spatial patterns of SOM and the associations between such patterns and pores of different origins. As noted previously, a voxel's overall grayscale value is the average attenuation of the elements occurring within that voxel. While mineralogy plays the largest role in the spatial characteristics of the solid material and would normally override any spatial characteristics from distribution of SOM and presence of pores with below image resolution

sizes, samples with similar mineralogy could allow for the spatial patterns caused by these other factors to be observed. There is some experimental evidence that, in samples with similar mineralogy, grayscale values of μCT images and SOM are correlated (Ananeyva, personal communications).

Studies have shown that geostatistics is helpful for describing the spatial characteristics of pores and, therefore, can be expected to also model well the spatial characteristics of the solid material (De Gryze et al, 2006; Feeney et al, 2006; Nunan et al, 2006). Therefore, to assess spatial patterns within the solid material, geostatistics will be used to quantify the range of spatial correlation, overall spatial variability, and the contribution of spatial variability that is below image resolution to the overall spatial variability.

Here I explore the utility of using the spatial patterns of grayscale values in μCT images as a proxy for the spatial patterns of SOM distribution. I will focus on SOM distribution patterns in the vicinity of soil pores of both non-biological and biological origin. This focus is driven by an expectation that, due to the role of biological pores in supplying new organic inputs and the role of non-biological pores in contributing to carbon losses, their comparison should yield contrasting gradients in SOM distributions. Identification of such gradients will indicate that grayscale values can provide useful information on SOM distribution patterns within intact soil samples.

To further test the utility of grayscale values as indicators of SOM spatial patterns, I will compare the gradients of grayscale values from conventional μCT images with gradients of Osmium (Os) stained organic matter from Os dual-energy images. Os staining has been proposed as an effective tool to visualize organic matter in μCT images (Peth et al, 2014) and was applied to estimate SOM spatial patterns (Rawlins et al, 2016). Os strongly binds with carbon-carbon

double bounds and its high atomic number increases the visibility of organic matter on μCT images. By taking images above and below the K-edge of Os, 3D maps of SOM within an intact soil sample can be constructed. From such maps I can then obtain direct measurements of SOM gradients in the vicinity of non-biological and biological soil pores.

Agricultural management is known to have an effect on overall SOM levels (Oades, 1984; Six et al, 2000; Syswerda et al, 2011; Paul et al, 2015), as well as on micro-scale SOM patterns (Ananyeva et al, 2013; Kravchenko et al, 2015). Since pores are known drivers of SOM protection, any change in the spatial pattern of pores would result in a change in SOM spatial patterns and potentially SOM levels. The distribution of non-biological and biological pores is known to be affected by agricultural management. Wang et al (2012) and Kravchenko et al (2014b) both observed that non-biological pores tended to dominate in systems with tillage, while pores of biological origin tended to dominate in conservation managements with little soil disturbance.

I hypothesized that areas dominated by non-biological pores will have relatively uniform microenvironmental conditions, and thus relatively uniform SOM spatial distribution patterns. Together with lack of point sources of organic matter in such pores, this will lead to smaller SOM gradients in their vicinity. On the other hand, areas dominated by biological pores provide spatially variable SOM inputs as well as a more diverse range of microenvironmental conditions for microorganisms. Thus, I expect greater spatial variability in SOM, as well as greater SOM gradients, in the vicinity of biological pores. In addition, I hypothesize that agricultural management practices that lead to a greater presence of biological pores will increase SOM spatial variability and result in larger SOM gradients than the management practices with greater presence of non-biological pores.

The first objective of the study is to explore utility of grayscale values of solid material from μCT images to characterize SOM patterns by comparing grayscale value spatial patterns with Os spatial patterns. The second objective is to explore spatial characteristics of the solid material in μCT images of intact soil samples from three contrasting land use and management practices and to analyze relationships between the spatial characteristics and the SOM levels of these practices. My third objective is to explore SOM and grayscale value gradients at distances from pores of different origins and in soils from different managements.

2.2 Materials and methods

2.2.1 Soil Collection and Imaging

The studied soil was collected from three different managements at Kellogg Biological Station Long Term Ecological Research site, Hickory Corners, MI (42°24´N, 85°24´W). The three managements were a conventional corn-soybean wheat rotation maintained with current best management practices, a biologically based corn-soybean-wheat with rye cover after corn and red clover interseeded into wheat with no additional inputs and rotary tillage between rows for weed management, and an early successional management, which is burned annually, but otherwise unmanaged. These management practices represent a management gradient with a highly managed system (conventional), a conservation management system (biologically based), and an unmanaged system (early successional). Further details can be found in Kravchenko et al (2015).

The soil (from 0-15 cm depth) was dry sieved and aggregates of 4-6.3 mm were collected for imaging. μCT images were obtained from beamline 13-BM-D of the GeoSoilEnvironCARS (GSECARS) at the Advanced Photon Source (APS), Argonne National Laboratory (ANL) in Argonne, Illinois. Two-dimensional projections were taken at 0.25° rotation angle steps with a one second exposure and combined into a three-dimensional image consisting of 520 slices with

696 by 696 pixels per slice for grayscale analysis and 1200 slices with 1920 by 1920 pixels per slice for analysis of pores below image resolution. The voxel size of the images was 13 μm for grayscale analysis and 2 μm for analysis of pores below image resolution. Pores were identified using the indicator kriging method in 3DMA-Rock (Oh and Lindquist, 1999; Wang et al, 2011) for grayscale analysis and through simple thresholding with Otsu's method for analysis of pores below image resolution.

2.2.2 Geostatistical Analysis

A total of 32 soil aggregate images were used in the geostatistical analysis, namely, 11 images from conventional and biologically based management and 10 images from early successional management. On each image I identified 5 soil cubes, 130 μm x 130 μm x 130 μm in size (Figure 2.1). Positions of the cubes were initially randomly selected, with further adjustments made to avoid major overlaps with other cubes, coarse sand grains that would not reflect the overall spatial characteristics of the aggregate, and aggregate boundaries. Soil pores identified by 3DMA-Rock were removed from the cubes prior to geostatistical analysis allowing for analysis of spatial patterns in the solid material only. 3D variograms were obtained using the gstat package in R (Pebesma, 2004) run on the High Performance Computing Center at Michigan State University. Variograms were fit with an exponential model using PROC NLIN in SAS 9.3 (SAS Inc., 2009). Spatial characteristics of the solid material can be determined from the components of the 3D variograms. The sill, where the variogram asymptotes, indicates the total spatial variability within a sample. The range of a variogram, lag distance at which the sill spatial autocorrelation exists in a sample. The nugget, the difference between the zero and the y-intercept, represents both measurement error and the variability at scales below the image resolution. The nugget to sill ratio describes the relative amount of spatial dependence at the voxel size.

Figure 2.1: Workflow for the geostatistical analysis. From each whole aggregate **(A)**, 5 cubes were selected **(B)**, **(C)** and then a 3D variogram obtained **(D)**. The whole aggregate is 5 mm in size, while the cubes in the slice **(B)** and 3D **(C)** are 130 µm on a side.

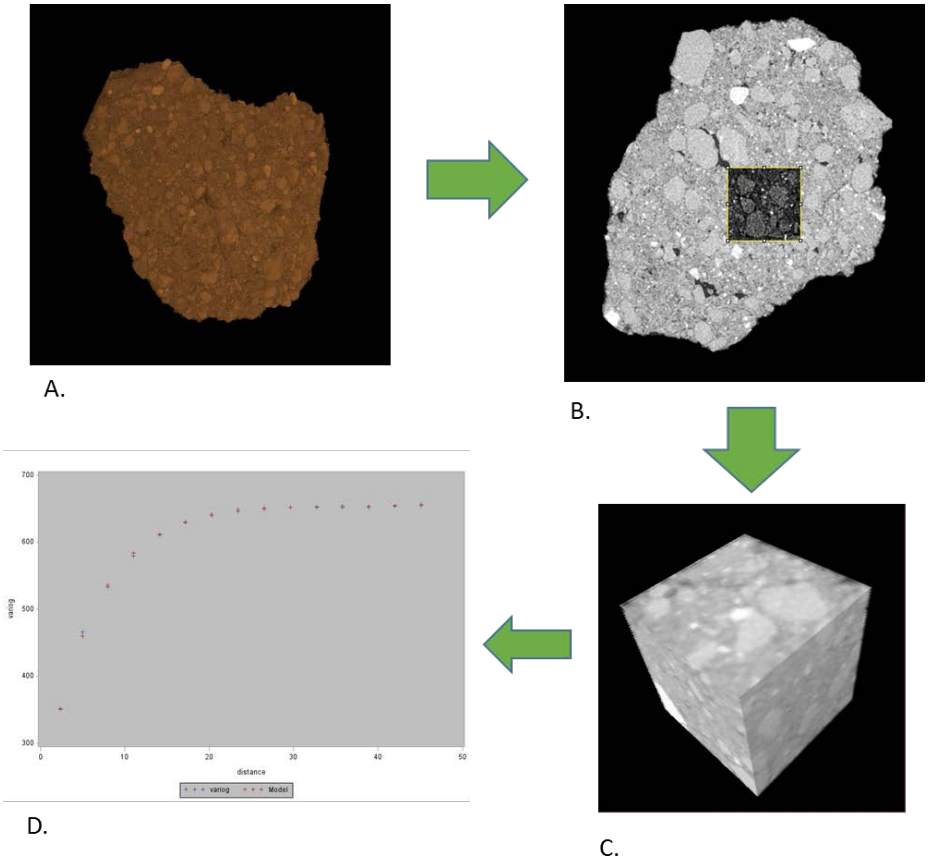

2.2.3 Os Gradients

Soil samples for Os analysis were taken as mini-cores. Only three mini-cores, all from the biological based management practice, were analyzed. The reason for the small number of samples used for this analysis is the very long image collection time for dual-energy Os scans limits the number of samples that could be processed. I choose biologically based management for these analyses, since I expected that pores of both non-biological and biological origin would be well represented in soil under this management. Samples were taken as 8 mm mini-cores, as opposed to dry sieved aggregates, because of concerns that aggregates would be too fragile for the multiple handling steps required by this method.

The mini-cores were taken at 3.5-5 cm depth using a beveled 3 mL Luer-Lok polypropylene syringe with an 8 mm inner diameter (BD, Franklin Lakes NJ, USA). There was minimal interference with Os staining, which binds to carbon-carbon double bonds, from polypropylene syringes as polypropylene contains almost no carbon-carbon double bounds. Cores were air dried and exposed to OsO_4 gas in a fume hood for one week. This allowed ample time for the OsO_4 gas to diffuse throughout the soil and to ensure maximum binding of Os to the soil organic material. The cores were then scanned at beamline 13-BM-D, GSECARS, APS ANL. Two-dimensional projections were taken at 0.25° rotation angle steps with a two second exposure and combined into a three-dimensional image consisting of 1200 slices with 1920 by 1920 pixels per slice. Final images had a 4 μm resolution. Three energies were used for the scans, 74 keV, 73.8 keV, and 28 keV. These energies provided, respectively, an image above Os K-edge, an image below Os K-edge, and an image at an energy optimal for soil pore and POM identification. By taking the difference between the above and below K-edge images, a map of the stained soil organic materials was created (Figure 2.2). Using the 28 keV images, non-biological pores were identified using simple thresholding, while POM pieces of both root and non-root origin were visually identified by hand. POM of non-root origin was defined as stand-alone organic fragments of round or irregular shape that were not connected to any obvious root remains.

Figure 2.2: An example of a µCT image from an Os stained soil sample from biologically based management at 4 µm resolution. **(A)** A 3D scan of an entire Os stained samples. The thickness of the sample was 1 mm. **(B)** Image of a slice of an Os stained sample above the K-edge (74 keV). **(C)** Image of a slice of an Os stained sample below the K-edge (73.8 keV). **(D)** Difference between above and below K-edge images with non-biological pore **(E)**, POM-NS **(G)**, and POM-Root **(F)** expanded. Total image size is 8 x 8 mm for **(B)**, **(C)**, and **(D)**.

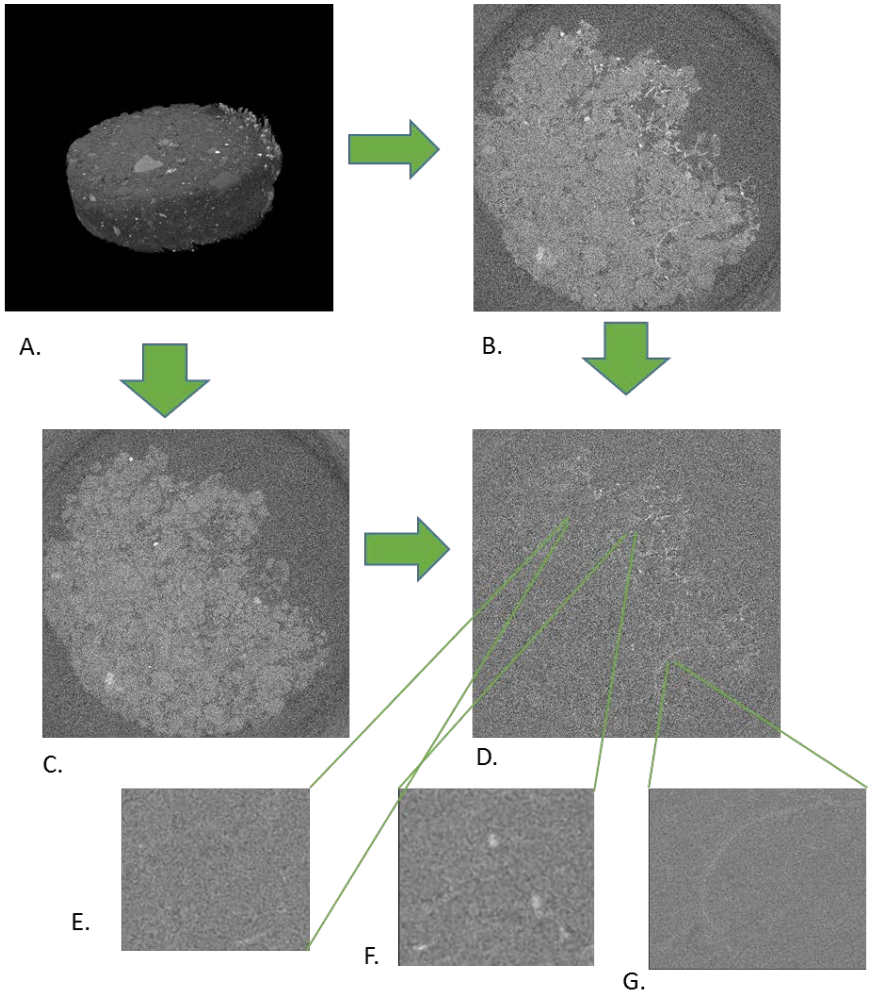

Two pores containing non-root derived POM (POM-NS), two pores containing root-derived POM (POM-Root) and four pores of non-biological origin were identified by hand for the analyses in each mini-core image (Figure 2.3). Identified pores varied in size from 20 to 300 µm. The identified pores were dilated by ~13 µm in all three dimensions to match the grayscale gradient results (described below). Then, a set of 4 µm layers were identified around each pore to a maximum distance of 213 µm. Grayscale values of the Os stained map were averaged for each 4 µm layer to obtain an Os gradient. The averages excluded the 0 value as that was the color of

the image background. To ensure comparability among the mini-cores, the Os gradients were standardized by subtracting the Os map's average grayscale value from each mini-core.

Figure 2.3: Examples of selected non-biological **(A, D)**, POM-Root **(B, E)**, and POM-NS pores **(C, F)** for 13 μm and 2 μm resolution. Non-biological pores were chosen so that no organic matter was visible in the pores and the pores were not round or oval in shape. POM-Root pores were chosen such that organic material was visible in the pores and were root shaped, i.e. round or oval with an elongated shape. POM-NS was chosen such that organic material was visible within the pores and the pore did not have a root like shape.

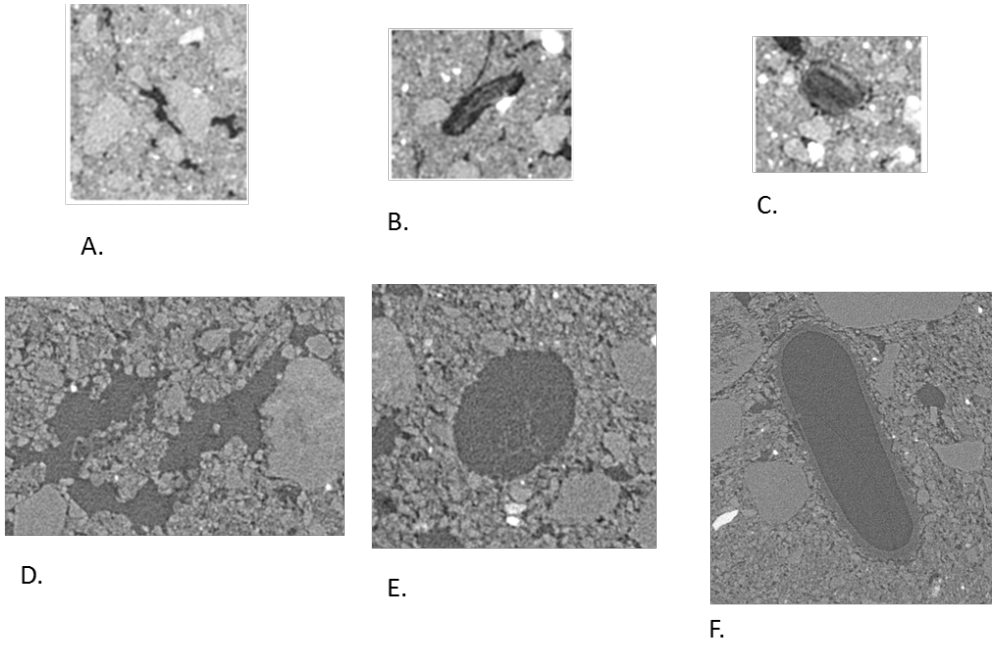

2.2.4 Grayscale Gradients

From each of the 32 images used in the geostatistical analysis, I identified three POM-NS, three POM-Root, and five non-biological origin pores (Figure 2.3). Identified pores ranged in sizes from 40 to 300 μm. In order to remove partial volume effects, the identified pores were dilated by one voxel in all three dimensions, thus they did not include the layer of border voxels that contained both pore and solid material. The grayscale value gradients were obtained by averaging voxels from 13 μm layers around each pore to a maximum distance of 208 μm (Figure 2.4). Averages did not include the 0 and 255 grayscale values as the 0 value was the value of the image background and excluding the 255 value corrected for any overly dense material, such as

iron minerals like magnetite or limonite, in the samples that might have skewed the grayscale averages. To enable direct comparisons between images, the grayscale value gradients were

Figure 2.4: Workflow for grayscale gradients. The whole aggregate **(A)** has all pores identified **(B)**. Individual pores are then identified **(C)**. Layers are collected for analysis of grayscale gradient **(D)**. Each color represents a different layer, while the white in the middle is the actual pore and the black layer adjacent to the white accounts for partial volume effects.

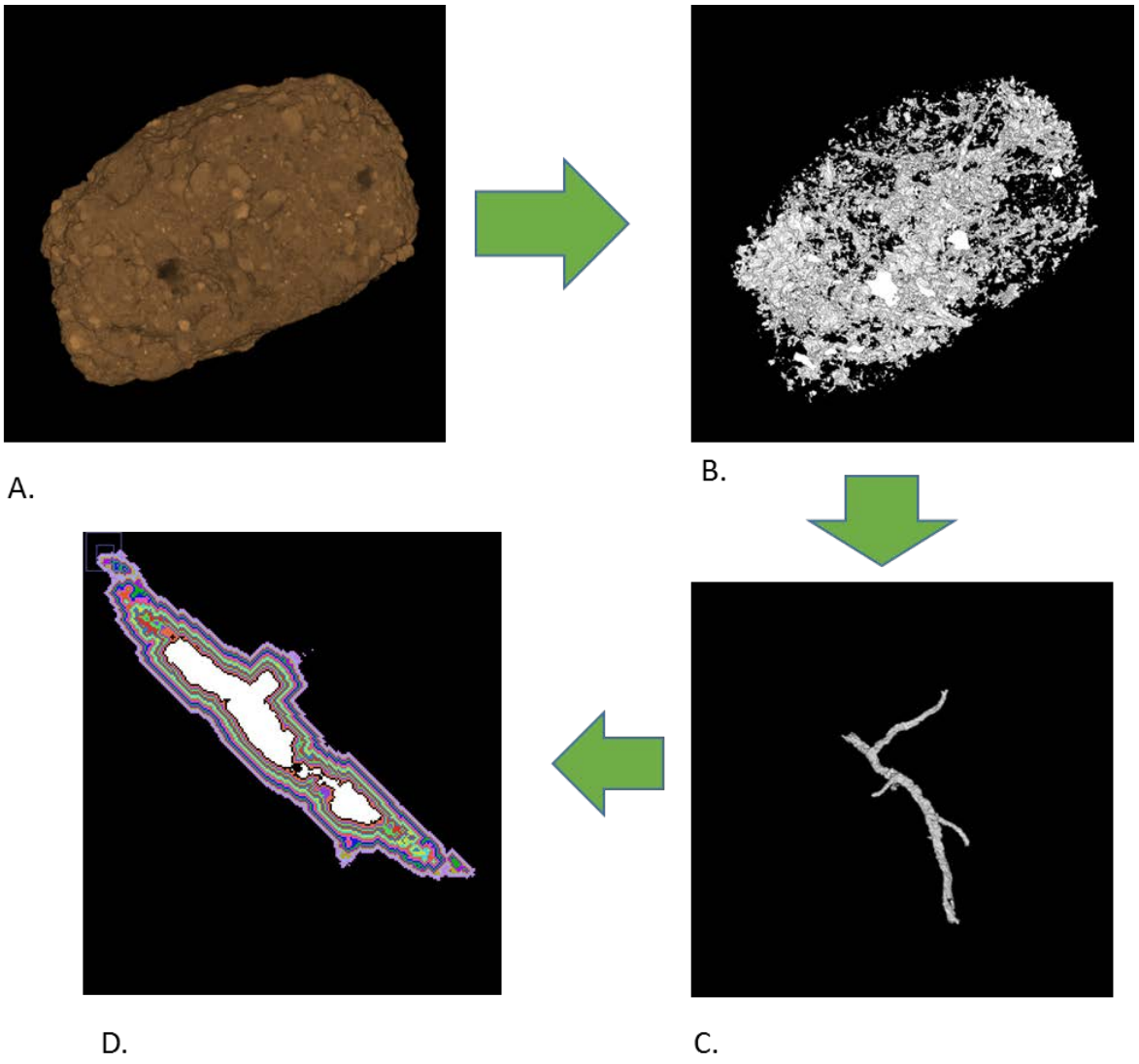

normalized so that the minimum grayscale value was 0 and the maximum grayscale value was 1 for each gradient. Calculation of the distance over which the gradient had influence was done by

fitting the individual gradients using PROC NLIN in SAS 9.4 (SAS Inc., 2009) with the following non-linear model:

$$f(x) = n + (s - n) \times \left(1 - e^{\left(-\frac{3x}{d}\right)}\right) \quad (2.1)$$

where x is distance from the pore, n is the y-intercept, s is the average grayscale value of the image, and d is the distance at which the pore stops affecting the grayscale values or effective distance of pore influence (EDPI).

2.2.5 Analysis of pores below image resolution (2-13 μm)

Presence of pores with sizes below the image resolution (<13 μm) can potentially affect gradients of grayscale values. If so, then it would not be possible to attribute the observed gradients in grayscale values to SOM. In order to explore the potential effect of such pores on the studied grayscale gradients, I scanned six of the 32 studied aggregates at 2 μm resolution. Two aggregates from each management were scanned.

I explored the differences among the studied managements of the presence of 2-13 μm pores. The purpose of this analysis was to ensure that the observed differences among the management practices were driven by SOM and not by below-resolution pores. For determination of presence of 2-13 μm, four cubes, 140 x 140 x 140 μm in size, were selected, using a selection process identical to that described above for the geostatistical analysis. Using Otsu's method, the overall porosity of each cube was determined. Binning was then used to compress the cube image to ~13 μm voxel size (Figure 2.5). Overall porosity of the binned image was then determined using the same threshold as the 2 μm samples. Subtracting the porosity of the binned images from the un-binned images resulted in the 2 to 13 μm porosity, referred to hereafter as the below image resolution porosity.

Figure 2.5: Example of a 2 µm image **(A)** and the same image reduced to 13 µm resolution **(B)**. Example of thresholding with Otsu's method of the same image at 2 µm **(C)** and 13 µm **(D)**.

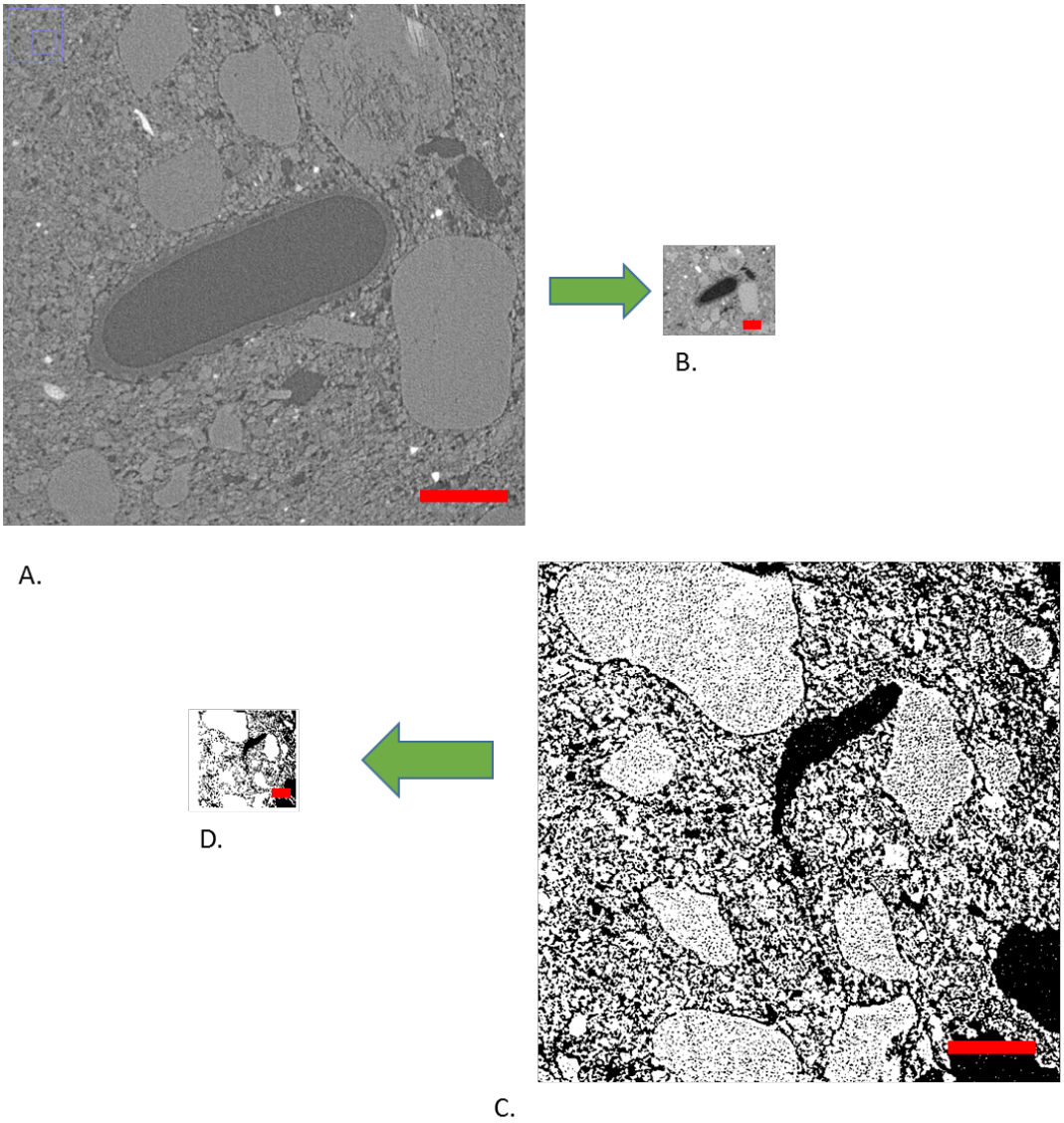

2.2.6 Statistical Analysis

Data analyses for all studied variables were conducted using the mixed model approach implemented in the PROC MIXED procedure of SAS Version 9.4 (SAS Inc., 2009). For comparisons of the geostatistical characteristics and total below image resolution porosity, the statistical model consisted of the fixed effect of management and the random effect of aggregates nested within management. For investigation of pore type and management effects on the grayscale gradients, the statistical model consisted of the fixed effects of management, pore

types, distances from the pores, and their interactions, as well as the random effect of aggregates nested within management and the random effect of individual pores nested within respective pore types and aggregates. In this analysis, distance was treated as a repeated measure factor.

Comparisons among pore types for the Os gradients were conducted using the statistical model with the fixed effects of pore type, distance, and their interaction and the random effects of soil core and soil core by pore type interaction. As with the grayscale gradients, the Os gradients distance factor was treated as a repeated measure. Comparisons among managements and pore types for the gradient influence distance were evaluated using the statistical model with the fixed effects of management, pore type, and the interactions between them and the random effect of aggregates nested within management.

The normality of residuals in all analyses was visually assessed using normal probability plots and stem-and-leaf plots, while equal variances assumption was assessed using Levene's test. Results are reported as statistically significant at α=0.05 level.

For all analyses, if the interactions were not significant, pairwise comparisons of the main effects using the LSMEANS statement were used. In the case where interactions were significant, slicing using the LSMEANS statement was employed. T-tests were conducted to determine if the mean values differed from zero.

2.3 Results

2.3.1 Geostatistical analysis of grayscale spatial patterns

Biologically based and early successional managements had greater overall spatial variability in grayscale values of the solid material than the conventional management system, as indicated by their higher sill values and histogram variance (Table 2.1). Spatial variations at distances less than the image resolution (13 μm) accounted for less than 50% of the overall variability, as indicated by nugget-to-sill ratios ranging from 39% in biologically based

management to 46 and 48% in early successional and conventional managements. The three managements did not differ in terms of their nugget and range values, indicating similarities in terms of variabilities at distances <13 μm and of distances at which spatial correlation were present.

Table 2.1: Characteristics of the variograms of soil material and variance of the histograms containing no >13 μm pores in three studied land use and management practices. Shown are means and standard errors (in parentheses) calculated based on a total of 157 subsection cubes from 32 aggregates. Different letters within each row denote statistically significant differences among the managements at α=0.05.

Variogram Characteristic	Conventional	Biologically Based	Early Successional
Range (μm)	334.1(1.4)a	309.4(1.4)a	297.7(1.4)a
Nugget	313(26)a	321(26)a	357(28)a
Sill	641(45)a	822(45)b	778(47)b
Nugget to Sill	0.48(0.02)a	0.39(0.02)b	0.46(0.02)a
Variance	637(45)a	817(45)b	782(47)b

2.3.2 Os levels as a function of distance from soil pores

The Os gradients were markedly different in pores of non-biological and biological origin (Figure 2.6). However, Os gradients did not differ between biological pores associated with POM-NS and POM-Root. Pores of biological origin had a large increase in Os labeled SOM immediately adjacent to the pores, which then slowly declined until returning to background levels at distances of 100-130 μm. Non-biological pores, on the other hand, had levels of Os labeled SOM that were statistically lower than background levels (P=0.045) at distances up to 30 μm from the pores.

Figure 2.6: **(A)** Mean difference from the background level for Os stained samples as a function of distance from pores of biological origin with plant roots (POM-Root) and with non-root derived POM (POM-NS) and from non-biological pores (n=6). The samples are from the biologically based system. Positive values indicate increased presence of Os labeled SOM, while negative values indicate a decrease in Os labeled SOM. **(B)** Normalized grayscale values for all three studied pore types from all three management practices. Dots are averages and the standard errors are equal to the size of the dots at each distance. The solid black lines represent the background Os labeled level (on **(A)**) and the background grayscale value (on **(B)**).

A.

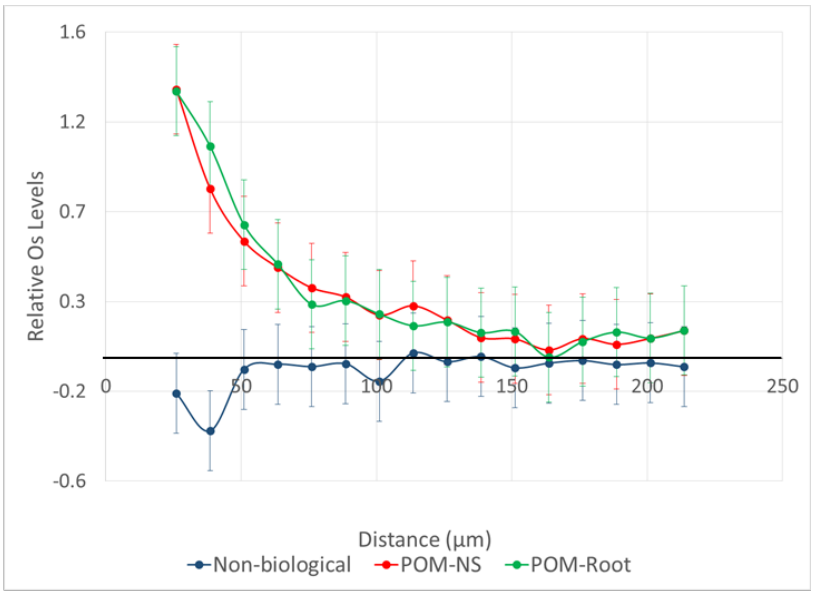

B.

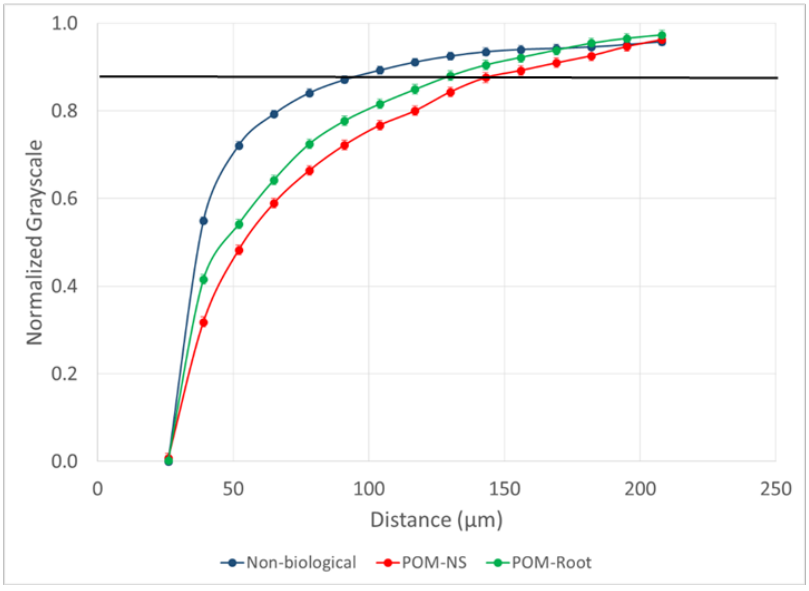

2.3.3 Grayscale levels as a function of distance from soil pores

The grayscale gradients for all managements and pore types had decreased grayscale values adjacent to the pores and then increased as distance from the pore increased (Figure 2.6).

This was similar to the biological pore results from the Os gradients. For biological pores, the grayscale gradients matched the Os gradients almost identically. When both grayscale and Os gradients for POM-NS and POM-Root in biologically based management were normalized to the average grayscale value (Figure 2.7), the overlap between the relationships was almost perfect, indicating that Os and grayscale value gradients were equivalent.

Figure 2.7: Normalized Os values from Os stained samples (n=6) and grayscale values (n=96) from non-stained samples as a function of distance from POM-NS and POM-Root pores in the soil of the biologically based management.

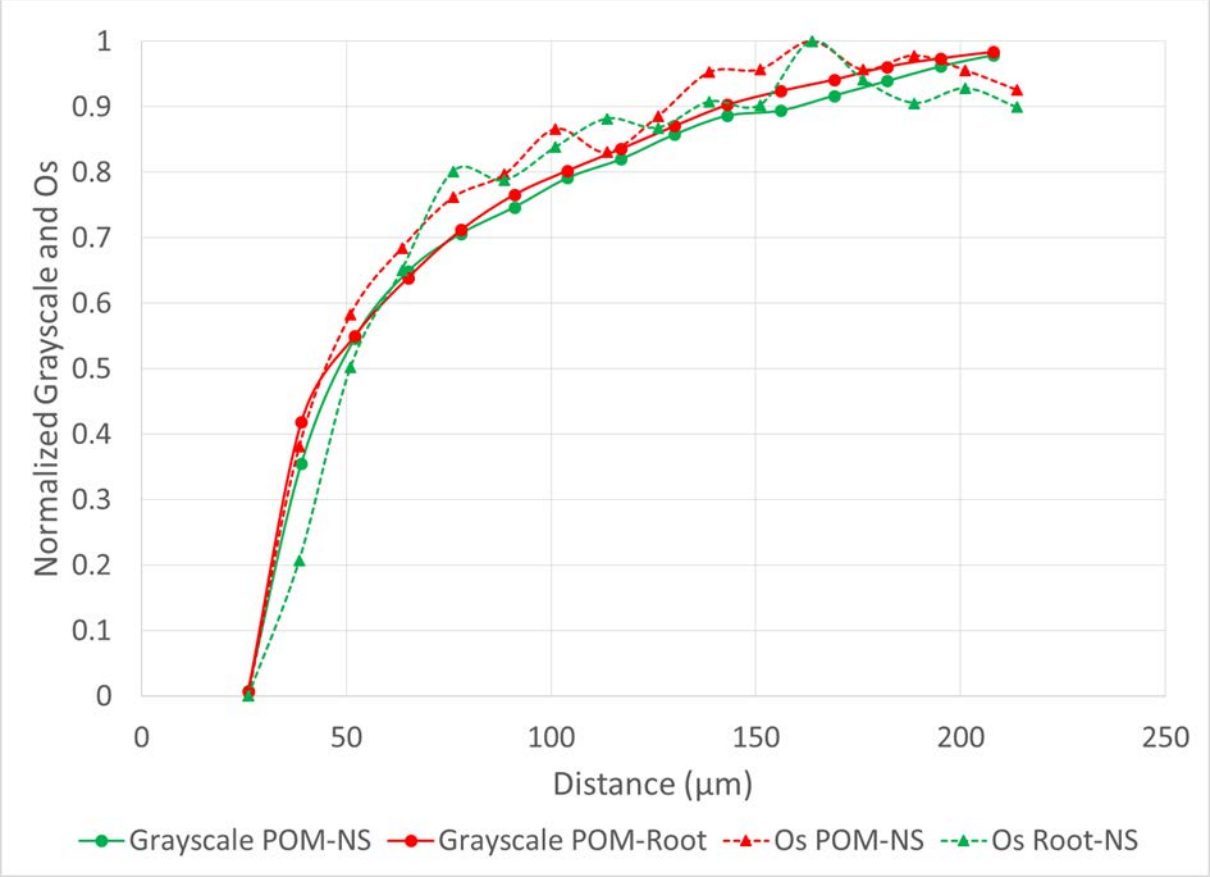

The grayscale levels in the solid material adjacent to non-biological pores were lower than the background grayscale values (average grayscale value of the whole aggregate). However, they increased much faster with increasing distance (Figure 2.6) and reached the background levels at much shorter distances than those of biological pores (Table 2.2). For

POM-NS and POM-Root, grayscale values returned to background levels at 123 μm, while non-biological pores at 74 μm.

Table 2.2: Effective distance of pore influence (EDPI) for the three studied pore types averaged across all studied aggregates. Means were calculated based on 32 aggregates with 3 POM-NS, 3 POM-Root, and 5 non-biological pores from each aggregate. Standard errors are shown in parentheses. Different letters denote significant differences among pore types at α=0.05.

Pore Type	EDPI(μm)
Non-biological	74.2(5.0)a
POM-Root	123.3(6.2)b
POM-NS	122.7(6.2)b

While no differences were observed between POM-NS and POM-Root grayscale gradients for biologically based and early successional managements (P=0.42, 0.23), POM-NS retained decreased grayscale values over longer distances than POM-Root in conventional management (P<0.001) (Figure 2.8). No significant differences were observed between managements for non-biological and POM-Root pores (P=0.85, 0.36), but conventional management again showed a shallower POM-NS grayscale gradient than the other managements (P=0.0096). EDPI only varied by pore type, indicating that management had no effect on this characteristic of grayscale value distributions (Table 2.2).

Figure 2.8: Normalized grayscale values as a function of distance from POM-NS pores for the three management practices (n=96). Error bars represent standard errors. The solid black line represents the background grayscale value, i.e. the average grayscale value of the entire aggregate.

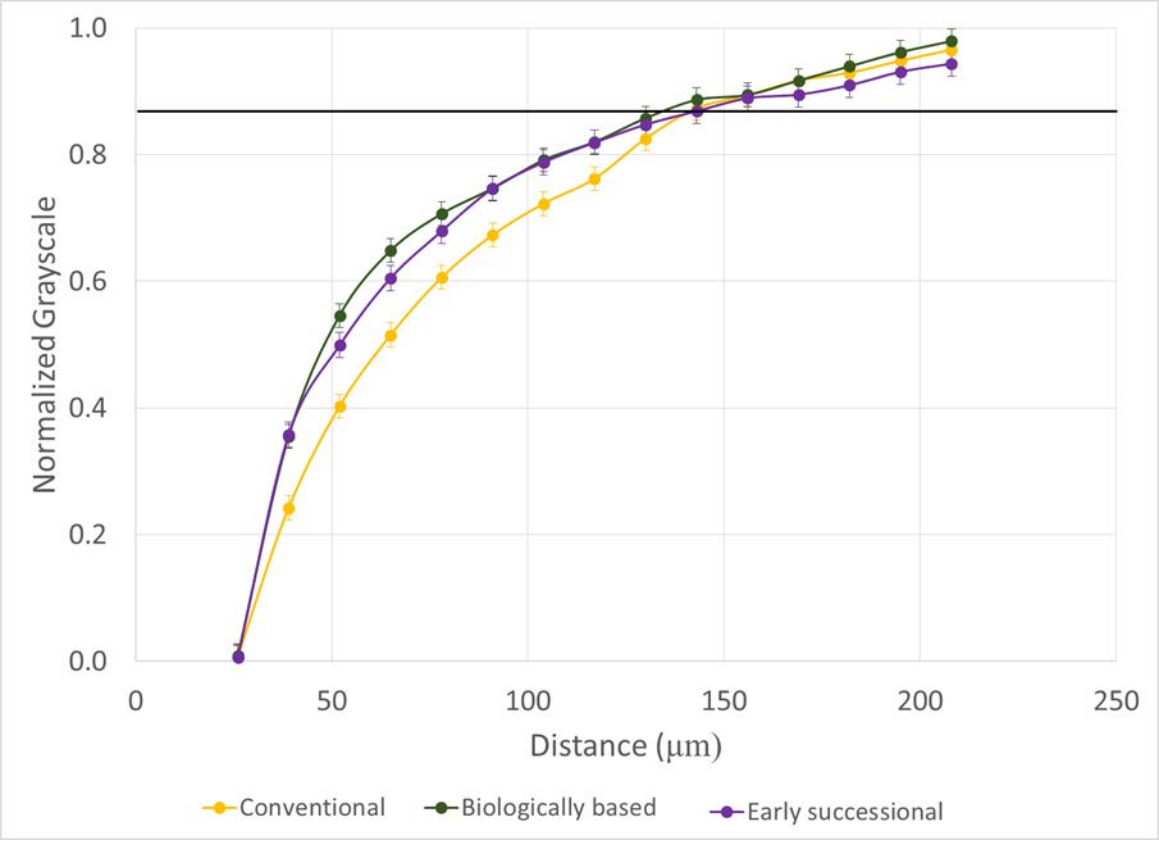

2.3.4 Pores below image resolution

While the >2 μm and the >13 μm porosities differed among the managements (P=0.044), the below image resolution porosity (2-13 μm) was the same for all three managements (P=0.45) (Figure 2.9). The >13 μm porosity and the >2 μm porosity were greater in the biologically based management than the conventional management, while the early successional management was not significantly different from either management.

Figure 2 9: Percentage of 2-13 µm and >2 µm pores in aggregates of the three managements. Letters indicate significant differences between managements for >2 µm pores at α= 0.05. The differences in 2-13 µm pores were not statistically significant. Error bars represent standard errors.

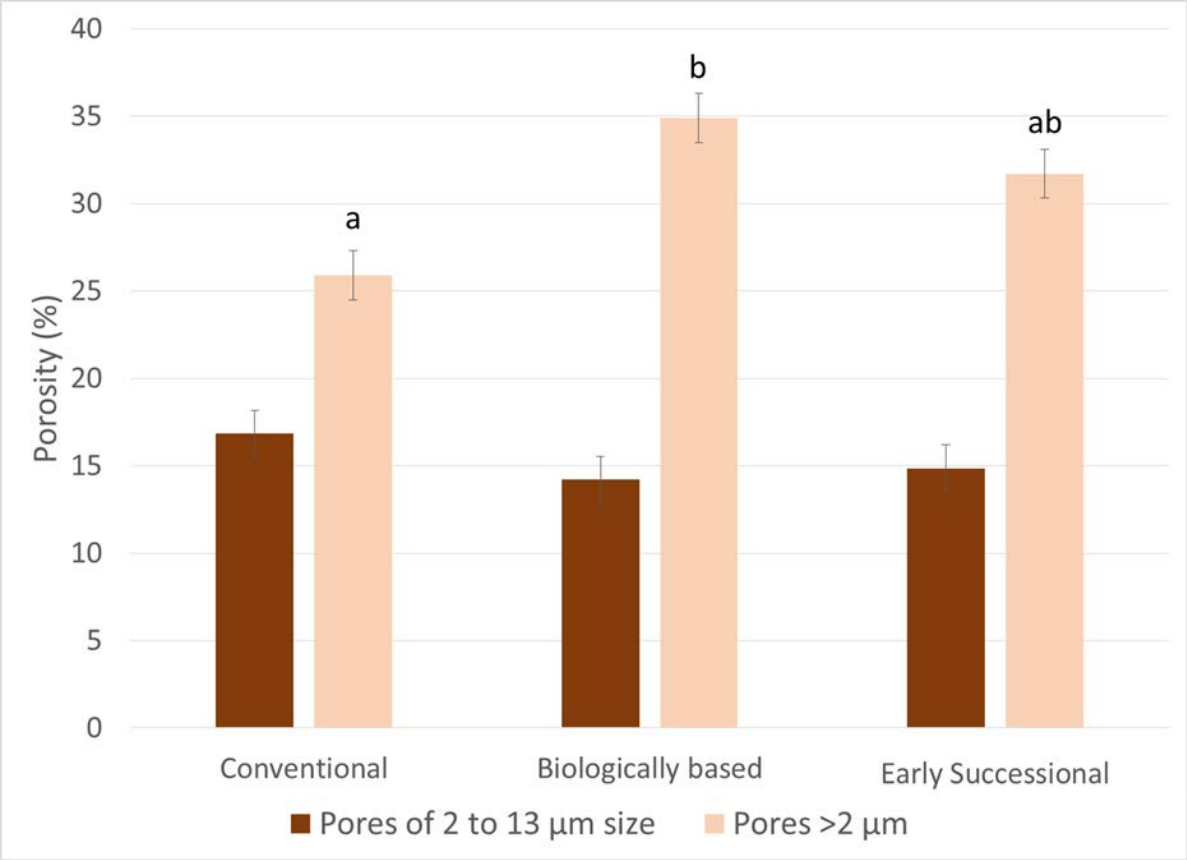

2.4 Discussion

2.4.1 Image grayscale values as a proxy for SOM patterns

My findings indicate that grayscale values can be a useful proxy for SOM, however, caution needs to be exercised in such use. Specifically, in the studied soil, a reliable correspondence between SOM gradients as determined via Os staining and grayscale value gradients was achieved only for pores of biological origin. As can be seen from Figure 2.7, the Os and grayscale gradients corresponded to each other remarkably well, indicating that grayscale gradients can be used as a suitable proxy when exploring SOM patterns near pores of biological origin. The EDPI observed (123 µm) is consistent with previously reported ranges for SOM distributions in soil of 38-175 µm determined through the use of Os staining and geostatistical

analyses, although these analyses were not correlated to pores specifically (Rawlins et al, 2016). Previous studies utilizing isotopically labeled materials have reported movement of decomposition products as far as 5-10 mm from carbon sources during soil incubations (Gaillard et al, 1999, 2003; Toosi et al, 2017). However, these studies do not specifically measure transport of DOM from individual pore, but overall transport of isotopic labeled materials from its source, which would account for the larger transport ranges seen in previous studies. Direct imaging of the spatial distribution of SOM near individual pores has previously been achieved using NanoSIMS, however, at spatial scales much lower (nm) than those used in this study. Mueller et al (2012) showed that, in the 5 mm and <63 μm samples used in their study, DOM moved ~2 μm from a carbon source, but also found indications of possibly larger spatial ranges at larger spatial scales. The 123 μm distance may indicate the typical diffusion distance of DOM from biological pores into the soil matrix in similarly textured soils.

For non-biological pores, Os staining and grayscale value gradient trends did not match. The grayscale levels increased with the distance from the pore, which could be interpreted as increased SOM concentrations near the pore. Yet, the Os gradients clearly indicate lower SOM levels in immediate vicinity (<30 micron) of non-biological pores (Figure 2.6). This result was hypothesized to be due to increased <13 μm porosity closer to non-biological origin pores. However, no difference in <13 μm porosity was observed among pore types (Figure 2.10).

Figure 2.10: Percentage of 2-13 µm pores as a function of distance from pores of biological origin with plant roots (POM-Root) and with non-root derived POM (POM-NS) and from non-biological pores (n=8). Error bars are standard errors at each distance.

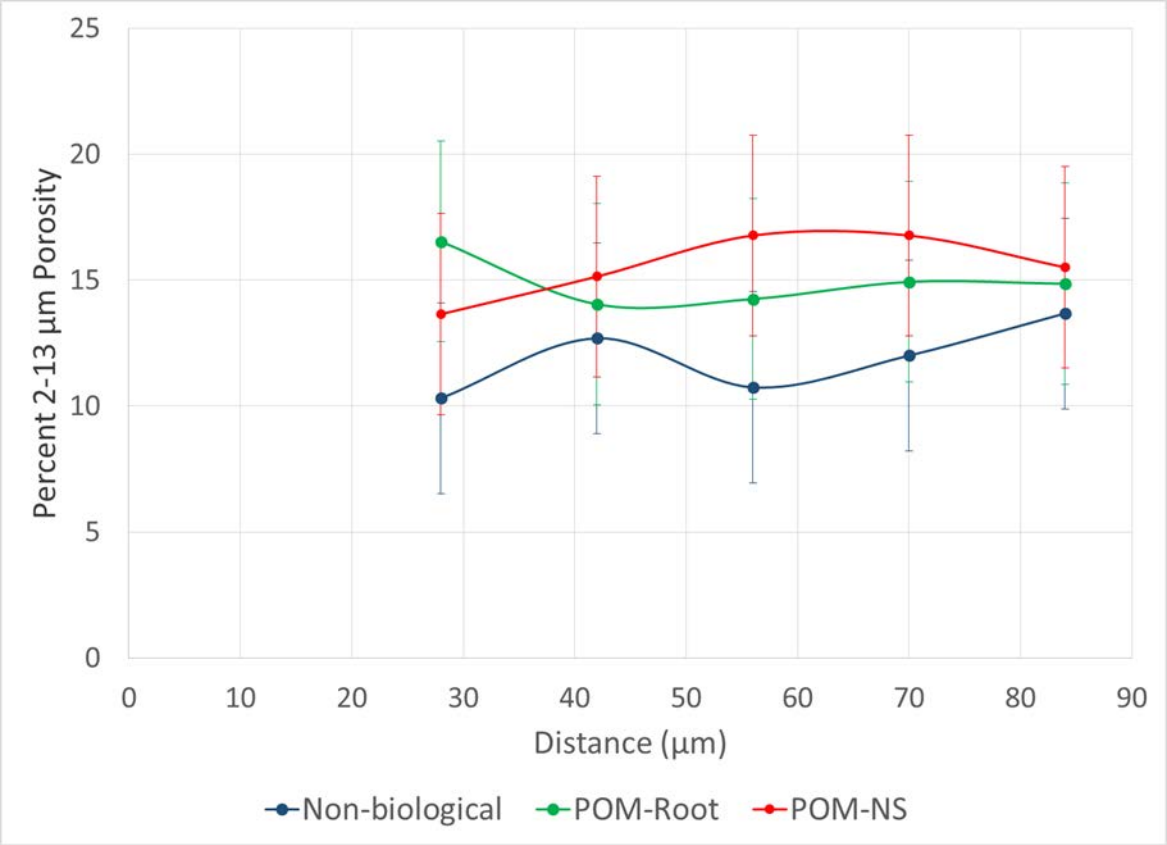

A possible explanation for this discrepancy is an artifact of image processing via 3DMA. 3DMA uses indicator kriging as a thresholding method, while the distance measures were conducted using Otsu's method due to computational and time limits resulting from the smaller image resolution. Indicator kriging performs well for identifying pores well above the image resolution, but may misidentify pores of sizes at or only slightly larger than the image resolution (Figure 2.11). Thus, the decreases in the grayscale values might be due to such missed porosity in non-biological pores. For non-biological pores, indicator kriging fails to identify small visible connections between larger pores that extend for several voxels between adjacent pores due to using the surrounding voxels to help determine if a voxel is pore or not, while Otsu's method correctly identifies these pores because it only uses the raw grayscale value to identify pores.

This artifact is less pronounced in biological pores as biological pores have no such small connections and, therefore, the true extent of the pore was accounted for.

Figure 2.11: Examples from the three different managements of how 3DMA missed pore material adjacent to non-biological pores, but identifies POM-Root and POM-NS pores correctly. **(A)** is from the conventional management, **(B)** is from the biologically based, and **(C)** is from the early successional. The blue outlines are the pores identified by 3DMA. Red arrows on each figure indicate an example of missed porosity on each figure.

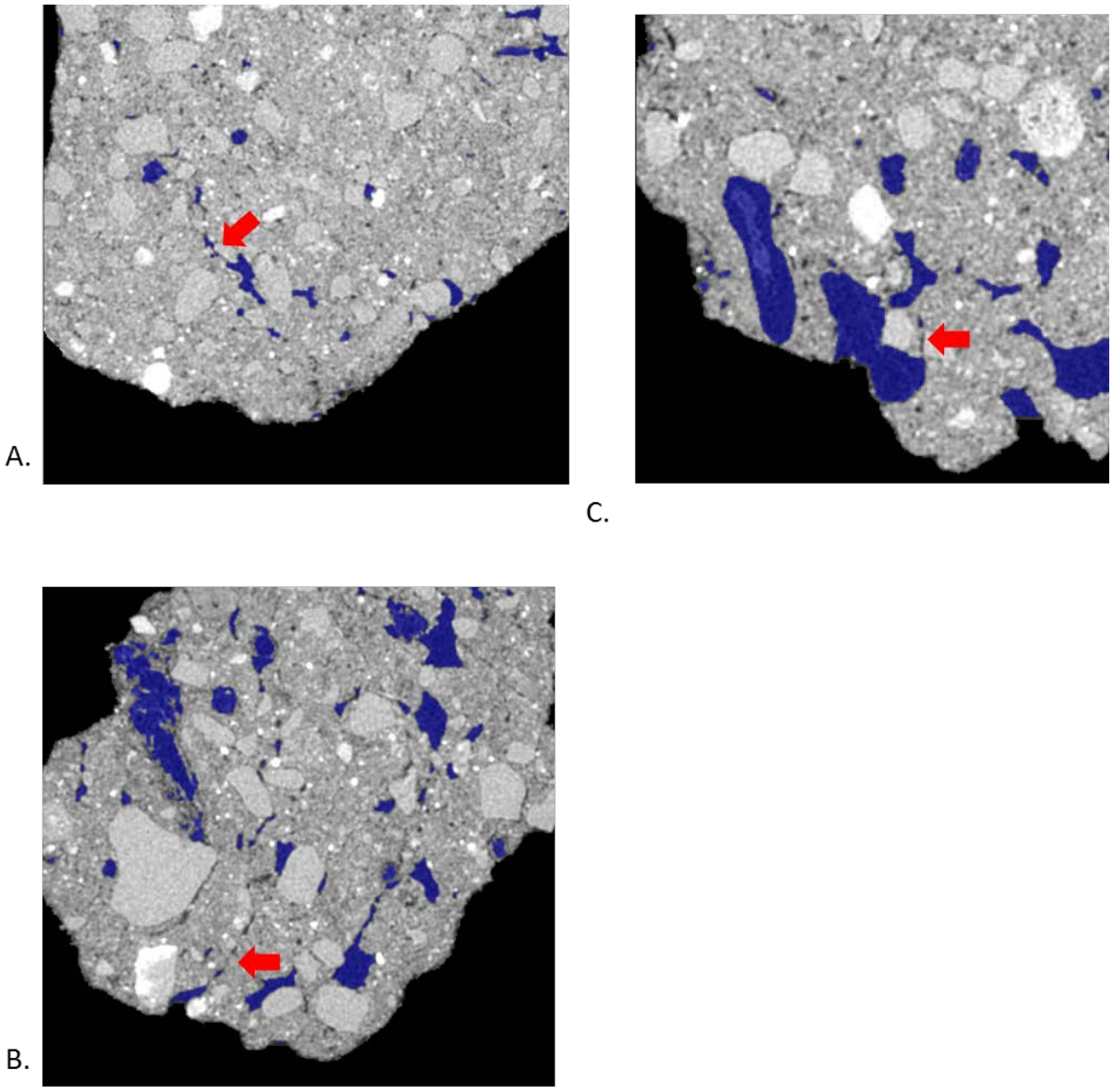

The reason for this artifact to be present in pores of non-biological but not biological origin can be explained by the processes that create the pores of these two different types. Biological pores are created through the radial compression of the surrounding matrix as a root

or macrofauna pushes through the soil and is then supported by organic binding agents, such as mucilage, mucus, and large amounts of DOM from decomposing organic matter, resulting in a clear boundary between pore and solid material (Gray and Lissmann, 1938; Greacen et al 1972; Greacen and Sands, 1980; Czarnes et al, 2000; Ruiz et al, 2017). Additionally, Helliwell et al (2017) found that while porosity near roots increased initially in sandy soils, which is similar to the texture of these soils, after eight days of growth, porosity was found to decrease adjacent to roots at this image resolution. Non-biological pores are created through the shrinking and expanding of clays, resulting in neither clear nor stable boundaries (Peng et al, 2007). However, using a different thresholding method may overcome the artifact effect.

2.4.2 Spatial patterns of grayscale values

The nugget to sill ratio values of the studied samples indicate that approximately 50-60% of the spatial variability in grayscale values of the solid material is accounted for at >13 μm distances. This matches the porosity data, where approximately 50% of the porosity occurs at >13 μm (Figure 2.9). Biologically based management had the most porosity above 13 μm and the lowest nugget to sill ratio, while conventional management had the lowest porosity above 13 μm and the highest nugget to sill ratio. Since nugget to sill ratio indicates the relative amount of spatial dependence at voxel size, this may indicate a connection between spatial dependence and porosity at image scale. This would support my hypothesis that spatial variability in the solid material of similar mineralogy is driven by pores. However, more research would be necessary to confirm this connection.

The lack of difference in spatial autocorrelation ranges among the aggregates from the three managements was surprising. Tillage, utilized both in conventional and biologically based management, homogenizes the soil, which, according to my expectations and previous findings (Garrett 2009), should be manifested in greater spatial correlation range values. Lack of such an

effect in my samples may indicate that the spatial correlation range in this soil is controlled more by the inherent mineralogy and/or texture, which are similar for the soil of all three managements, than by the management-driven SOM differences. The EDPI was much smaller than the spatial correlation range (123 μm vs. 312 μm) lending further support to the notion that the SOM distribution was not a driver of the spatial correlation range values. Rawlins et al (2016) investigated the spatial ranges of SOM, pores, minerals, and bulk from μCT images. While the spatial ranges for SOM (38-175 μm) were greater than mineral and pores alone, the spatial ranges for bulk variograms were <250 μm, which is congruent with my results.

Observed similarity in the nugget values from the three studied managements was in agreement with the results of Nunan et al (2006), who found similar nuggets between three different amendment managements. The lack of differences between nuggets corroborates the below image resolution porosity measurements where the below image resolution porosity was similar between all three managements (Figure 2.9). The differences observed in the overall porosity matched results previously reported for these aggregates with biologically based ≥ early successional ≥ conventional (Kravchenko et al, 2015).

Greater overall spatial variability in less intense management practices, i.e., biologically based and early successional managements, manifested via greater sill values (Table 2.1), is likely a result of management-induced changes in SOM. As mentioned above, soil mineralogy and texture of the studied managements were very similar, as well as their below image resolution porosity values (Figure 2.9 & 2.10). Yet, after almost 20 years of implementation, the biologically based and early successional management practices resulted in higher SOM than the conventionally managed practice (Paul et al, 1999; Senthilkumar et al, 2009). Observed greater variability in grayscale values of biologically based and early successional managements

suggests that these SOM inputs were not uniformly distributed. This assertion is supported by previous findings of Ananyeva et al (2013) who reported greater variability in soil carbon within the macro-aggregates from early successional management as compared to conventional management practice; while Feeney et al (2006) observed that active biota, in particular roots, increased spatial correlation of soil pores. Spatial gradients in SOM associated with pores of biological origin is one possible mechanism contributing to the increased variability.

The increased spatial variability observed in the grayscale values of the biologically based and early successional managements, if driven by SOM distributions, would indicate increased occurrence of different microenvironments of either increased or decreased amounts of SOM, while conventional management would have less of these differing microenvironments. Greater presence of biological pores may result in an increased diversity of microenvironmental conditions, including different levels of microbial accessibility, nutrient availability, and potentially water and gas fluxes. Such microenvironmental differences affect microbial activities (Ekschmitt et al, 2005; Ekschmitt, 2008; Kravchenko and Guber, 2017); and greater SOM decomposition can be expected in microenvironments conducive to high microbial activity, while SOM protection in microenvironments where microbial activity is reduced. This increase in microenvironment heterogeneity, and therefore, greater presence of microsites where SOM might not be available to microbial decomposers and/or reduction of microbial decomposition due to anaerobic microsites (Keiluweit et al, 2016, 2017), may be reflective of the increased carbon protection/sequestration observed in the biologically based and early successional managements as compared to conventional management (Paul et al, 1999; Senthilkumar et al, 2009).

2.4.3 SOM pattern in relation to soil pores

My Os results demonstrated that pores were the drivers of SOM's spatial variability in the studied soil (Figure 2.6). Biological pores had a clear spatial gradient of SOM with highest levels in the vicinity of pores and decreasing when moving into the surrounding solid material. Biological pores are observed more frequently in biologically base and early successional managements as biological pores tend to be <90 μm, which have a higher abundance in these managements. Non-biological pores had a small decrease in SOM adjacent to the pores, but otherwise their presence was not related to SOM distribution patterns. Non-biological pores are observed more frequently in conventional management as non-biological pores tend to be 40-90 μm in size, which have a higher abundance in this management. Oxygen availability may control the decrease in SOM observed adjacent to non-biological pores. In the studied soil, <13 μm pores (below image resolution sizes) are water filled during most of the year. This would hamper the diffusion of oxygen and lead to dominance of anaerobic conditions, which can result in as much as a 10-fold decrease in decomposition rates (Keiluweit et al, 2017). The likely outcome is, thus, organic matter's decomposition near large (20-300μm) pore boundaries, where oxygen is available, and organic's preservation in anaerobic (<13 μm pore) zones.

2.4.4 Effect of management practices on SOM pattern in relation to soil pores

The effect of management on the SOM gradients as inferred from the grayscale gradient was unanticipated. There were no differences among managements observed for non-biological and POM-Root pores. However, there were observed differences between the managements in POM-NS pores. Biologically based and early successional managements had no differences between POM-Root and POM-NS pores. Conversely, in conventional management, POM-NS gradients tended to retain decreased grayscale values over longer distances. I inferred that this decrease is related to an increase in SOM content. A possible explanation is that, per visual

observations, POM-NS within conventional soil aggregates tended to be located closer to the interior of soil aggregates and/or away from pores of > 13 μm size, while POM-NS in biologically based and early successional managements were located closer to the aggregate exterior and/or nearer to pores of 13 μm size. Such isolation in conventional soil would result in restriction of microorganism, water, and oxygen access to POM-NS, resulting in incomplete decomposition. The incomplete decomposition produces decomposition products of a more hydrophobic nature. This hydrophobicity would decrease the ability of these products to be transported by water, resulting in a build-up of organic matter closer to the pore. Toosi et al (2017) observed that as maximum pore size decreases the presence of SOM compounds with fewer oxygen functional groups and greater aromaticity increases; this observation supports my increased hydrophobicity explanation.

2.5 Conclusion

Analysis of grayscale gradients near pores of biological origin were found to be a useful proxy for assessing SOM spatial distribution patterns at micro-scale. Grayscale gradients of non-biological pores, in contrast, were found to not be a useful proxy for SOM due to a pore identification artifact. Utilizing a different thresholding method may overcome this limitation. Os and grayscale value gradients indicate increased SOM concentrations adjoining biological pores, decreasing to background levels as distance from the pore increases. The average distance of positive influence of biological pores on SOM levels was 123 μm. Os gradients indicate that SOM concentrations decreased in the direct vicinity of non-biological pores then returned to the background levels. The average distance of negative influence of non-biological pores on SOM levels was 30 μm.

Soil material without >13 μm pores was more variable in its grayscale values in biologically based and early successional management than in conventional management

practice. The greater variability is likely to be driven by SOM spatial distribution patterns, which reflect presence of soil pores, especially, pores of biological origin. This spatial variability likely results in greater variability of microenvironmental conditions for microbial functioning with possible implications for soil carbon protection.

Funding

Support for this research was provided in part by the USDA-NIFA, Award No. 2016-67011-24726 “Using stable isotopes and computer tomography to determine mechanisms of soil carbon protection in cover crop based agricultural systems” and by the US National Science Foundation Long-Term Ecological Research Program (DEB 1027253) at the Kellogg Biological Station and by Michigan State University AgBioResearch. Portions of this work were performed at GeoSoilEnviroCARS (The University of Chicago, Sector 13), Advanced Photon Source (APS), Argonne National Laboratory. GeoSoilEnviroCARS is supported by the National Science Foundation - Earth Sciences (EAR - 1634415) and Department of Energy- GeoSciences (DE-FG02-94ER14466). This research used resources of the Advanced Photon Source, a U.S. Department of Energy (DOE) Office of Science User Facility operated for the DOE Office of Science by Argonne National Laboratory under Contract No. DE-AC02-06CH11357.

REFERENCES

REFERENCES

Ananyeva, K., Wang, W., Smucker, A. J. M., Rivers, M. L., and Kravchenko, A. N. (2013). Can intra-aggregate pore structures affect the aggregate's effectiveness in protecting carbon? *Soil Biol. Biochem.* 57, 868-875. doi: 10.1016/j.soilbio.2012.10.019

Aravena, J. E., Berli, M., Ruiz, S., Suárez, F., Ghezzehei, T. A., and Tyler, S. W. (2014). Quantifying coupled deformation and water flow in the rhizosphere using X-ray microtomography and numerical simulations. *Plant Soil*. 376, 95-110. doi: 10.1007/s11104-013-1946-z

Bailey, V. L., Smith, A. P., Tfaily, M., Fansler, S. J., and Bond-Lamberty, B. (2017). Differences in soluble organic carbon chemistry in pore waters sampled from different pore size domains. *Soil Biol. Biochem.* 107, 133-143. doi: 10.1016/j.soilbio.2016.11.025

Bengough, A. G., McKenzie, B. M., Hallett, P. D., and Valentine, T. A. (2011). Root elongation, water stress, and mechanical impedance: a review of limiting stresses and beneficial root tip traits. *J. Exp. Bot.* 62, 59-68. doi: 10.1093/jxb/erq350

Chun, H. C., Giménez, D., and Yoon, S. W. (2008). Morphology, lacunarity and entropy of intra-aggregate pores: aggregate size and soil management effects. *Geoderma*. 146, 83-93. doi: 10.1016/j.geoderma.2008.05.018

Czarnes, S., Hallett, P. D., Bengough, A. G., and Young, I. M. (2000). Root- and microbial-derived mucilages affect soil structure and water transport. *Eur. J. Soil Sci.* 51, 435-443. doi: 10.1046/j.1365-2389.2000.00327.x

De Gryze, S., Jassogne, L., Six, J., Bossuyt, H., Wevers, M., and Merckx, R. (2006). Pore structure changes during decomposition of fresh residue: X-ray tomography analyses. *Geoderma*. 134, 82-96. doi: 10.1016/j.geoderma.2005.09.002

Denef, K., Six, J., Bossuyt, H., Frey, S. D., Elliot, T. E., Merckx, R., et al. (2001). Influence of dry-wet cycles on the interrelationship between aggregate, particulate organic matter, and microbial community dynamics. *Soil Biol. Biochem.* 33, 1599-1611. doi: 10.1016/S0038-0717(01)00076-1

Dungait, J. A. J., Hopkins, D. W., Gregory, A. S., and Whitmore, A. P. (2012). Soil organic matter turnover is governed by accessibility not recalcitrance. *Global Change Biol.* 18, 1781-1796. doi: 10.1111/j.1365-2486.2012.02665.x

Ekschmitt, K., Kandeler, E., Poll, C., Brune, A., Buscot, F., Friedrich, M., et al. (2008). Soil-carbon preservation through habitat constraints and biological limitations on decomposer activity. *J. Plant Nutr. Soil Sci.* 171, 27-35. doi: 10.1002/jpln.200700051

Ekschmitt, K., Liu, M., Vetter, S., Fox, O., and Wolters, V. (2005). Strategies used by soil biota to overcome soil organic matter stability – why is dead organic matter left over in soil? *Geoderma*. 128, 167-176. doi: 10.1016/j.geoderma.2004.12.024

Falconer, R. E., Battaia, G., Schmidt, S., Baveye, P., Chenu, C., and Otten, W. (2015). Microscale heterogeneity explains experimental variability and non-linearity in soil organic matter mineralization. *PloS One*. 10(5): e0123774. doi: 10.1371/journal.pone.0123774

Feeney, D. S., Crawford, J. W., Daniell, T., Hallett, P. D., Nunan, N., Ritz, K., et al. (2006). Three-dimensional microorganization of the soil-root-microbe system. *Microb. Ecol.* 52, 151-158. doi: 10.1007/s00248-006-9062-8

Gaillard, V., Chenu, C., and Recous, S. (2003). Carbon mineralization in soil adjacent to plant residues of contrasting biochemical quality. *Soil Biol. Biochem.* 35, 93-99. doi: 10.1016/S0038-0717(02)00241-9

Gaillard, V., Chenu, C., Recous, S. and Richard, G. (1999). Carbon, nitrogen and microbial gradients induced by plant residues decomposing in soil. *Eur. J. Soil Sci.* 50, 567-578. doi: 10.1046/j.1365-2389.1999.00266.x

Garrett, R. G. (2009). Relative spatial soil geochemical variability along two transects across the United States and Canada. *Appl. Geochem.* 24, 1405-1415. doi: 10.1016/j.apgeochem.2009.04.011

Gibson, J. R., Lin, H., and Bruns, M. A. (2006). A comparison of fractal analytical methods on 2- and 3-dimensional computed tomographic scans of soil aggregates. *Geoderma*. 134, 335-348. doi: 10.1016/j.geoderma.2006.03.052

Greacen, E. L., and Oh, J. S. (1972). Physics of root growth. *Nat. New Biol.* 235, 24-25. doi: 10.1038/newbio235024a0

Greacen, E. L., and Sands, R. (1980). Compaction of forest soils. a review. *Aust. J. Soil. Res.* 18, 163-189. doi: 10.1071/SR9800163

Gray, J., and Lissmann, H. W. (1938). An apparatus for measuring the propulsive forces of the locomotory muscles of the earthworm and other animals. *J. Exp. Biol.* 15, 518-521.

Helliwell, J. R., Sturrock, C. J., Mairhofer, S., Craigon, J., Ashton, R. W., Miller, A. J., et al. (2017). The emergent rhizosphere: imaging the development of the porous architecture at the root-soil interface. *Sci. Rep.* 7: 14875. doi:10.1038/s41598-017-14904-w

Keiluweit, M., Nico, P. S., Kleber, M., and Fendorf, S. (2016). Are oxygen limitations under recognized regulators of organic carbon turnover in upland soils? *Biogeochemistry*. 127, 157-171. doi: 10.1007/s10533-015-0180-6

Keiluweit, M., Wanzek, T., Kleber, M., Nico, P., and Fendorf, S. (2017). Anaerobic microsites have an unaccounted role in soil carbon stabilization. *Nat. Commun.* 8: 1771. doi: 10.1038/s41467-017-01406-6

Kiem, R., and Kögel-Knabner, I. (2002). Refractory organic carbon in particle-size fractions of arable soils II: organic carbon in relation to mineral surface area and iron oxides in fractions <6 μm. *Org. Geochem.* 33, 1699-1713. doi: 10.1016/S0146-6380(02)00112-2

Ketcham, R. A. (2005). Three-dimensional grain fabric measurements using high-resolution X-ray computed tomography. *J. Struc. Geol*. 27, 1217-1228. doi: 10.1016/j.jsg.2005.02.006

Kravchenko, A. N., and Guber, A. K. (2017). Soil pores and their contributions to soil carbon processes. *Geoderma*. 287, 31-39. doi: 10.1016/j.geoderma.2016.06.027

Kravchenko, A. N., Negassa, W. C., Guber, A. K., Hildebrandt, B., Marsh, T. L., and Rivers, M. L. (2014b). Intra-aggregate pore structure influences phylogenetic composition of bacterial community in macroaggregates. *Soil Sci. Soc. Am. J.* 78, 1924-1939. doi: 10.2136/sssaj2014.07.0308

Kravchenko, A. N., Negassa, W. C., Guber, A. K., and Rivers, M. L. (2015). Protection of soil carbon within macro-aggregates depends on intra-aggregate pore characteristics. *Sci. Rep.* 5:16261. doi: 10.1038/srep16261

Kravchenko, A. N., Negassa, W., Guber, A. K., and Schmidt, S. (2014a). New approach to measure soil particulate organic matter in intact samples using X-ray computed microtomography. *Soil Sci. Soc. Am. J.* 78, 1177-1185. doi: 10.2136/sssaj2014.01.0039

Kravchenko, A. N., Wang, W., Smucker, A. J. M., and Rivers, M. L. (2011). Long-term differences in tillage and land use affect intra-aggregate pore heterogeneity. *Soil Sci. Soc. Am. J.* 75, 1658-1666. doi: 10.2136/sssaj2011.0096

Kuzyakov, Y., and Blagodatskaya, E. (2015). Microbial hotspots and hot moments in soil: concept & review. *Soil Biol. Biochem.* 83, 184-199. doi: 10.1016/j.soilbio.2015.01.025

Mooney, S. J., Pridmore, T. P., Heliwell, J., and Bennett, M. J. (2012). Developing X-ray computed tomography to non-invasively image 3-D root systems architecture in soil. *Plant Soil*. 352, 1-22. doi: 10.1007/s11104-011-1039-9

Mueller, C. W., Kölbl, A., Hoeschen, C., Hillion, F., Heister, K., Herrmann, A. M., et al. (2012). Submicron scale imaging of soil organic matter dynamics using NanoSIMS – from single particles to intact aggregates. *Org. Geochem.* 42, 1476-1488. doi: 10.1016/j.orggeochem.2011.06.003

Negassa, W. C., Guber, A. K., Kravchenko, A. N., Marsh, T. L., Hildebrandt, B., and Rivers, M. L. (2015). Properties of soil pore space regulate pathways of plant residue decomposition and community structure of associated bacteria. *PLoS One*. 10(4): e0123999 doi: 10.1371/journal.pone.0123999

Nunan, N., Ritz, K., Rivers, M., Feeney, D. S., and Young, I. M. (2006). Investigating microbial micro-habitat structure using X-ray computed tomography. *Geoderma*. 133, 398-407. doi: 10.1016/j.geoderma.2005.08.004

Oades, J. M. (1984). Soil organic matter and structural stability: mechanisms and implications for management. *Plant Soil.* 76, 319-337. doi: 10.1007/BF02205590

Oh, W., and Lindquist, W. B. (1999). Image thresholding by indicator kriging. *IEEE Trans. Pattern Anal. Mach. Intell.* 21, 590-602. doi: 10.1109/34.777370

Papadopoulos, A., Bird, N. R. A., Whitmore, A.P., and Mooney, S. J. (2009). Investigating the effects of organic and conventional management on soil aggregate stability using X-ray computed tomography. *Eur. J. Soil Sci*. 60, 360-368. doi: 10.1111/j.1365-2389.2009.01126.x

Paul, E. A., Harris, D., Collins, H. P., Schulthess, U., and Robertson, G. P. (1999). Evolution of CO_2 and soil carbon dynamics in biologically managed, row-crop agroecosystems. *Appl. Soil Ecol.* 11, 53-65. doi: 10.1016/S0929-1393(98)00130-9

Paul, E. A., Kravchenko, A., Grandy, S., and Morris, S. (2015). "Soil organic matter dynamics: controls and management for sustainable ecosystem functioning," in *The ecology of agricultural landscapes: long-term research on the path to sustainability*, eds. S. K. Hamilton, J. E. Doll, and G. P. Robertson, (New York, New York, USA: Oxford University Press), 104-134.

Pebesma, E. J. (2004). Multivariable geostatistics in S: the gstat package. *Comput. Geosci.* 30, 683-691. doi: 10.1016/j.cageo.2004.03.012

Peng, X., Horn, R., and Smucker, A. (2007). Pore shrinkage dependency of inorganic and organic soils on wetting and drying cycles. *Soil Sci. Soc. Am. J.* 71, 1095-1104. doi: 10.2136/sssaj2006.0156

Peth, S. (2010). "Applications of microtomography in soils and sediments," in *Developments in Soil Science, Vol. 34*, eds. B. Singh and M. Gräfe, (The Netherlands: Elsevier B. V.), 73-101.

Peth, S., Chenu, C., Leblond, N., Mordhorst, A., Garnier, P., Nunan, N., et al. (2014). Localization of soil organic matter in soil aggregates using synchrotron-base X-ray microtomography. *Soil Biol. Biochem.* 78, 189-194. doi: 10.1016/j.soilbio.2014.07.024

Peth, S., Horn, R., Beckmann, F., Donath, T., Fischer, J., and Smucker, A. J. M. (2008). Three-dimensional quantification of intra-aggregate pore-space features using synchrotron-radiation-based microtomography. *Soil Sci. Am. J*. 72, 897-907. doi: 10.2136/sssaj2007.0130

Rasse, D. P. and Smucker, A. J. M. (1998). Root recolonization of previous root channels in corn and alfalfa rotations. *Plant Soil* 204, 203-212. doi: 10.1023/A:1004343122448

Rawlins, B. G., Wragg, J., Reinhard, C., Atwood, R. C., Houston, A., Lark, R. M., et al. (2016). Three-dimensional soil organic matter distribution, accessibility and microbial respiration in macroaggregates using osmium staining and synchrotron X-ray computed tomography. *SOIL*. 2, 659-671. doi: 10.5194/soil-2-659-2016

Ruiz, S., Schymanski, S. J., and Or, D. (2017). Mechanics and energetics of soil penetration by earthworms and plant roots: higher rates cost more. *Vadose Zone J.* 16:8. doi: 10.2136/vzj2017.01.0021

SAS Inc. (2009). *SAS user's guide. Version 9.2*. Cary, NC: SAS Inst.

Senthilkumar, S., Basso, B., Kravchenko, A. N., and Robertson, G. P. (2009). Contemporary evidence of soil carbon loss in the U.S. corn belt. *Soil Sci. Soc. Am. J.* 73, 2078-2086. doi: 10.2136/sssaj2009.0044

Six, J., Conant, R. T., Paul, E. A., Paustian, K. (2002). Stabilization mechanisms of soil organic matter: implications for C-saturation of soils. *Plant Soil*. 241, 155-176. doi: 10.1023/A:1016125726789

Six, J., Elliott, E. T., and Paustian, K. (2000). Soil macroaggregate turnover and microaggregate formation: a mechanism for C sequestration under no-tillage agriculture. *Soil Biol. Biochem.* 32, 2099-2103. doi: 10.1016/S0038-0717(00)00179-6

Smucker, A. J. M., Park, E.-J., Dorner, J., and Horn, R. (2007). Soil micropore development and contributions to soluble carbon transport within macroaggregates. *Vadose Zone J.* 6, 282-290. doi: 10.2136/vzj2007.0031

Sørensen, L. H. (1974). Rate of decomposition of organic matter in soil as influenced by repeated air drying-rewetting and repeated additions of organic material. *Soil Biol. Biochem.* 6, 287-292. doi: 10.1016/0038-0717(74)90032-7

Syswerda, S. P., Corbin, A. T., Mokma, D. L., Kravchenko, A. N., and Robertson, G. P. (2011). Agricultural management and soil carbon storage in surface vs. deep layers. *Soil Sci. Soc. Am. J.* 75, 92-101. doi: 10.2136/sssaj2009.0414

Toosi, E. R., Kravchenko, A. N., Mao, J., Quigley, M. Y., and Rivers, M. L. (2017). Effects of management and pore characteristics on organic matter composition of macroaggregates: evidence from characterization of organic matter and imaging. *Eur. J. Soil Sci.* 68, 200-211. doi: 10.1111/ejss.12411

Wang, W., Kravchenko, A. N., Johnson, T., Srinivasan, S., Ananyeva, K. A., Smucker, A. J. M., et al. (2013). Intra-aggregate pore structures and *Escherichia coli* distribution by water flow within and movement out of soil macroaggregates. *Vadose Zone J.* 12:4. doi: 10.2136/vzj2013.01.0012

Wang, W., Kravchenko, A. N., Smucker, A. J. M., Liang, W., and Rivers, M. L. (2012). Intra-aggregate pore characteristics: X-ray computed microtomography analysis. *Soil Sci. Soc. Am. J.* 76, 1159-1171. doi: 10.2136/sssaj2011.0281

Wang, W., Kravchenko, A. N., Smucker, A. J. M., and Rivers, M. L. (2011). Comparison of image segmentation methods in simulated 2D and 3D microtomographic images of soil aggregates. *Geoderma*. 162, 231-241. doi: 10.1016/j.geoderma.2011.01.006

Young, I. M., and Crawford, J. W. (2004). Interactions and self-organization in the soil-microbe complex. *Science*. 304, 1634-1637. doi: 10.1126/science.1097394

Chapter 3: Influence of Pore Characteristics on the Fate and Distribution of Newly Added Carbon*

Abstract

Pores create a transportation network within a soil matrix, which controls the flow of air, water, nutrients, and movement of microorganisms.The flow of air, water, and movement of microbes, in turn, control soil carbon dynamics. Computed microtomography (μCT) allows for the visualization of pore structure at micron scale, but quantitative information on contribution of pores to the fate and protection of soil carbon, essential for modeling, is still lacking. I used the natural difference between carbon isotopes of C3 and C4 plants to determine how the presence of pores of different sizes affects spatial distribution patterns of newly added carbon immediately after plant termination and then after one-month incubation. I considered two contrasting soil structure scenarios: soil with the structure kept intact and soil for which the structure was destroyed via sieving. For the experiment, soil was collected from 0-15 cm depth at a 20-year continuous maize (*Zea mays* L., C4 plant) experiment into which cereal rye (*Secale cereale* L., C3 plant) was planted. Intact soil fragments (5-6 mm) were procured after 3 months rye growth in a greenhouse. Pore characteristics of the fragments were determined through μCT imaging. Each fragment was sectioned and total carbon, total nitrogen, $\delta^{13}C$, and $\delta^{15}N$ were measured. The results indicate that, prior to incubation, greater presence of 40-90 μm pores was associated with higher levels of C3 carbon, pointing to the positive role of these pores in transport of new C inputs. Nevertheless, after incubation, the association became negative, indicating greater losses of newly added C in such pores. These trends were statistically significant in destroyed-structure soil and numerical in intact-structure soil. In soils of intact-structures, after incubation, higher

* Originally published as: Quigley, M. Y., Negassa, W. C., Guber, A. K., Rivers, M. L., and Kravchenko, A. N. (2018a). Influence of pore characteristics on the fate and distribution of newly added carbon. Front. Environ. Sci. 6:51. doi: 10.3389/fenvs.2018.00051

levels of total carbon were associated with greater abundance of 6.5-15 and 15-40 μm pores, indicating a lower carbon loss associated with these pores. The results indicate that, in the studied soil, pores of 40-90 μm size range are associated with the fast influx of new C followed by its quick decomposition, while pores <40 μm tend to be associated with C protection.

3.1 Introduction

Soils contain twice as much carbon as the atmosphere and have the potential to store even more, especially in agricultural soils (Lal, 1999; Swift, 2001; Dungait et al, 2012; Kell, 2012). Soil carbon content is an important component of soil fertility as it drives several defining criteria of soil quality, including cation exchange capacity, soil aggregation, and water holding capacity (Dou et al, 2014). This makes utilization of agricultural management practices that increase and/or conserve soil carbon vitally important to sustainability (Grandy and Robertson, 2007).

One such practice is the utilization of cover crops, a crop that is planted between main crops for the purpose of increasing water infiltration, stabilizing the soil surface, preventing erosion, decreasing weeds, and increasing soil fertility. The activity of cover crop roots may benefit the physical protection of new carbon inputs. Physical protection of soil carbon occurs when physical disconnections separate decomposers from carbon sources (Dungait et al, 2012). This disconnect is not limited to access of decomposers and their enzymes to soil carbon, but also includes availability of other components necessary for decomposition, such as oxygen and water (Schmidt et al, 2011, Keiluweit et al, 2017).

Long-term cover crop based management increases soil aggregation (Tiemann and Grandy, 2015), and soil carbon is known to be better protected within soil aggregates (Six et al, 2000; Grandy and Robertson, 2007). Yet, mechanistically, it is the soil pore-space that controls not only movement of soil microbes, but also air and water fluxes and transport of nutrients

necessary for decomposition (DeGryze et al, 2006; Negassa et al, 2015; Young and Crawford, 2004;). Pores within the soil matrix serve as planes of breakage along which the aggregates form; and their sizes and spatial positions not just define soil aggregate-size distributions but determine micro-environmental conditions driving physical carbon protection within the aggregates (Young et al, 2001; Ekschmitt et al, 2005, 2008; Kravchenko and Guber, 2017; Rabot et al, 2018).

Pores of different sizes have different origins, connectivities, accessibilities, and hydraulic properties (Park and Smucker, 2005; Peth et al, 2008). As pore size decreases, higher suction is required to drain the pore. This means that while pores of >10 μm sizes may only require gravity to fully or partially drain, under normal soil moisture regimes, pores <10 μm remain water filled (Marshall et al, 1996).

Plant root diameters are typically > 40 μm and, therefore, roots can only access and/or create pores exceeding that size (Wiersum, 1957; Cannell, 1977). Root pores are formed by compressing the soil matrix radially as the root pushes through the soil and then their walls are stabilized through mucilage and often refilled by roots of the next generation crops (Gray and Lissmann, 1938; Greacen and Oh 1972; Greacen and Sands, 1980; Rasse and Smucker, 1998; Czarnes et al, 2000; Ruiz et al, 2017). Fungal hyphae are known to create pores of 20-30 μm size by pushing aside silt particles and exuding binding agents to buttress the pores (Dorioz et al, 1993; Bearden, 2001, and Emerson and McGarry, 2003). However, fungi are typically excluded from pores less than 10 μm (Six et al, 2006).

Roots provide carbon into the soil system in two ways: as a source of biomass when they die and as a source of easily decomposable carbon via root exudates. Roots tend to consist of more difficult to decompose molecules (such as lignin and tannin), which, in addition to being

harder to decompose, are easier to adsorb to mineral surfaces, sequestering them (Rasse et al, 2005; Jackson et al, 2017). Root exudates, on the other hand, tend to be small, soluble, and easily decomposable materials, such as organic acids, carbohydrates, and amino acids (Dungait et al, 2012) or water insoluble materials, such as mucilage (Brimecombe et al, 2001). The easily decomposable materials stimulate microbial growth, which increases decomposition of native soil organic matter (SOM) (Kuzyakov and Blagodatskaya, 2015). There is some indication that microorganisms can also stimulate root growth and exudation (Neumann et al, 2014).

Agricultural management influences pore size distributions. Wang et al (2012) showed that soil under long-term conventional tillage had more pores of 37.5-97.5 μm, while early succession agricultural management had greater proportions of >97.5 μm and <15 μm pores. Kravchenko et al (2014) found that organic management with cover crops had fewer 32-58 μm pores and a greater amount of >188 μm pores than conventional tillage management. In that study, the difference in pores from organic cover crop management were attributed to increased root activity, while conventional management promoted 32-58 μm pores created through wetting/drying cycles. Ananyeva et al (2013) found that higher carbon concentrations were found in sections of soil aggregates with an increased presence of 15-37.5 μm pores. The presence of 37.5-97.5 μm pores was associated with aggregate sections containing less carbon.

Stable carbon isotopic signatures can be used to track carbon within a system. Plants preferentially incorporate ^{12}C into their tissues, but the extent of ^{12}C incorporation depends on which metabolic pathway the plant utilizes. Plants that utilize the C3 photosynthetic pathway incorporate more ^{12}C than plants utilizing the C4 photosynthetic pathway. Therefore, it is possible to differentiate between carbon derived from C3 and C4 plants isotopically due to this

natural isotopic difference. Stable carbon isotopes are reported in δ notation as per mil (‰) differences between the $^{13}C/^{12}C$ ratio of the sample compared to a standard:

$$\delta^{13}C = \left[\left(R_{Sample} - R_{Standard}\right)/R_{Standard}\right] * 1000 \qquad (3.1)$$

SOM and particulate organic matter (POM) $\delta^{13}C$ values reflect the $\delta^{13}C$ values of the original plant material source. Therefore, the measured $\delta^{13}C$ of a soil reflects the C3/C4 history of the soil (Ehleringer et al, 2000; Bowling et al, 2008). Experiments that utilize C3/C4 transitions have been used extensively for determination of soil C turnover rates (Bernoux et al, 1998; Derrien and Amelung, 2011) and for analyses of the fresh carbon input distribution within soil aggregates (Smucker et al, 2007; Urbanek et al, 2011).

The goal of this study was to determine how the abundance of different pore sizes relates to the preservation or loss of newly added carbon. I utilized a C3/C4 natural abundance greenhouse experiment with soil collected from a long term C4 cropping system and planted a C3 plant, cereal rye (*Secale cereale* L.), which is one of the most commonly used cover crops in the US Midwest. The first objective of this study was to examine the relationships between newly added carbon and soil pores of different sizes. I used $\delta^{13}C$ to "track" newly added C3 carbon and determined pore characteristics via computed microtomography (μCT). The second objective was to examine the relationships between the decomposition of carbon and soil pores sizes after incubating the studied soil.

3.2 Materials and methods

3.2.1 Greenhouse experimental setup

Soil for the greenhouse study was obtained in the summer of 2013 from the Living Field Lab (LFL) experiment established in 1993 at W. K. Kellogg Biological Site, Hickory Corners, MI (42°24´N, 85°24´W). The soil is a fine-loamy, mixed mesic Typic Hapludalf (Oshtemo and Kalamazoo series) developed on glacial outwash. Soil was collected from the LFL's conventional

management continuous maize (*Zea mays* L) treatment. This treatment has been planted with maize, a C4 plant, and no other crop since 1993. Detailed management and site information is available at http://lter.kbs.msu.edu/Data/LTER and https://lter.kbs.msu.edu/research/long-term-experiments/living-field-lab/.

Six soil blocks of 40 cm x 26 cm x 15 cm size were collected at 0-15 cm depth. Three of the blocks were placed directly into plastic bins with as little disturbance as possible to retain intact soil structure, and are referred to hereafter as intact-structure treatment. However, I was concerned that, due to the tendency of roots to follow existing pore structure, the root effects generated during out experiment might be masked by the legacy of the existing pores. Therefore, soil from the other three blocks was crushed and sieved through a 1 mm sieve to destroy the existing soil structure, and is referred to hereafter as destroyed-structure treatment. One of the intact soil bins was left unplanted as a control, and the remaining bins had cereal rye (*Secale cereale* L.) hand planted at a depth of 3 cm and a plant density of ~23.5 plants per m^2. Rye was grown in the greenhouse for 3 months and watered daily to allow for the development of a good stand of rye biomass; the control bin was watered along with the rest. Soil bulk density was taken in each tub using a 7.5 cm brass ring.

After 3 months of rye growth, approximately an eighth of the soil was taken from a random side in each bin was removed using a trowel and allowed to air dry. The soil was allowed to break along natural planes of weakness through manual crushing. Intact soil fragments of 5 mm size were hand selected (n=5, 11, and 11 for control, destroyed-structure and intact-structure treatments, respectively) for analyses and incubation. Soil fragments were selected based on proximity to rye roots to best determine the effect of rye root growth on the aggregates. Two rye roots per bin were hand collected for isotope analysis from intact plants

from the soil used for soil fragment selection. Selected intact soil fragments were mounted on top of plastic stands using rubber cement for subsequent scanning and incubation.

The experiment and data collection are briefly summarized here and then described in detail in the sections below. First, all intact soil fragments were air-dried and subjected to μCT scanning (Section 2.2). Then half of the intact soil fragments were physically cut into ~0.5-1 mm^3 sections, with the physical positions of the procured sections matching their virtual positions in 3D μCT images (Section 2.4). In each cut section, I measured $\delta^{13}C$, $\delta^{15}N$, total C (%C), and total N (%N). These intact soil fragments are hereafter referred to as Pre for preincubation soil. The remaining intact fragments were subjected to a 28 day incubation during which respired CO_2 was measured and collected for $\delta^{13}C$ analysis (Section 2.3). After incubation, the intact soil fragments were re-scanned and also cut into sections, then $\delta^{13}C$, $\delta^{15}N$, total C (%C), and total N (%N) measurements were taken. These intact soil fragments are hereafter referred to as Post for post incubation soil.

3.2.2 μCT image collection and analysis

The μCT images for both Pre and Post intact soil fragments were obtained on the bending magnet beam line, station 13-BM-D of the GeoSoilEnvironCARS (GSECARS) at the Advanced Photon Source (APS), Argonne National Laboratory (ANL), IL. Images were collected with the Si (111) double crystal monochromator tuned to 28 keV incident energy, the distance from sample to source was approximately 55 m, and the X-ray dose is estimated to be 1 kGy. Two-dimensional projections were taken at 0.25° rotation angle steps with a one second exposure and combined into a three-dimensional image consisting of 1040 slices with 1392 by 1392 pixels per slice for Pre scans, resulting in a voxel size of 6.5 μm, while Post scans had 1100 slices with 1920 by 1920 pixels, resulting in a voxel size of 6.2 μm. The data were pre-processed by

correcting for dark current and flat field and reconstructed using the GridRec fast Fourier transform reconstruction algorithm (Rivers, 2012).

Pore/solid segmentation of the images was conducted using the indicator kriging method in 3DMA-Rock software (Oh and Lindquist, 1999; Wang et al, 2011). Based on the analysis of the segmented data I obtained the total porosity of the intact soil fragments, the total image porosity (pores > 6.5 μm in diameter), and the size distribution of > 6.5 μm diameter pores. Total porosity of each intact fragment was calculated using the dry weight of the fragment and its volume as determined from the μCT images. The total image porosity was calculated as the percent of pore voxels within the total intact soil fragment's voxels. Size distribution of image identified pores was determined using the burn number distribution approach in 3DMA-Rock software (Lindquist et al, 2000, Ananyeva et al, 2013). Briefly, the burn number represents the shortest distance from the pore medial axis to the pore wall. For clarity, burn numbers have been converted into pore diameters. I specifically focused the data analyses on the pores of the following four diameter size ranges: 6.5-15 μm, 15-40 μm, 40-95 μm, and >95 μm. These pore sizes were chosen to match pore sizes previously studied in macro-aggregates and which demonstrated strong associations with carbon (Wang et al, 2012, 2013; Ananyeva et al, 2013; Kravchenko et al, 2014, 2015).

3.2.3 Incubation experimental set up

The soil fragments used in incubation (Post soil) consisted of two intact soil fragments from control treatment, 6 intact soil fragments from destroyed-structure treatment, and 5 intact soil fragments from intact-structure treatment. Water was added to the fragments to achieve 60% of water filled pore space. The fragments were then placed into 10 ml vacutainers (BD Franklin Lakes NJ, USA) with 1 mL of de-ionized water added to the bottom to maintain high humidity. Incubations were carried out for 28 days at 22.4±0.1°C. CO_2 emission measurements were taken

on days 1, 2.5, 4, 8, 13, 19, and 28. Gas samples for isotope analysis were collected on days 13, 19, and 28 only. The CO_2 emission measurements were conducted using an LI-820 CO_2 infrared gas analyzer (Lincoln, Nebraska, USA). After each sampling, the remaining gas in the headspace was flushed with CO_2-free air. Flushing was found to dry out the soil, so de-ionized water (~10-20 μL) was added directly to the fragments to maintain the moisture level after day 4. One intact-structure fragment and four destroyed-structure fragments broke during the incubation and, while chemical analyses were possible, the broken fragments could not be re-scanned.

3.2.4 Soil fragment cutting and chemical analyses

To assess patterns of $\delta^{13}C$, $\delta^{15}N$, total C and total N and their relationship to pore characteristics, each intact soil fragment was cut into 5 to 13 sections. This was done to account for variation between the soil fragments. The number of sections into which the fragment was cut depended on its size and shape. To facilitate cutting, de-ionized water was added to fill 30% of the pore volume immediately prior to cutting. Cutting was performed with a #11 scalpel and a 24x magnifying glass. The relative position of each cut was recorded. Then, the relative positions were used to virtually cut the 3D μCT image to match the physical cutting. Virtual cutting yielded regions in the three-dimensional tomographic images that corresponded to the physically cut sections. Image based porosity and pore size distributions were determined in each virtual section of each soil fragment.

Prior to chemical analyses, visibly identifiable particulate organic matter (POM) was separated from physically cut sections and analyzed separately. The identifiable POM consisted primarily of plant root remains, but occasional plant residue fragments of unknown origin were also observed. Soil from cut sections, POM from cut sections, and separately collected rye roots were analyzed for $\delta^{13}C$, $\delta^{15}N$, total C, and total N at the Stable Isotope Facility at the University of California Davis. Fragment sections were analyzed using an Elementar Vario EL Cube or

Micro Cube elemental analyzer (Elementar Analysensysteme GmbH, Hanau, Germany) interfaced to a PDZ Europa 20-20 isotope ratio mass spectrometer (Sercon Ltd., Cheshire, UK). POM material and rye roots were analyzed using a PDZ Europa ANCA-GSL elemental analyzer interfaced to a PDZ Europa 20-20 isotope ratio mass spectrometer (Sercon Ltd., Cheshire, UK).

Gas samples were analyzed for $\delta^{13}C$ at the Stable Isotope Facility at the University of California Davis. Gas samples were analyzed using a ThermoScientific GasBench system interfaced to a ThermoScientific Delta V Plus isotope ratio mass spectrometer (ThermoScientific, Bremen, Germany).

The carbon isotopes are reported relative to Vienna PeeDee Belemnite (VPDB) with a 0.1‰ standard deviation for solid samples and 0.02‰ standard deviation for gas samples. The nitrogen isotopes are reported relative to AIR and had a standard deviation of 0.1‰.

3.2.5 Grayscale Gradients

Grayscale gradients were used to identify spatial patterns in the soil matrix adjacent to root pores of 40-90 μm size. The grayscale value of an individual voxel from a μCT image is a function of the atomic number and relative density of the material within the voxel. Higher atomic number elements, such as iron, have higher grayscale values on images, while lower atomic number elements, such as carbon and nitrogen, have lower grayscale values on images. Therefore, the value of each grayscale voxel reflects elements present within it. Quigley et al (*2018*) showed that spatial gradients in grayscale values adjacent to the pores formed through plant root activities matched well with SOM gradients determined by the osmium staining method (Peth et al, 2014; Rawlins et al, 2016). Thus, in this study I will use the grayscale gradients adjacent to the root pores as indicators of SOM distributions.

Three root pores of 40-90 μm size range were identified on Pre and Post images from 4 soil fragments. The root pores were then 3D dilated by one voxel to exclude any voxels

containing both pore and solid material. Voxels were averaged in ~13 μm layers around the pore to a distance of 194 μm and the grayscale gradients were obtained by averaging the grayscale values of each layer (Figure 3.1). Averages excluded 0 values that represented the background and 255 values to prevent skewing the gradients by the occasional presence of inclusions of high atomic number elements, e.g., Fe. For direct comparison of the images, the values were normalized such that the lowest average grayscale value within the gradient was 0 and the highest average grayscale value within the gradient was 1.

Figure 3.1: Example of a selected root used for grayscale gradient analyses. The color overlay indicates the extent of the grayscale gradient with the colors indicating each individual 13 μm layer.

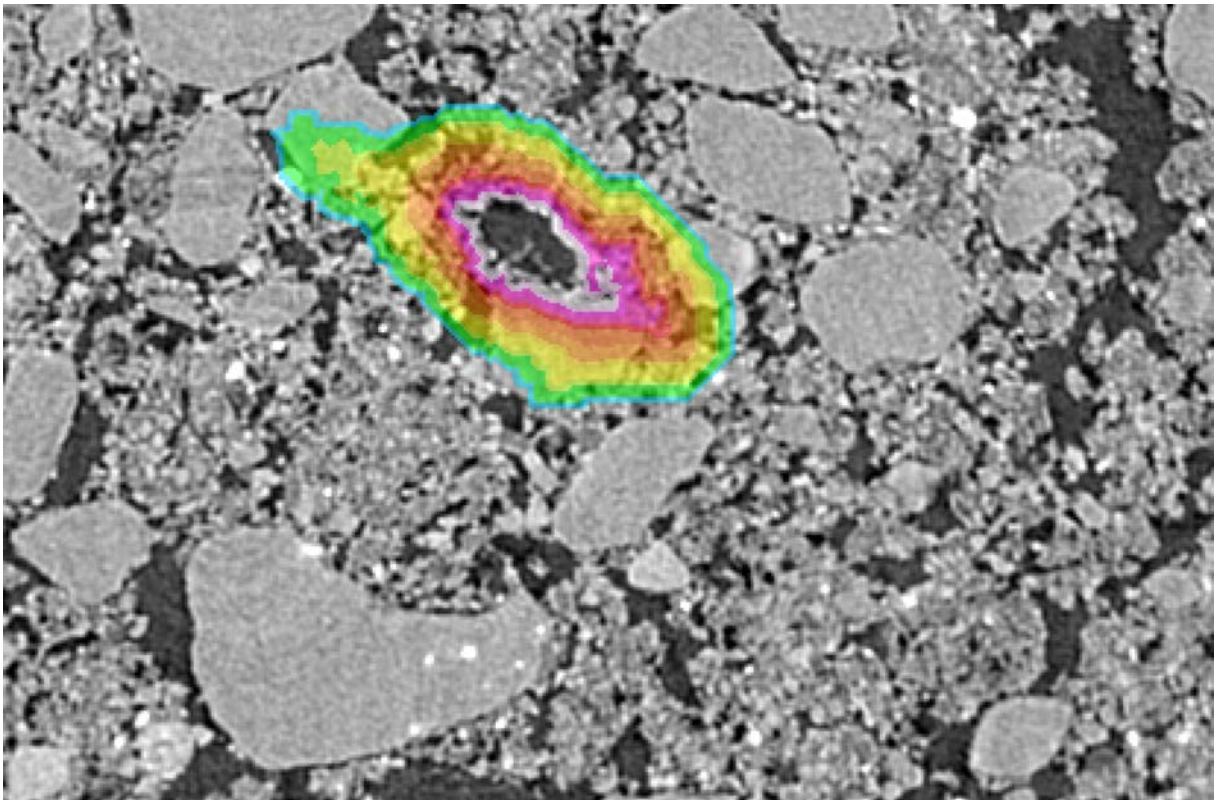

3.2.6 Statistical Analysis

Comparisons between intact- and destroyed-structure treatments as well as between Pre and Post in terms of pore characteristics and $\delta^{13}C$, $\delta^{15}N$, total C, and total N were conducted using the mixed model approach implemented in the PROC MIXED procedure of SAS Version

9.4 (SAS, 2009). The statistical model for the analyses consisted of the fixed effects of treatment, Pre and Post, and their interaction; and a random effect of soil fragments nested within treatment and Pre and Post. The normality was visually assessed using normal probability plots and stem-and-leaf plots, while equal variances was assessed using Levene's test. Where the equal variance assumption was violated, analysis with unequal variances was conducted (Milliken and Johnson, 2009).

For analysis of $\delta^{13}CO_2$ and CO_2 data obtained during soil fragment incubations, the statistical model consisted of the fixed effects of treatment, time, and their interaction. Time was treated as a repeatedly measured fixed factor using the REPEATED statement of PROC MIXED. Comparisons between the $\delta^{13}CO_2$ and the $\delta^{13}C$ of the fragments prior to incubation were conducted by defining the $\delta^{13}C$ of the soil in each treatment as a control and analyzed using Dunnett's comparison-with-control test. The significant differences at the 0.05 level were reported, while trends are reported at the 0.1 level.

Regression analyses between pore characteristics and $\delta^{13}C$ and total C were conducted using the PROC REG procedure in SAS Version 9.4 (SAS, 2009). The significant slopes at the 0.05 level were reported.

To investigate the correlation between the pore sizes (6.5-15, 15-40, 40-90 and >90 μm) and chemical measures ($\delta^{13}C$, total C, and total N), canonical correlation analysis was conducted using the cancor function in R (R Core Team, 2013). Canonical correlation compares how one set of variables is correlated to another set of variables in multidimensional space. The correlations are described through axes, which can be represented as orthogonal planes of maximum correlation, known as correlation axes. Each correlation axis is defined by canonical variates. Canonical variates are latent variables, which are not observed, but derived from a

combination of the observed variables. Collinearity within the observed variables was checked through the calculation of the determinant prior to canonical correlation analysis. As canonical correlations requires a larger data set, only the Pre data set was used for canonical correlations due to the small sample size of the Post data set.

3.3 Results

3.3.1 Soil and plant characteristics

Soil bulk density was lower in the treatments with rye as compared to control treatment (Table 3.1). The lower bulk density was the result of root growth and carbon addition. The average $\delta^{13}C$ values of particulate organic matter (POM), that is, the visible root remains and unidentifiable plant fragments isolated from intact soil fragments during their cutting, showed that the control treatment had significantly more C4 POM than the destroyed-structure treatment and numerically more C4 POM than the intact-structure treatment (Table 3.1). The destroyed-structure and intact-structure treatments were significantly different from each other at α=0.1, but not α=0.05. The $\delta^{13}C$ of rye roots grown in destroyed-structure soil were depleted by ~1.5‰ more than rye roots grown in intact-structure soil, while the $\delta^{15}N$ of rye roots in destroyed-structure was depleted by ~3.3‰ as compared to intact (Table 3.1).

Table 3.1: Means of soil bulk density (n=2) and characteristics of rye roots (n=4) from the studied treatments. Standard errors are shown in parentheses. Letters indicate significant differences among treatments at α=0.1 and bold letters indicate differences at α=0.05.

Treatment	Bulk Density, g/cm^3	$\delta^{13}C$ roots	$\delta^{15}N$ roots	C:N roots	$\delta^{13}C$ POM
Control	1.40(0.1)**a**	NA	NA	NA	-18.4(2.3)**a**
Intact	1.13(0.1)**b**	-28.6(0.3)b	2.3(0.4)**b**	18.6(1.5)b	-22.5(1.3)**b**
Destroyed	1.16(0.1)**b**	-30.1(0.4)a	-1.0(0.3)**a**	12.1(1.8)a	-26.0(1.8)**ab**

Prior to incubation, intact-structure and destroyed-structure soil had significantly higher total C than the control soil (Table 3.2). However, after incubation, this significance disappeared.

The C:N ratio was significantly lower for control soil fragments than for the fragments from the intact-structure treatment both in Pre and Post. The $\delta^{13}C$ values in destroyed-structure soil significantly increased, indicating losses in C3 carbon during incubation. The numerical trend in $\delta^{15}N$ of Destroyed>Intact>Control observed in the Pre increased and became statistically significant post-incubation. The total N was not affected by either treatment or incubation.

Table 3.2: Means of soil carbon and nitrogen characteristics for the three studied treatments Pre and Post. Standard errors are shown in parentheses. Means and standard errors in each treatment are calculated based on 2-6 aggregates with 1-13 sections per aggregate. Letters indicate significant differences among treatments within Pre and Post groups at α=0.05. Stars indicate the cases where there was a statistically significant difference between Pre and Post results within each treatment at α=0.05. Total C and total N are expressed as %C and %N.

Time	Treatment	Total C	$\delta^{13}C$	Total N	$\delta^{15}N$	C:N ratio
Pre	Intact	0.87(0.03)a	-21.4(0.2)	0.10(0.01)	4.0(0.2)	9.1(0.4)a
	Destroyed	0.87(0.05)a	-22.0(0.2)*	0.12(0.01)	4.2(0.2)	8.0(0.4)ab
	Control	0.74(0.04)b	-21.5(0.2)	0.10(0.01)	3.6(0.3)	7.7(0.6)b
Post	Intact	0.86(0.04)	-21.4(0.2)	0.10(0.01)	4.3(0.2)a	8.9(0.4)a
	Destroyed	0.80(0.03)	-21.2(0.2)	0.10(0.01)	4.8(0.2)b	8.3(0.4)ab
	Control	0.77(0.07)	-21.3(0.2)	0.11(0.02)	3.2(0.3)c	7.1(0.7)b

3.3.2 Pore characteristics

Total porosity of individual soil fragments ranged from 10-30% for all three treatments. The average image porosity, that is presence of pores >6 μm in diameter, was around 12% in fragments from control and 20% in fragments from rye treatments (Figure 3.2). After incubation, pore abundances tended to numerically increase in soils from all three treatments (Figure 3.3), however, the increases were only statistically significant for the pores from the 6.5-15 μm size group (Figure 3.2). Pores with diameters >90 μm tended to be the least abundant in the control treatment, followed by the intact-structure and destroyed-structure soils. This tendency was observed in the soils prior to incubation and remained after incubation. Differences between treatments were only observed for the >90 μm pores.

Figure 3.2: Relative abundances of 6.5-15, 15-40, 40-95, >95 µm pores, and porosity in the soil fragments of the three studied treatments before and after incubation. Relative pore abundance refers to the percent of medial axes per total soil volume as determined from 3DMA-Rock software. Bars represent standard errors. Letters indicate significant differences between Treatments, across Pre and Post (α= 0.05). Stars indicated significant differences between Pre and Post within each treatment at α=0.05.

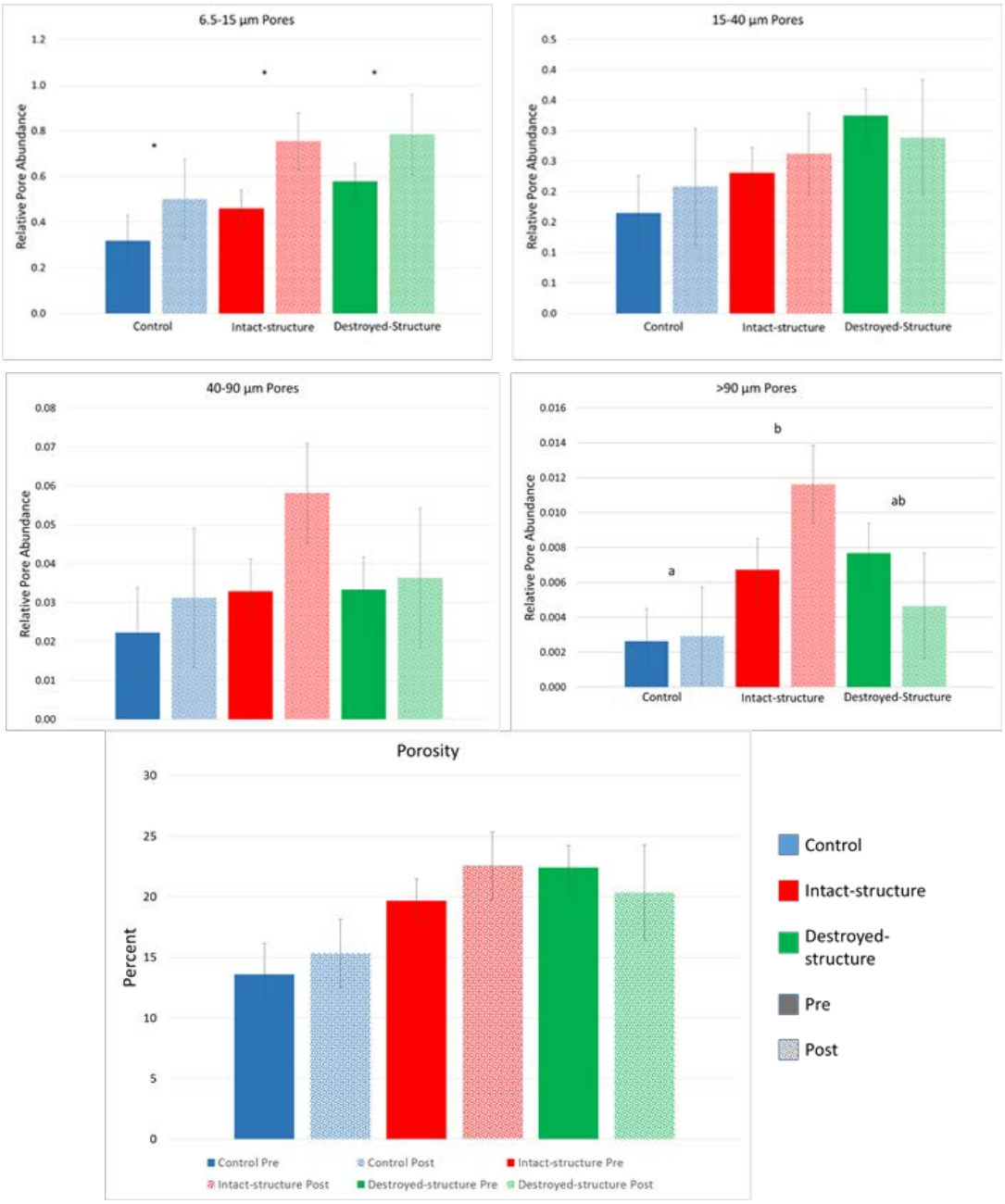

Figure 3.3: Representative slices of the same soil fragment for Pre-Intact **(A)**, Post-Intact **(B)**, Pre-Destroyed **(C)**, and Post-Destroyed **(D)**. Red arrows highlight an area where porosity visibly increased during incubation. Each soil fragment is approximately 5 mm across.

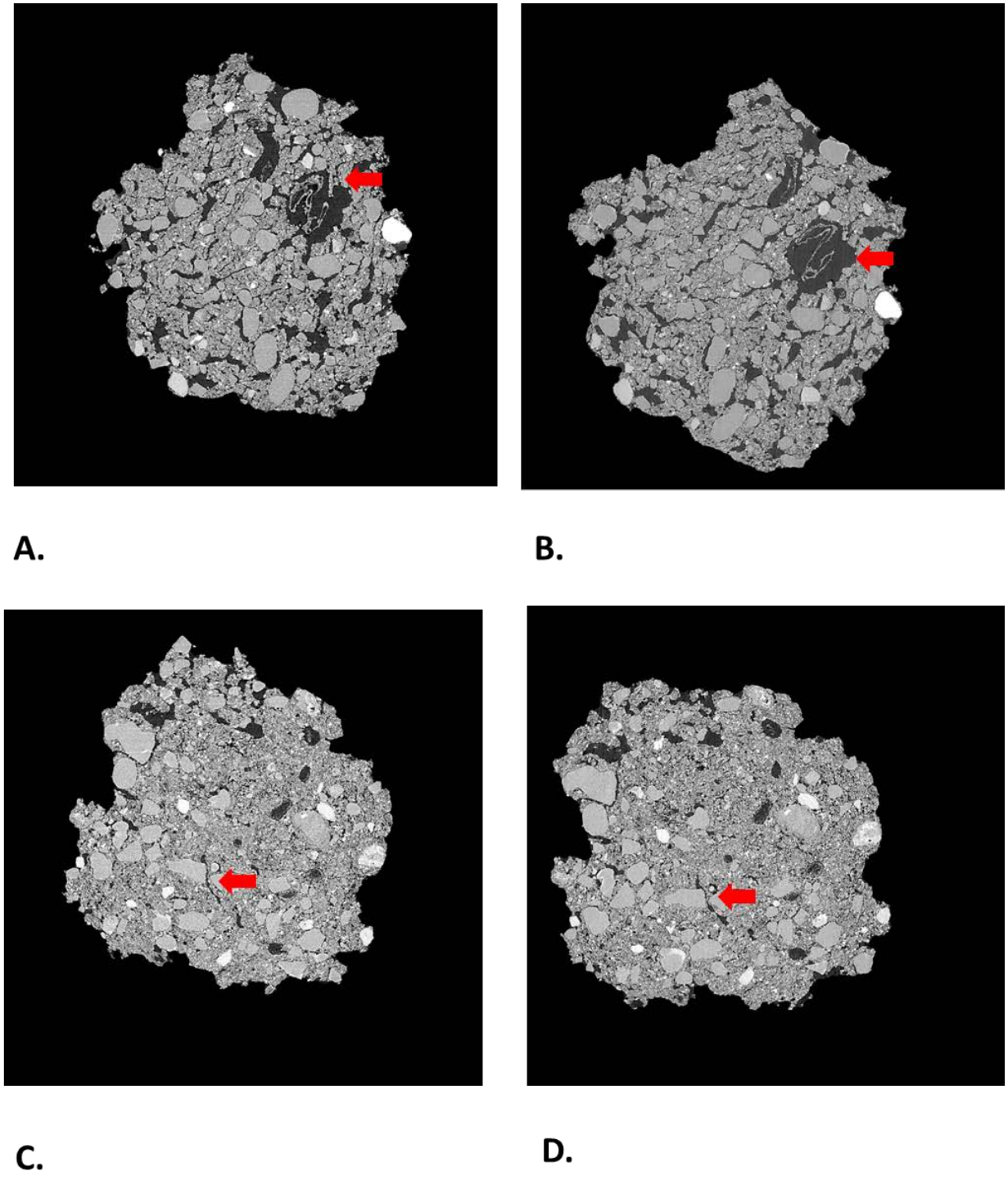

3.3.3 Associations between pores and chemical characteristics

In soil from the control treatment there were no significant correlations observed between the two studied carbon characteristics (total C and $\delta^{13}C$) and pore abundances of any of the studied sizes, either before or after incubation. There was also no correlation observed between the two nitrogen characteristics (total N and $\delta^{15}N$) and pore abundances (results not shown).

An interesting pattern emerged in the correlation of $\delta^{13}C$ and abundance of pores of different sizes in the Pre destroyed-structure treatment. Correlation with 6.5-15 μm pores was positive, no correlation was observed with 15-40 μm pores, and correlation was negative with 40-90 μm pores (Figure 3.4, Table 3.3). This indicates that in the soil from destroyed-structure

Table 3.3: Correlation coefficients for Pre and Post soil for total C and $\delta^{13}C$ with relative abundances of 6.5-15 μm, 15-40 μm, 40-90 μm, and >90 μm pores for intact and destroyed-structure treatments. Positive correlation with $\delta^{13}C$ indicate more new carbon was associated with a higher presence of specified pore. Stars indicate significant correlation at α=0.05.

Structure	Pore size, μm	Incubation	Total C	$\delta^{13}C$
Destroyed	6.5-15	Pre	-0.25	0.33*
		Post	-0.75*	0.76*
	15-40	Pre	-0.28	0.17
		Post	-0.78*	0.79*
	40-90	Pre	0.05	-0.39*
		Post	-0.47*	0.40*
	>90	Pre	0.25	-0.07
		Post	0.1	-0.19
Intact	6.5-15	Pre	0.19	0.02
		Post	0.50*	0.52*
	15-40	Pre	0.18	0.01
		Post	0.37*	0.45*
	40-90	Pre	0.26	-0.18
		Post	0.11	0.17
	>90	Pre	0.12	-0.14
		Post	0.09	-0.08

treatment prior to its incubation, the sections with greater abundance of 6.5-15 μm pores tended to have less C3 carbon while the sections with greater abundance of 40-90 μm tended to have

Figure 3.4: Correlations between total C (%C) and relative abundances of 40-95 µm pores **(A)** and between $\delta^{13}C$ and 40-90 µm pores **(B)** for intact-structure treatment and destroyed-structure treatment for both Pre and Post. Relative pore abundances refer to the percent of medial axes per total soil volume as determined from 3DMA-Rock software. Gray area indicates 95% confidence interval. Correlation coefficients are shown in Table 3.3.

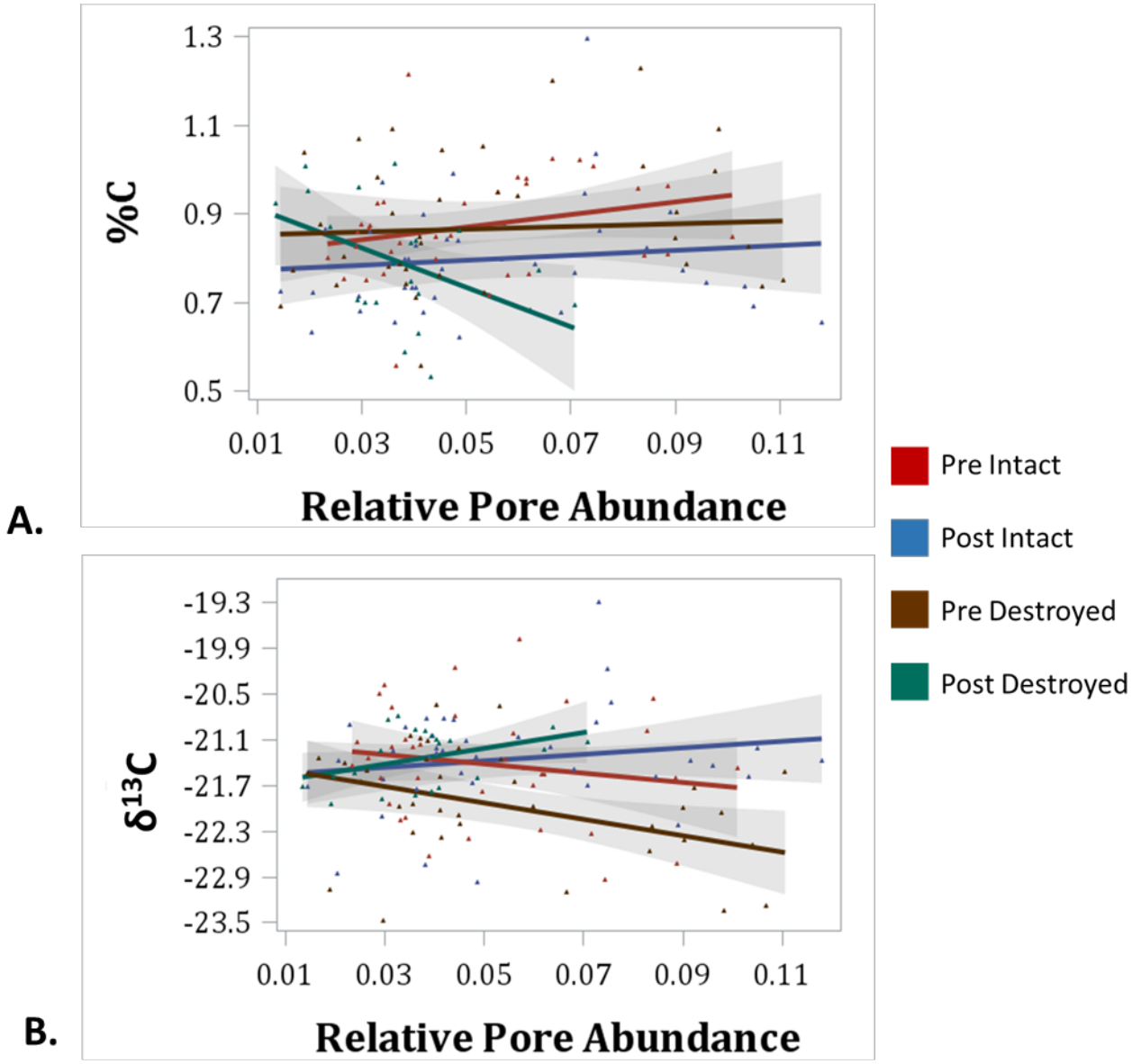

more C3 carbon. Post $\delta^{13}C$ was positively correlated with 6.5-15, 15-40, and 40-90 µm pores, indicating that the sections with greater abundance of pores of all three sizes tended to have less C3 carbon after incubation. The trend of negative correlations Pre and positive correlations Post between $\delta^{13}C$ and 40-90 µm pores was statistically significant in destroyed-structure soil and

numeric in intact-structure soil. In the soil from the intact-structure treatment, $\delta^{13}C$ was positively correlated to 6.5-15 and 15-40 μm pores Post.

There was no significant correlations between total C and any pore sizes in either intact-structure or destroyed-structure soils Pre (Table 3.3). In Post intact-structure soil total C was positively correlated with 6.5-15 μm pores and 15-40 μm pores. However, in destroyed-structure soil total C was negatively correlated with these pores.

3.3.4 Incubation CO_2

The cumulative amount of CO_2 emitted from the soil fragments during the 28-day incubation was the highest in the soil from the intact-structure treatment, followed by the destroyed-structure and control treatments (Figure 3.5a). The $\delta^{13}C$ values of the CO_2 emitted during the incubation indicate that microorganisms preferentially used more C3 carbon in the destroyed-structure and intact-structure treatments than in the control, but the difference was only statistically significant on day 28 (Figure 3.5b).

The $\delta^{13}C$ values of the CO_2 emitted during the incubation indicate that during the last three measurements (days 13, 19, and 28), the CO_2 gas became more depleted for all three treatments.

Figure 3.5: **(A)** Cumulative CO_2 and **(B)** average isotopic signature of CO_2 respired during 28 day incubation experiment. Bars represent standard errors. Bold lines indicate the mean $\delta^{13}C$ values of the soil fragment sections prior to incubation for each treatment while boxes indicate the standard errors (-22.0±0.1‰, -21.4±0.1‰, and -21.6±0.1‰ for destroyed-structure, intact-structure, and control, respectively). Letters indicate significant differences among treatments at α=0.05. Stars indicate significant differences between the $\delta^{13}C$ of the emitted CO_2 and the soil sections Pre at α=0.05.

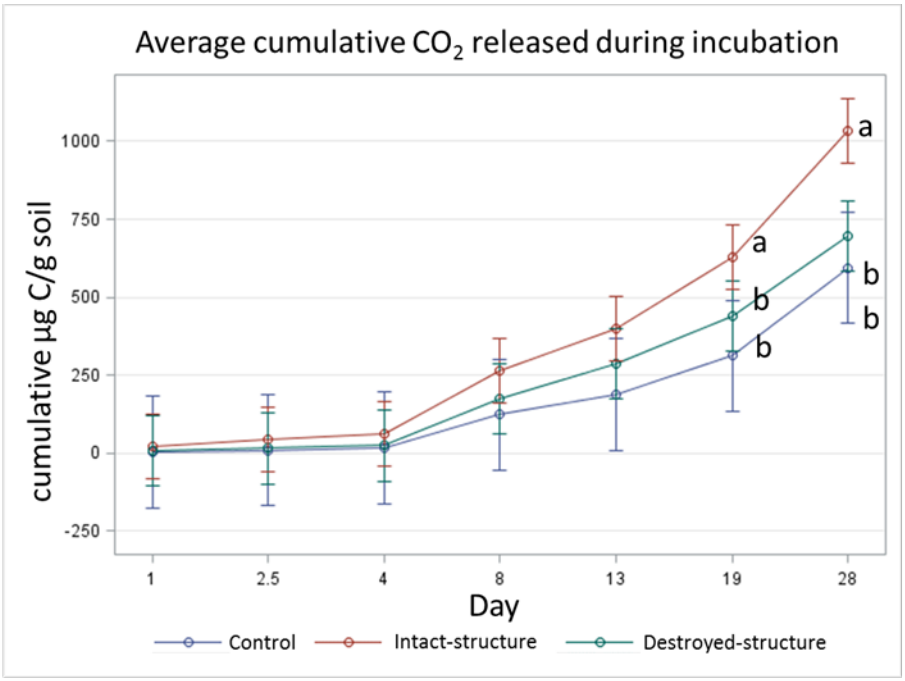

A.

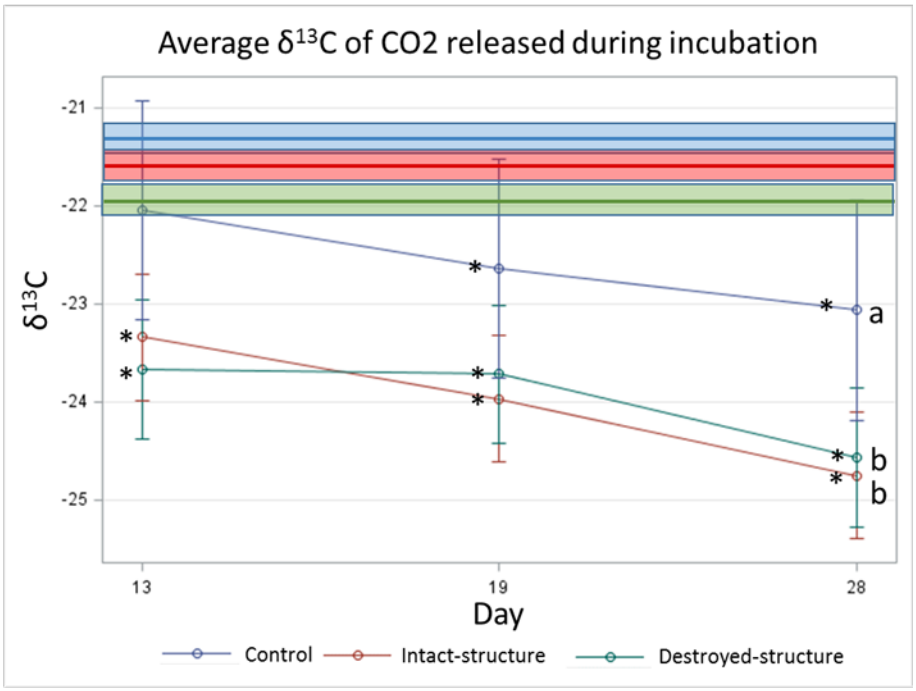

B.

3.3.5 Grayscale Gradients

Both intact- and destroyed-structure Pre and Post soils had similar general patterns of very high grayscale values directly adjacent to the pores, followed by a sudden decrease (Figure 3.6). Then, the grayscale values slowly increased until reaching a plateau at 120-140 µm distances from the pore. The plateau grayscale value roughly corresponded to the background grayscale value. However, the differences in Pre and Post grayscale gradients had opposite signs in the two treatments. In destroyed-structure soil, Pre soils had lower grayscale values than Post at the same distance, while Pre intact-structure soil had higher grayscale values than the Post soil.

Figure 3.6: Normalized grayscale values from µCT images of soil fragments as a function of distance from 40-90 µm pores for intact-structure and destroyed-structure at Pre and Post. Error bars indicate standard error. Note that values of the normalized grayscale reflect a combination of contributors, including atomic numbers of the elements and density of the material located within an image voxel. Specifically, lower normalized values here correspond to lower atomic number elements and lower densities, while higher values correspond to higher atomic number elements and higher densities. As such, lower values roughly represent more carbon in the soil matrix, while higher values represent less carbon in the soil matrix and/or denser soil matrix.

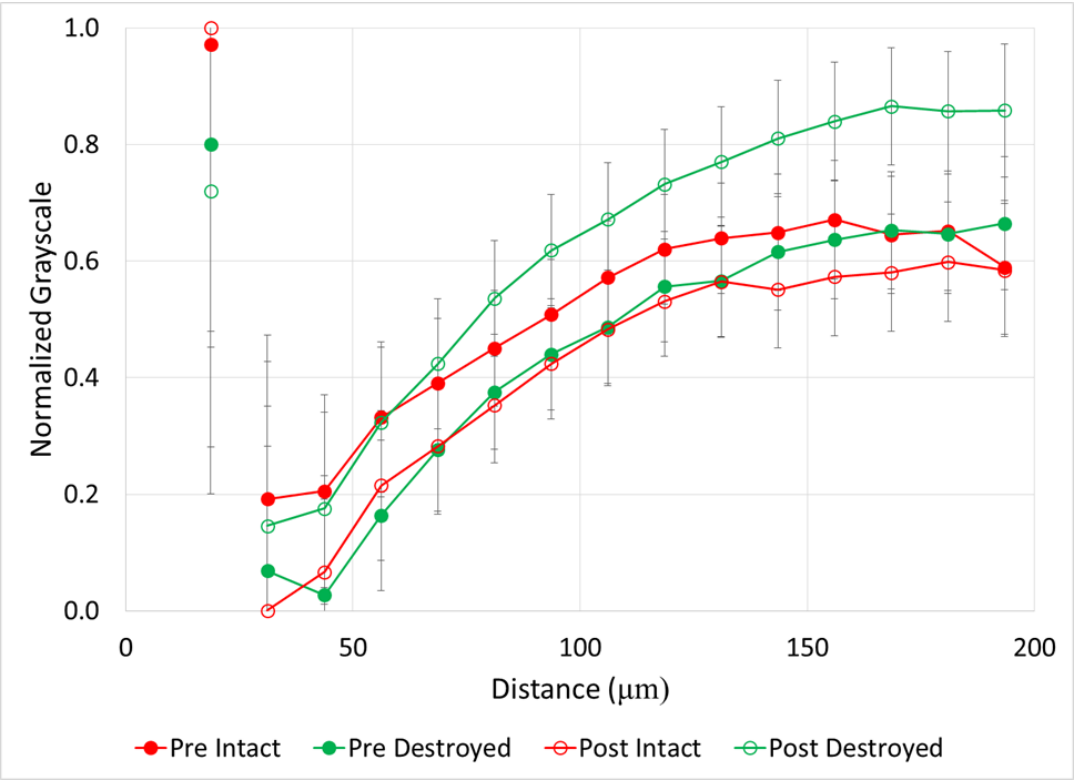

3.3.6 Canonical Correlations

The first two canonical correlation axes were significant at the 0.05 level (Figure 3.7). The first canonical variates can be described by the relationship between total C (negatively correlated) and total N (positively correlated) with 6.5-15 µm (negatively correlated) and 15-40 µm (positively correlated) pores. This indicates that pores of 6.5-15 µm were associated with higher C:N ratios while 15-40 µm pores were associated with lower C:N ratios. There was a treatment difference observed in this axis between destroyed-structure and intact-structure soils: the destroyed-structure soil contained more carbon with lower C:N ratios and a higher abundance of 15-40 µm pores than intact-structure soil.

Figure 3.7: Canonical correlation of pore sizes with total C (%C), total N (%N) and $\delta^{13}C$. The first two canonical correlations were significant at α=0.05 and are shown. The correlation factors that define the latent variables for each axes are shown on the right. The sign indicates the direction of correlation and the number indicates the amount each observed variable contributes to the latent variable. Lines indicate the (0,1) line **(A)** and (0, -1) line **(B)**, while letters indicate treatment (destroyed-structure (D) and intact-structure (I)).

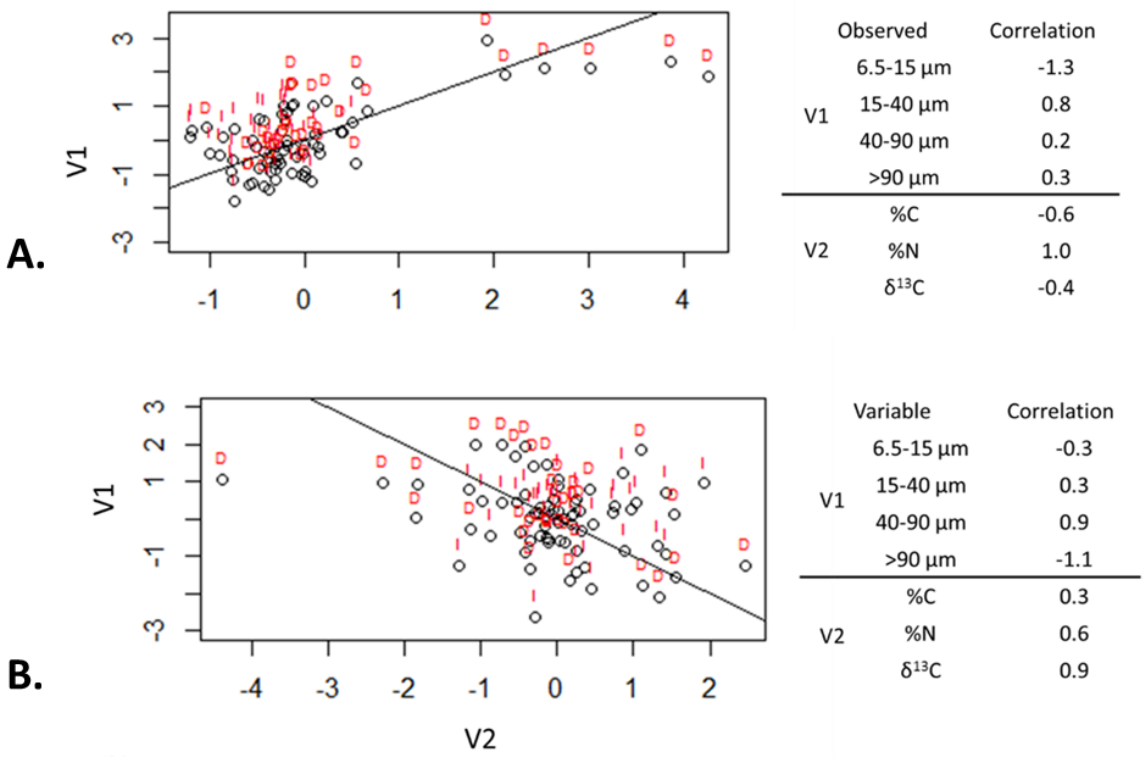

The second canonical variates can be described by the relationship between $\delta^{13}C$ (positive correlation) and total N (positive correlation) with 40-90 μm pores (positive correlation) and >90 μm pores (negative correlation). This indicates that 40-90 μm pores tend to have newer carbon with higher nitrogen concentrations, while >90 μm pores tend to have older carbon with lower nitrogen concentrations. There was no effect of treatment observed in the second canonical correlation axis.

3.4 Discussion

Three months of rye growth increased total C and the C:N ratio within both the intact-structure and destroyed-structured soils. However, in the subsequent incubation, gains of total C tended to disappear. As indicated by the $\delta^{13}C$ results, the carbon losses, at least in the destroyed-structure fragments, were dominated by losses in C3 carbon. Gains and losses of C3 and of total carbon were associated with presence of soil pores. However, the relationships between carbon and pores differed for different pore sizes, suggesting different microscale mechanisms by which these pores contribute to carbon accrual processes.

3.4.1 Relationship between C3 carbon and 40-90 μm pores

The correlations between $\delta^{13}C$ and pores of the studied size ranges had similar signs in both intact- and destroyed-structure soils, but in the intact-structure soil, the correlations were not statistically significant (Table 3.3). This is likely the outcome of the legacy of soil pore architecture of the intact-structure soil, which contributed to greater variability, thus lowering statistical significance in that treatment, as well as differences in decomposability of plant root material in the two treatments (as discussed below).

Negative correlation between $\delta^{13}C$ and 40-90 μm pores, indicated that greater levels of C3 were associated with the presence of 40-90 μm pores (Figure 3.4, Table 3.3). It is assumed that the increase in C3 carbon is associated with the newly added carbon. I surmise that a

possible cause for this association is that many of the 40-90 μm pores, especially those in the destroyed-structure soil, were created by fine plant roots. Since old root pores were destroyed during the sieving process, any 40-90 μm pores in the destroyed-structure soil, which were of root origin, would have been directly produced by the growth of the rye. On the contrary, in the intact-structure treatment such pores could have been produced by both new and historically grown plants, increasing variability that weakened the correlation.

After incubation, the gains in new carbon in the destroyed-structure soil in relation to the abundance of 40-90 μm pores were quickly lost. The 40-90 μm pores went from being positively correlated with new carbon in Pre to being negatively correlated with new carbon in Post. The grayscale gradients in the Post destroyed-structure soil had higher grayscale values than in the Pre (Figure 3.6). This further supports the notion that, while prior to incubation the SOM levels in the vicinity of such newly formed pores were relatively high, in samples subjected to incubation the SOM levels adjacent to 40-90 μm pores were low.

Greater decomposition of newly added carbon in 40-90 μm pores could result both from a more labile nature of the new carbon and from greater microbial activities in these pores. The second canonical correlation axis (Figure 3.7) shows that the 40-90 μm pores tend to have newer carbon and a higher concentration of nitrogen, thus possibly, containing more decomposable organic compounds. Indeed, the small plant roots located within such pores could have been more easily decomposable since fine roots tend to have less lignin and a lower lignin:N ratio is an indication of root decomposability (Rasse et al, 2005). Bailey et al (2017) observed that water extracted from pores between 20 and 200 μm contained more lipids, which are more easily decomposable, than lignin and tannin, which are more difficult to decompose. Moreover, the increased decomposition/carbon loss in such pores was reported as related to greater microbial

presence, transport, and activity in 40-90 μm pores (Strong et al, 2004; Wang et al, 2013; Kravchenko et al, 2014).

Some of the differences between the intact- and destroyed-structure treatments in terms of pore associations with new carbon might be related to differences in root decomposability. The intact-structure roots had a higher C:N ratio, as well as $\delta^{15}N$ and $\delta^{13}C$ (Table 3.1). The $\delta^{15}N$ of plant roots is controlled by the nitrogen use efficiency. Large differences between root and shoot $\delta^{15}N$ values can result from pooling of nitrate in plant roots (Kalcsits et al, 2015; Kalcsits and Guy, 2016). The shoot $\delta^{15}N$ was 2.08‰ for rye samples collected from both intact-structure and destroyed-structure soils, but, while the intact-structure roots were similar to the shoot values, destroyed-structure roots were ~3‰ more depleted. This suggests that pooling of nitrate could have taken place in the destroyed-structure roots, lowering C:N ratio and increasing decomposability. In addition, more depleted $\delta^{13}C$ values of roots from the destroyed-structure soil would make it slightly easier for microorganisms to decompose them than intact-structure roots. The differences in the $\delta^{13}C$ of C3 plants are related to water availability with more depleted values occurring where water is more plentiful (Farquhar et al, 1989, Stewart et al, 1995). The differences in overall pore size distributions of the two treatments could be the cause for the differences in nitrate and water availability. However, since the normal range of values for C3 plants is from -24 to -34‰, the difference between intact-structure and destroyed-structure roots observed in this study can be regarded as relatively small.

3.4.2 Relationship between carbon and 6.5-15 μm, 15-40 μm, and >90 μm pores

After incubation, there was a notably decreased association with C3 carbon in both intact-structure and destroyed-structure soil. This implies a preferential utilization of newer carbon in these pores. This preference could be the result of anaerobic conditions that existed within the soil. During incubation, the soil moisture level was kept at 60% water filled porosity, which

would have resulted in water filling the majority of both the 6.5-15 and 15-40 μm pores during the incubation, resulting in anaerobic conditions prevailing there during incubation. Keiluweit et al (2017) observed that in anaerobic microsites within upland soils, decomposition rates were reduced by a factor of 10, which may also explain the slower decomposition of materials from these pores as seen in the association with increased amounts of carbon. The anaerobic conditions may also explain why newer carbon was preferentially used in association with these pores. Newer carbon would likely contain more oxidized functional groups than older carbon. These functional groups would be quickly used under anaerobic conditions, resulting in biased decomposition of newer carbon in relation to pores of 6.5-15 and 15-40 μm sizes.

The association between total C and 15-40 μm pores (Figure 3.8) was identical to those observed by Ananeyva et al (2013). The two data sets, while of the same soil type and collected from the same geographic area, were of two completely different agricultural managements. This study is from a 20 year conventional management continuous corn treatment, while Ananeyva et al (2013) used aggregates from a 19 year native succession management, which was essentially unmanaged. This seems to suggest a universal mechanism for the relationship between soil carbon and the presence of 15-40 μm pores. One possible driver of this relationship might be the presence of fungi in these pores. The first canonical correlation axis (Figure 3.7), shows a difference in the C:N ratio of the two pore sizes. This potentially could signal a difference in decomposability between 6.5-15 μm and 15-40 μm pores. Bailey et al (2017) and Smith et al (2017) both observed that pores of >6 μm contained more easily decomposable material, while

Figure 3.8: Correlation between total carbon and abundance of 15-37.5 µm pores (Ananyeva et al, 2013, blue reproduced with permission from Elsevier) or 15-40 µm pores (this study, green). The y-axis is presented as total C, g/kg instead of %C to align with the original Anayeva et al (2013) graph.

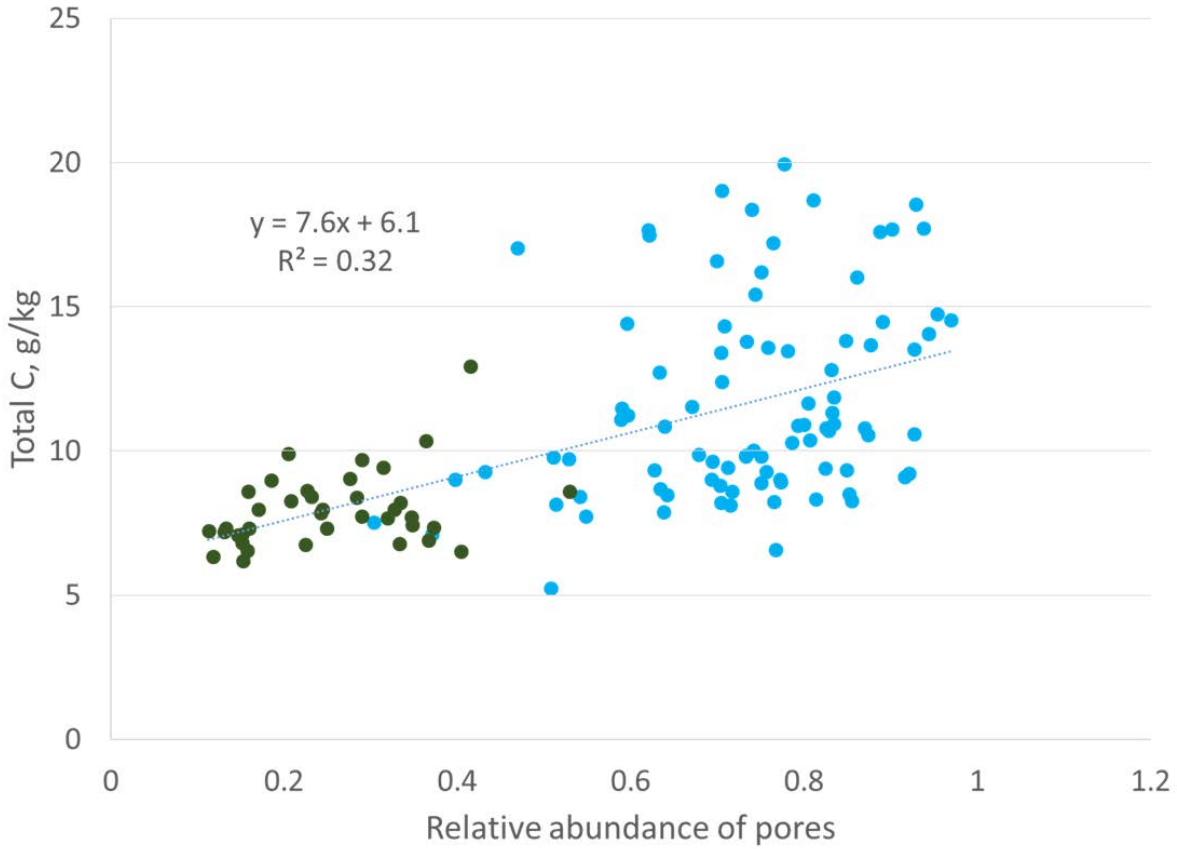

pores <6 µm contained more difficult to decompose material. They attributed this difference to accessibility of fungi, which preferential decompose more complex organic materials, but, as fungal hyphae are typically 10 µm in size, cannot access pores smaller than 10 µm (Six et al, 2006). Fungi are also known to create pores of 20-30 µm size by pushing aside silt particles and extruding binding agents, which would create micro-environments with more decomposable material in these created pores (Dorioz et al, 1993; Bearden, 2001, and Emerson and McGarry, 2003). Another potential explanation might be the presence of root hairs. Root hairs are also 10 µm in size and therefore, would also occur in the 15-40 µm pore range. More research is necessary to explore the cause of this correlation between total C and 15-40 µm pores. Caution,

however, should also be applied to these results as some of these correlations might be the result of soil handling, i.e. water addition during incubation, drying during scanning, etc., and not neccesarily management effects.

3.4.3 Additional considerations

The CO_2 results seem to indicate a different story than the soil fragment data. In the soil fragment data, destroyed-structure soil lost the most carbon during incubation, while the intact-structure soil lost a negligible amount of carbon during incubation. The CO_2 data, on the other hand, indicates that the intact-structure lost the most carbon as CO_2. This discrepancy is due to the removal of POM from the soil fragments prior to total C, total N, $\delta^{13}C$, and $\delta^{15}N$ measurements. The amount of POM removed from the intact-structure soil was almost twice as large as the amount of POM removed from the destroyed-structure soil. This means that the discrepancy between the CO_2 data and soil fragments was most likely due to the difference in the amount of POM.

I recognize that in terms of exploring associations between carbon and soil pores my work is, in essence, an observational study. Thus, it possesses a limitation common to all observational studies, that is, an inability to unequivocally declare cause and effect relationships. Yet, I posit that, at present it is impossible to recreate soil environments with specific pore characteristics for controlled cause-effect determination. Even though creation of artificial soil materials with contrasting pore architecture by either using soil fractions of different sizes or by soil compaction is possible (Negassa et al, 2015, Sleutel et al, 2012,Thomson et al, 2010; Stenger et al, 2002; De Neve and Hofman, 2000) such constructions fail to recreate biological conditions. By biological conditions, I refer to the structure and abundance of resident microbial communities, formed in pores of different sizes *in situ* and acclimated to specific

microenvironments existing there. Since it is microbial activities that largely drive carbon processing, failure to correctly represent them will likely mislead findings. This leaves no alternative, but observational studies, such as this study, to explore the role of pores within soil micro-environments.

3.5 Conclusion

My findings confirm previous results on the importance of pores in tens of microns size range for processing of organic carbon in soil, specifically in regards to fate and distribution of newly added carbon. I demonstrated that pores of 40-90 μm size range play a particularly intriguing role in new carbon gains as well as its subsequent losses. Such pores seem to be "easy come easy go" locations which receive the greatest amounts of new carbon from growing plant roots, but then rapidly lose that newly added carbon. On the other hand, both 6.5-15 and 15-40 μm pores are associated with preferential use of newer carbon. Carbon protection associated with the 6.5-15 μm pores could be associated with lack of accessibility by fungal hyphae and pervasiveness of anaerobic conditions when soils are near field capacity. Pores of 15-40 μm pore size are also associated with a prevalence of anaerobic conditions when soils are above field capacity, but fungal hyphae are not excluded and are potential drivers of carbon dynamics in pores of this size.

Funding

Support for this research was provided in part by the USDA-NIFA, Award No. 2016-67011-24726 “Using stable isotopes and computer tomography to determine mechanisms of soil carbon protection in cover crop based agricultural systems”, USDA-NIFA, Award No. 2011-68002-30190 “Cropping Systems Coordinated Agricultural Project (CAP): Climate Change, Mitigation, and Adaptation in Corn-based Cropping Systems” sustainablecorn.org, and by the US National Science Foundation Long-Term Ecological Research Program (DEB 1027253) at the Kellogg

Biological Station and by Michigan State University AgBioResearch. Portions of this work were performed at GeoSoilEnviroCARS (The University of Chicago, Sector 13), Advanced Photon Source (APS), Argonne National Laboratory. GeoSoilEnviroCARS is supported by the National Science Foundation - Earth Sciences (EAR - 1634415) and Department of Energy- GeoSciences (DE-FG02-94ER14466). This research used resources of the Advanced Photon Source, a U.S. Department of Energy (DOE) Office of Science User Facility operated for the DOE Office of Science by Argonne National Laboratory under Contract No. DE-AC02-06CH11357.

REFERENCES

REFERENCES

Ananyeva, K., Wang, W., Smucker, A. J. M., Rivers, M. L., and Kravchenko, A. N. (2013). Can intra-aggregate pore structures affect the aggregate's effectiveness in protecting carbon? *Soil Biol. Biochem.* 57, 868-875. doi: 10.1016/j.soilbio.2012.10.019

Bailey, V. L., Smith, A. P., Tfaily, M., Fansler, S. J., and Bond-Lamberty, B. (2017). Differences in soluble organic carbon chemistry in pore waters sampled from different pore size domains. *Soil Biol. Biochem.* 107, 133-143. doi: 10.1016/j.soilbio.2016.11.025

Bearden, B. N. (2001). Influence of arbuscular mycorrhizal fungi on soil structure and soil water characteristics of vertisols. *Plant Soil* 229, 245– 258. doi: 10.1023/A:1004835328943

Bernoux, M., Cerri, C. C., Neill, C. and de Moraes, J. F. L. (1998). The use of stable carbon isotopes for estimating soil organic matter turnover rates. *Geoderma* 82, 43-58. doi: 10.1016/S0016-7061(97)00096-7

Bowling, D. R., Pataki, D. E., and Randerson, J. T. (2008). Carbon isotopes in terrestrial ecosystem pools and CO_2 fluxes. *New Phytol.* 178, 24-40. doi: 10.1111/j.1469-8137.2007.02342.x

Brimecombe, M. J., de Leij, F. and Lynch, J. M. (2001). "The effect of root exudates on rhizosphere microbial populations," in *The rhizosphere: biochemistry and organic substances at the soil-plant interface*, eds. R. Pinton, Z. Varanini and P. Nannipieri. (New York, New York, USA: Marcel Dekker), 95–140.

Cannell, R. Q. (1977). Soil aeration and compaction in relation to root growth and soil management. *Appl. Biol.* 2, 1-86.

Czarnes, S., Hallett, P. D., Bengough, A. G., and Young, I. M. (2000). Root- and microbial-derived mucilages affect soil structure and water transport. *Eur. J. Soil Sci.* 51, 435-443. doi: 10.1046/j.1365-2389.2000.00327.x

De Gryze, S., Jassogne, L., Six, J., Bossuyt, H., Wevers, M., and Merckx, R. (2006). Pore structure changes during decomposition of fresh residue: X-ray tomography analyses. *Geoderma* 134, 82-96. doi: 10.1016/j.geoderma.2005.09.002

De Neve, S. and Hofman, G. (2000). Influence of soil compaction on carbon and nitrogen mineralization of soil organic matter and crop residues. *Biol. Fertil. Soils* 30, 544-549. doi: 10.1007/s003740050034

Derrien, D. and Amelung, W. (2011). Computing the mean residence time of soil carbon fractions using stable isotopes: impacts of the model framework. *Eur. J. Soil Sci.* 62, 237-252. doi: 10.1111/j.1365-2389.2010.01333.x

Dorioz, J. M., Robert, M., and Chenu, C. (1993). The role of roots, fungi and bacteria on clay particle organization. An experimental approach. *Geoderma* 56, 179– 194. doi:10.1016/0016-7061(93)90109-X

Dou F., Hons F. M., Wright A. L., Boutton, T. W. and Yu, X. (2014). Soil carbon sequestration in sorghum cropping systems: evidence from stable isotopes and aggregate-size fractionation. *Soil Sci.* 179, 68-74. doi: 10.1097/SS.0000000000000045

Dungait, J. A. J., Hopkins, D. W., Gregory, A. S., and Whitmore, A. P. (2012). Soil organic matter turnover is governed by accessibility not recalcitrance. *Global Change Biol.* 18, 1781-1796. doi: 10.1111/j.1365-2486.2012.02665.x

Ehleringer, J. R., Buchmann, N., and Flanagan, L. B. (2000). Carbon isotope ratios in belowground carbon cycle processes. *Ecol. Appl*. 10, 412-422. doi: 10.2307/2641103

Ekschmitt, K., Kandeler, E., Poll, C., Brune, A., Buscot, F., Friedrich, M., et al. (2008). Soil-carbon preservation through habitat constraints and biological limitations on decomposer activity. *J. Plant Nutr. Soil Sci.* 171, 27-35. doi: 10.1002/jpln.200700051

Ekschmitt, K., Liu, M., Vetter, S., Fox, O., and Wolters, V. (2005). Strategies used by soil biota to overcome soil organic matter stability – why is dead organic matter left over in soil? *Geoderma* 128, 167-176. doi: 10.1016/j.geoderma.2004.12.024

Emerson,W. W. and McGarry, D. (2003). Organic carbon and soil porosity. *Aust. J. Soil Res.* 41, 107–118. doi: 10.1071/SR01064

Farquhar, G. D., Ehleringer, J. R., and Hubick, K. T. (1989). Carbon isotope discrimination and photosynthesis. *Annu. Rev. Plant Physiol. Plant Mol. Biol.* 40, 503-537. doi: 10.1146/annurev.pp.40.060189.002443

Grandy, A. S. and Robertson, G. P. (2007). Land-use intensity effects on soil organic carbon accumulation rates and mechanisms. *Ecosystems* 10, 58-73. doi: 10.1007/s10021-006-9010-y

Gray, J., and Lissmann, H. W. (1938). An apparatus for measuring the propulsive forces of the locomotory muscles of the earthworm and other animals. *J. Exp. Biol.* 15, 518-521.

Greacen, E. L., and Oh, J. S. (1972). Physics of root growth. *Nat. New Biol.* 235, 24-25. doi: 10.1038/newbio235024a0

Greacen, E. L., and Sands, R. (1980). Compaction of forest soils. a review. *Aust. J. Soil. Res.* 18, 163-189. doi: 10.1071/SR9800163

Jackson, R. B., Lajtha, K., Crow, S. E., Hugelius, G., Kramer, M. G., and Piñeiro, G. (2017). The ecology of soil carbon: pools, vulnerabilities, and biotic and abiotic controls. *Annu Rev Ecol Evol Syst*. 48, 419-445. doi: 10.1146/annurev-ecolsys-112414-054234

Kalcsits, L. A. and Guy, R. D. (2016). Variation in fluxes estimated from nitrogen isotope discrimination corresponds with independent measures of nitrogen flux in *Populus balsamifera* L. *Plant Cell Environ.* 39, 310-319. doi: 10.1111/pce.12614

Kalcsits, L. A., Min, X., and Guy, R. D. (2015). Interspecific variation in leaf-root differences in $\delta^{15}N$ among three tree species grown with either nitrate or ammonium. *Trees.* 29, 1069-1078. doi: 10.1007/s00468-015-1186-3

Kell, D. B. (2012). Large-scale sequestration of atmospheric carbon via plant roots in natural and agricultural ecosystems: why and how. *Philos T R Soc B.* 367, 1589-1597. doi: 10.1098/rstb.2011.0244

Keiluweit, M., Wanzek, T., Kleber, M., Nico, P., and Fendorf, S. (2017). Anaerobic microsites have an unaccounted role in soil carbon stabilization. *Nat. Commun.* 8: 1771. doi: 10.1038/s41467-017-01406-6

Kravchenko, A. N., and Guber, A. K. (2017). Soil pores and their contributions to soil carbon processes. *Geoderma* 287, 31-39. doi: 10.1016/j.geoderma.2016.06.027

Kravchenko, A. N., Negassa, W. C., Guber, A. K., Hildebrandt, B., Marsh, T. L., and Rivers, M. L. (2014). Intra-aggregate pore structure influences phylogenetic composition of bacterial community in macroaggregates. *Soil Sci. Soc. Am. J.* 78, 1924-1939. doi: 10.2136/sssaj2014.07.0308

Kravchenko, A. N., Negassa, W. C., Guber, A. K., and Rivers, M. L. (2015). Protection of soil carbon within macro-aggregates depends on intra-aggregate pore characteristics. *Sci. Rep.* 5:16261. doi: 10.1038/srep16261

Kuzyakov, Y., and Blagodatskaya, E. (2015). Microbial hotspots and hot moments in soil: concept & review. *Soil Biol. Biochem.* 83, 184-199. doi: 10.1016/j.soilbio.2015.01.025

Lal, R. (1999). Soil management and restoration for carbon sequestration to mitigate the accelerated greenhouse effect. *Prog. Env. Sci.* 1, 307-326. doi: 10.1055/s-2008-1072270

Lindquist, W. B., Venkatarangan, A., Dunsmuir, J., and Wong, T. (2000). Pore and throat size distributions measured from synchrotron X-ray tomographic images of Fontainebleau sandstornes. *J. Geophys. Res.* 105, 21,509-21,527. doi: 10.1029/2000JB900208

Marshall, T. J., Holmes, J. W., and Rose, C. W. (1996). Soil Physics, third ed. Cambridge, England: Cambridge University Press.

Milliken, G .A., and Johnson, D. E. (2009). Analysis of Messy Data Volume I: Designed Experiments, second ed. Boca Raton, FL: CRC Press.

Negassa, W. C., Guber, A. K., Kravchenko, A. N., Marsh, T. L., Hildebrandt, B., and Rivers, M. L. (2015). Properties of soil pore space regulate pathways of plant residue decomposition and community structure of associated bacteria. *PLoS One* 10(4): e0123999 doi: 10.1371/journal.pone.0123999

Neumann, G., Bott, S., Ohler, M. A., Mock, H.-P., Lippmann, R., R. Grosch, et al. (2014). Root exudation and root development of lettuce (*Lactuca sativa* L. cv. Tizian) as affected by different soils. *Front. Microbol.* 5:2. doi: 10.3389/fmicb.2014.00002

Oh, W., and Lindquist, W. B. (1999). Image thresholding by indicator kriging. *IEEE Trans. Pattern Anal. Mach. Intell.* 21, 590-602. doi: 10.1109/34.777370

Park, E. J. and Smucker, A. J. M. (2005). Saturated hydraulic conductivity and porosity within macroaggregates modified by tillage. *Soil Sci. Soc. Am. J.* 69, 38-45. doi: 10.2136/sssaj2005.0038

Peth, S., Horn, R., Beckmann, F., Donath, T., Fischer, J., and Smucker, A. J. M. (2008). Three-dimensional quantification of intra-aggregate pore-space features using synchrotron-radiation-based microtomography. *Soil Sci. Soc. Am. J.* 72, 897-907. doi: 10.2136/sssaj2007.0130

Peth, S., Chenu, C., Leblond, N., Mordhorst, A., Garnier, P., Nunan, N., et al. (2014). Localization of soil organic matter in soil aggregates using synchrotron-base X-ray microtomography. *Soil Biol. Biochem.* 78, 189-194. doi: 10.1016/j.soilbio.2014.07.024

Quigley, M. Y., Rivers, M. L., and Kravchenko, A. N. (2018). Patterns and sources of spatial heterogeneity in soil matrix from contrasting long term management practices. *Front. Environ. Sci.* 6:28 doi: 10.3389/fenvs.2018.00028

R Core Team (2013). R: A language and environment for statistical computing. R Foundation for Statistical Computing, Vienna, Austria. http://www.R-project.org/.

Rabot, E., Wiesmeier, M., Schlüter, S., and Vogel, H.-J. (2018). Soil structure as an indicator of soil functions: a review. *Geoderma* 314, 122-137. doi:10.1016/j.geoderma.2017.11.009

Rasse, D. P., Rumpel, C. and Dignac, M.-F. (2005). Is soil carbon mostly root carbon? Mechanisms for a specific stablisation. *Plant Soil* 269, 341-356. doi: 10.1007/s11104-004-0907-y

Rasse, D. P. and Smucker, A. J. M. (1998). Root recolonization of previous root channels in corn and alfalfa rotations. *Plant Soil* 204, 203-212. doi: 10.1023/A:1004343122448

Rawlins, B. G., Wragg, J., Reinhard, C., Atwood, R. C., Houston, A., Lark, R. M., et al. (2016). Three-dimensional soil organic matter distribution, accessibility and microbial respiration in macroaggregates using osmium staining and synchrotron X-ray computed tomography. *SOIL*. 2, 659-671. doi: 10.5194/soil-2-659-2016

Rivers, M. L. (2012). tomoRecon: High-speed tomography reconstruction on workstations using multi-threading. *Proc. SPIE* 8505:OU. doi:10.1117/12.930022

Ruiz, S., Schymanski, S. J., and Or, D. (2017). Mechanics and energetics of soil penetration by earthworms and plant roots: higher rates cost more. *Vadose Zone J.* 16:8. doi: 10.2136/vzj2017.01.0021

SAS Inc. (2009). *SAS user's guide. Version 9.2*. Cary, NC: SAS Inst.

Schmidt, M. W., Torn, M. S., Abiven, S., Dittmar, T., Guggenberger, G., Janssens, I. A., et al. (2011). Persistence of soil organic matter as an ecosystem property. *Nature* 478, 49-56. doi:10.1038/nature10386

Six, J., Elliott, E. T., and Paustian, K. (2000). Soil macroaggregate turnover and microaggregate formation: a mechanism for C sequestration under no-tillage agriculture. *Soil Biol. Biochem*. 32, 2099-2103. doi: 10.1016/S0038-0717(00)00179-6

Six, J., Frey, S. D., Thiet, R. K., and Batten, K. M. (2006). Bacterial and fungal contributions to carbon sequestration in agroecosystems. *Soil Sci. Soc. Am. J.* 70, 555-569. doi:10.2136/sssaj2004.0347

Sleutel, S., Bouckaert, L. Buchan, D., Van Loo, D., Cornelis, W. M., and Sanga, H. G. (2012). Manipulation of the soil pore and microbial community structure in soil mesocosm incubation studies. *Soil Biol. Biochem.* 45, 40-48. doi: 10.1016/j.soilbio.2011.09.016

Smith, A. P, Bond-Lamberty, B., Benscoter, B. W., Tfaily, M. M., Hinkle, C. R., Liu, C., et al (2017). Shifts in pore connectivity from precipitation versus groundwater rewetting increases soil carbon loss after drought. *Nature Comm*. 8:1335. doi: 10.1038/s41467-017-01320-x

Smucker, A. J. M., Park, E.-J., Dorner, J., and Horn, R. (2007). Soil micropore development and contributions to soluble carbon transport within macroaggregates. *Vadose Zone J.* 6, 282-290. doi: 10.2136/vzj2007.0031

Stewart, G. R., Turnbull, M. H., Schmidt, S., and Erskine, P. D. (1995). ^{13}C natural abundance in plant communities along a rainfall gradient: a biological integrator of water availability. *Aust. J. Plant Physiol*. 22, 51-55. doi: 10.1071/PP9950051

Stenger, R., Barkle, G. F., and Burgess, C. P. (2002). Mineralisation of organic matter in intact versus sieved/refilled soil cores. *Aust. J. Soil Res.* 40, 149-160. doi: 10.1071/SR01003

Strong, D. T., De Wever, H., Merckx, R., and Recous, S. (2004). Spatial location of carbon decomposition in the soil pore system. *Eur. J. Soil Sci.* 55, 739-750. doi: 10.1111/j.1365-2389.2004.00639.x

Swift, R. S. (2001). Sequestration of carbon by soil. *Soil Sci.* 166, 858-871. doi: 10.1097/00010694-200111000-00010

Thomson, B. C., Ostle, N. J., McNamara, N. P., Whiteley, A. S., and Griffiths, R. I. (2010). Effects of sieving, drying and rewetting upon soil bacterial community structure and respiration rates. *J. Microbiol. Methods* 83, 69-73. doi: 10.1016/j.mimet.2010.07.021

Tiemann, L. K. and Grandy, A. S. (2015). Mechanisms of soil carbon accrual and storage in bioenergy cropping systems. *Glob Change Biol Bioenergy* 7, 161-174. doi: 10.1111/gcbb.12126

Urbanek, E., Smucker, A. J. M., and Horn, R. (2011). Total and fresh organic carbon distribution in aggregate size classes and single aggregate regions using natural $^{13}C/^{12}C$ tracer. *Geoderma* 164, 164-171. doi:10.1016/j.geoderma.2011.05.020

Wang, W., Kravchenko, A. N., Johnson, T., Srinivasan, S., Ananyeva, K. A., Smucker, A. J. M., et al. (2013). Intra-aggregate pore structures and *Escherichia coli* distribution by water flow within and movement out of soil macroaggregates. *Vadose Zone J.* 12:4. doi: 10.2136/vzj2013.01.0012

Wang, W., Kravchenko, A. N., Smucker, A. J. M., Liang, W., and Rivers, M. L. (2012). Intra-aggregate pore characteristics: X-ray computed microtomography analysis. *Soil Sci. Soc. Am. J.* 76, 1159-1171. doi: 10.2136/sssaj2011.0281

Wang, W., Kravchenko, A. N., Smucker, A. J. M., and Rivers, M. L. (2011). Comparison of image segmentation methods in simulated 2D and 3D microtomographic images of soil aggregates. *Geoderma*. 162, 231-241. doi: 10.1016/j.geoderma.2011.01.006

Wiersum, L. K. (1957). The relationship of the size and structural rigidity of pores to their penetration by roots. *Plant Soil* 9, 75-85. doi: 10.1007/BF01343483

Young, I. M., and Crawford, J. W. (2004). Interactions and self-organization in the soil-microbe complex. *Science* 304, 1634-1637. doi: 10.1126/science.1097394

Young, I. M., Crawford, J. W., and Rappoldt, C. (2001). New methods and models for characterizing structural heterogeneity of soil. *Soil Tillage Res.* 61, 33-45. doi: 10.1016/S0167-1987(01)00188-X

Chapter 4: Effect of management and pore size distribution on the input and persistence of new carbon

Abstract

Agricultural management can have a large effect on soil carbon concentrations with some managements triggering losses and others generating accumulation. However, the mechanisms behind these effects are not sufficiently understood, especially at a scale of a few to hundreds of microns where the physical protection of soil carbon takes place. Understanding where new carbon is added and how it is used could refine current management recommendations for enhancing C accrual and improving soil health. As soil pores control the movement of gasses, water, and microorganisms, soil pores may also control new carbon gains and losses. In order to determine how new carbon is added in relation to abundance and size distribution of soil pores, I utilized cereal rye (*Secale cereale* L.) enriched with ^{13}C to track the addition of new carbon. Pulse labeling was used to enrich the rye during growth and to track the fate of plant derived C in soil after plant growth and after subsequent 3 week incubation. Computed microtomography was used to characterize pore size distributions. Soil from two contrasting agricultural managements, conventional and biologically based, was used. In order to better differentiate the effect of roots, soil was either kept intact or destroyed with a 1 mm sieve. Soil mini-cores were taken after rye termination and analyzed for $\delta^{13}C$ and total C. Results indicate that in soils with legacy root channels, new carbon is added evenly between pores of different sizes. In soils without pre-existing root channels, new carbon was preferentially added to 15-40 and 40-90 μm pores. Relationships between new carbon and pores were lost after incubation, indicating rapid new carbon loss from pores where new carbon was added, although the loss was less severe in 4-40 μm pores. This has implications for understanding underlying mechanisms of why some soils retain carbon, while others do not.

4.1. Introduction

Soil carbon stocks are roughly equivalent to twice the amount of carbon stored in the atmosphere (Lal, 1999; Swift, 2001; Falkowski et al, 2000; Davidson and Janssens, 2006). While a substantial portion of this carbon is stored in arctic regions, agricultural soils have a large untapped storage capacity that can help with climate change mitigation (Oechel and Vourlitis, 1994; Lal, 2011; Dungait et al, 2012; Kell, 2012). Additionally, soil carbon is strongly linked with higher soil fertility and greater crop yields, thus making increased storage of soil carbon in agricultural soils important to agricultural sustainability and soil health (Melsted, 1954; Bauer and Black, 1994; Lal, 2006).

Agricultural management can have a substantial effect on soil carbon gains and losses (Senthilkumar et al, 2009; Syswerda et al, 2011). Conventionally managed systems, i.e., those receiving tillage, chemical fertilizers, and no winter cover, are associated with carbon losses (Grandy and Robertson, 2007; Ruan and Robertson, 2013; Abraha et al, 2018). Including cover crops in the rotation, i.e. planting of a non-cash crop between cash crops, can provide erosion control, suppress weeds, increase water holding capacity and fertility, as well as enable soil carbon gains; although the gains can take years to be reliably detected (Necpálová et al, 2014; Rorick and Kladivko, 2017).

The mechanisms behind carbon gains in agricultural systems with cover crops are not fully understood (Austin et al, 2017). For example, increasing plant biomass inputs is believed to be one of the best ways to improve soil carbon (Paustian et al, 2016). However, crops producing large amounts of biomass do not always lead to substantial carbon gains (Garten and Wullschleger, 1999; Chimento et al, 2016; Sprunger and Robertson, 2018). This observation indicates that not only the amount of C input, but it subsequent protection within the soil matter is required for increasing soil C levels. Protection of soil C is driven by micro-scale soil

processes, including accessibility of new C to microbial decomposers that is achieved via soil pores. Already, the addition of microscale information has been shown to increase model accuracy over use of the macroscale characteristics for modelling carbon respiration and hydraulic properties (Falconer et al, 2015; Smet et al, 2018). Lack of accounting for microscale processes may explain the wide variability in performance of soil carbon models (Keel et al, 2017).

The presence of diverse microenvironments is believed to be the key driver of carbon protection within soils (Kuzyakov and Blagodatskaya, 2015). However, characteristics and properties of soil microenvironments are largely defined by soil pores that control the fluxes of water and gases, microbial access to carbon sources, as well as microorganism movement and nutrient transport (Young et al, 2001; Ekschmitt et al, 2005, 2008; Park et al, 2007; Kravchenko and Guber, 2017; Rabot et al, 2018). Through their control of soil microenvironment creation, soil pores are also essential to soil carbon protection. While a link between pores of specific size ranges and soil carbon loss/protection has been established (Strong et al, 2004; Ananyeva et al, 2013; Bailey et al, 2017; Quigley et al, 2018a), the mechanisms behind these correlations have yet to be elucidated. Moreover, how roots contribute to these relationships is also poorly understood as root growth can affect the pore size distribution (Graecen et al 1968; Dexter, 1987), but pore size distribution can also affect root growth (Bowen, 1981; Bengough et al, 2006).

Numerous studies have shown that roots, as compared to shoots, contribute a disproportionate amount (up to 75%) to soil carbon (Gale et al, 2000; Rasse et al, 2005; Kong and Six, 2010; Mazzilli et al, 2015; Austin et al, 2017). This contribution can be in the form of actual root biomass or through root exudates. Studies have shown that around 30-50% of

belowground biomass can be attributed to root exudates (Barber and Martin, 1976; Meharg and Killham, 1991; Kuzyakov et al, 2003). The exudates consist of organic acids, amino acids, and other small, highly soluble and easy to decompose compounds, although mucilage and other harder to decompose materials can also be produced (Brimecombe et al, 2011; Dungait et al, 2012). The easily decomposable compounds can then be quickly taken up by soil microbes, contributing to microbial biomass. It has been found that up to 25-30% of microbial biomass carbon can be derived from actively growing plants (Williams et al, 2006; Austin et al, 2017). Processing carbon by soil microorganism is also known to be one of the first steps in soil organic matter production. This processed carbon can then easily attach to mineral particles, where they are protected from further degradation (Grandy and Neff, 2008; Wieder et al, 2014; Kallenbach et al, 2015, 2016; Jackson et al, 2017). Therefore, spatial patterns in the distribution of roots and their exudates can also play an important role in soil carbon protection.

The distribution of soil pore sizes varies depending on agricultural management. Conventional management has been associated with an increased presence of 40-90 μm pores (Wang et al, 2012), which has also been linked with carbon losses (Ananeyeva et al, 2013), especially of newer carbon (Quigley et al, 2018a). These pores are created through either mechanical wetting/drying and freeze/thaw cycles or by smaller plant roots. On the other hand, management with continuous presence of live vegetation cover, e.g., cover crops, has been related to a higher presence of >84 μm pores and higher total porosity, which are associated with larger roots (Kravchenko et al, 2014). However, existing root pores also are preferentially used by new plants, potentially masking any new root effects (Rasse and Smucker, 1998).

I examined the associations between pore size distributions, i.e., abundances of pores of different sizes, and the addition and usage of newly added carbon in soils from two long-term

contrasting agricultural practices: conventional chemical fertilization and biologically based management with cover crops. A greenhouse experiment using soil from these two different agricultural managements was planted with cereal rye (*Secale cereale* L.), a common cover crop in the Midwestern US. Two soil treatments were considered, one with the original soil structure intact and one where soil structure was destroyed by sieving through 1 mm sieve. Destroying the existing structure destroys the existing roots pores, allowing for the root effects on soil pore formation and carbon protection to be separated from root legacy effects and to be more easily detected. The rye was enriched with ^{13}C during 3 months of growth via pulse labeling. The enriched rye was used to track newly added carbon within the soil after 3 months of rye growth and a subsequent 21-day incubation. The first objective was to determine the localization of the new carbon added to soil by growing rye roots. The second objective was to determine if and where this new carbon was lost in a subsequent incubation. The particular focus of the study was on evaluating the role of pores on new carbon localization and subsequent losses.

4.2. Materials and methods

4.2.1 Soil collection

Soil for the greenhouse experiment was collected from two different management practices established in 1989 at Kellogg Biological Station Long Term Ecological Research site, located in Hickory Corners, MI (42°24´N, 85°24´W). The soil is a fine-loamy, mixed mesic Typic Hapludalf developed on glacial outwash with an intermixed loess layer of the Oshtemo and Kalamazoo series (Crum and Collins, 1995; Luehmann et al, 2016). The two practices were the conventional and biologically based systems. The conventional practice is a corn-soybean-wheat rotation maintained with current best management practices (tillage, chemical fertilizer additions, pesticide and herbicide as needed, no winter cover). The biologically based practice is

a corn-soybean-wheat rotation with rye cover after corn and red clover inter-seeded into wheat. Rotary tillage was used between rows for weed control and no additional inputs were added. Detailed management and site information is available at http://lter.kbs.msu.edu/Data/LTER.

Soil was collected between rows in May of 2016 during the wheat rotation prior to red clover establishment in the biologically based system. From each practice, soil was collected at the 0-10 cm depth with minimal disturbance and placed into three 30 x 21 cm size containers to a depth of 8 cm. This soil will be referred to as intact-structure soil. Additional soil was collected from each treatment and sieved through a 1 mm sieve to destroy the existing soil structure. The sieved soil was placed in three 30 x 21 cm containers to an 8 cm depth for each practice. This soil will be referred to as destroyed-structure soil. Two containers from each management and structure had circular enclosures, 6 cm in diameter, of 35 μm mesh inserted to create a zone free of the immediate influence of plant roots. Rye was then hand planted at a 3 cm depth outside of the root excluding mesh every 4 cm with a total of nine rye plants per container.

4.2.2 Pulse labeling

Enriched stable isotopes can be used to easily track carbon in a system. Stable carbon isotopes are reported in δ notation as per mil (‰) differences between the $^{13}C/^{12}C$ ratio of the sample compared to a standard:

$$\delta^{13}C = \left[\left(R_{Sample} - R_{Standard}\right)/R_{Standard}\right] * 1000 \quad (4.1)$$

Pulse labeling is a technique used to uniformly label plant material via enriched $^{13}CO_2$ (Thompson, 1996; Bromand et al, 2001; Sangster et al, 2010). Pulse labeled plant material can then be tracked through the system using the following calculation:

$$F = \frac{\left(\delta^{13}C_{final} - \delta^{13}C_{non-enriched}\right)}{\left(\delta^{13}C_{enriched} - \delta^{13}C_{non-enriched}\right)} \quad (4.2)$$

where F is the fraction of enriched material in the final sample, $\delta^{13}C_{final}$ is the $\delta^{13}C$ value of the sample, $\delta^{13}C_{enriched}$ is the $\delta^{13}C$ of the enriched plant material, and $\delta^{13}C_{non\text{-}enriched}$ is the $\delta^{13}C$ of the original material. Decomposition is believed to have a negligible effect on $\delta^{13}C$ values, and therefore its effects can be safely ignored. Enriched material has previously been successfully used to track the decomposition of organic material within soils at micron scale (Gaillard et al, 1999, 2003; Toosi et al, 2017).

Rye was grown in the greenhouse for a total of three months. Pulse labeling began two weeks after rye establishment and was repeated every 10 days until the end of the three month growth period. At each labeling event, the rye containers were moved into a plexiglass chamber. One gram of 99% ^{13}C enriched $CaCO_3$ was placed in the chamber with a fan to circulate the ^{13}C labeled CO_2. The chamber was then sealed with duct tape to create an air tight enclosure (Figure 4.1). Excess H_2SO_4 was added to the 99% ^{13}C enriched $CaCO_3$ to evolve CO_2. Plants were labeled for 24 hours (Bird et al, 2003; Toosi et al, 2017) and then removed from the plexiglass chamber until the next labeling event. A total of eight labeling events occurred during the experiment. The four containers where rye was not planted (1 per treatment combination) were not subjected to pulse labeling, but were watered throughout the experiment as an isotopic control.

Figure 4.1: Image of the pulse labeling plexiglass chamber and pulse labeling set up. Note the fan in the corner to circulate the evolved $\delta^{13}C$ enriched CO_2. Samples were rotated between rack positions for each pulse labeling event.

4.2.3 Sample collection

At the end of the three month rye growth period, four intact mini-cores were taken from each container at 0-5 cm depth using a beveled 3 mL Luer-Lok polypropylene syringe with an 8 mm inner diameter (BD, Franklin Lakes NJ, USA). In each container, two cores were taken from

the root exclusion zone and two adjacent to rye plants. Two additional cores per container were taken to calculate bulk density. The bulk density was used to verify if mini-core sampling resulted in significant compaction of the samples. If compaction took place during sampling, the bulk density would be significantly higher than the 1.43 g/cm^3 bulk density of the original soil (Crum and Collins, 1995; Wickings and Grandy, 2013). The cores were then air dried for collection of computed microtomography (μCT) images. Roots and shoots were collected and air dried, then analyzed for $\delta^{13}C$ to determine the enrichment of the rye in each container.

All mini-cores were subjected to μCT scanning (see below). After that, half of the samples were sacrificed for $\delta^{13}C$ analysis. The other half was incubated for 21 days (see below), scanned again, and then sampled for $\delta^{13}C$. The two halves will be referred to as Pre and Post (incubation) samples. Samples for $\delta^{13}C$ analysis were collected using a custom-made soil sampling device (Figure 4.2), which facilitated matching of the $\delta^{13}C$ data with μCT images. The device consisted of five 2 mm diameter and 5 mm deep soil cylinders. Approximately 10-20 μg of soil was collected into each cylinder for $\delta^{13}C$ and total C analysis.

Figure 4.2: Pictorial schematic of soil sampling using the sample device. First, the top 1.5 mm of the sample was removed **(A)**. The sample was then aligned to match the μCT images (red mark) and the 5 mm sample **(B)**. The soil sampling device **(C)** was then aligned with the red mark **(D)** and five samples collected simultaneously **(E)**. The samples were then placed into tins for total carbon and $\delta^{13}C$ analysis **(F)**.

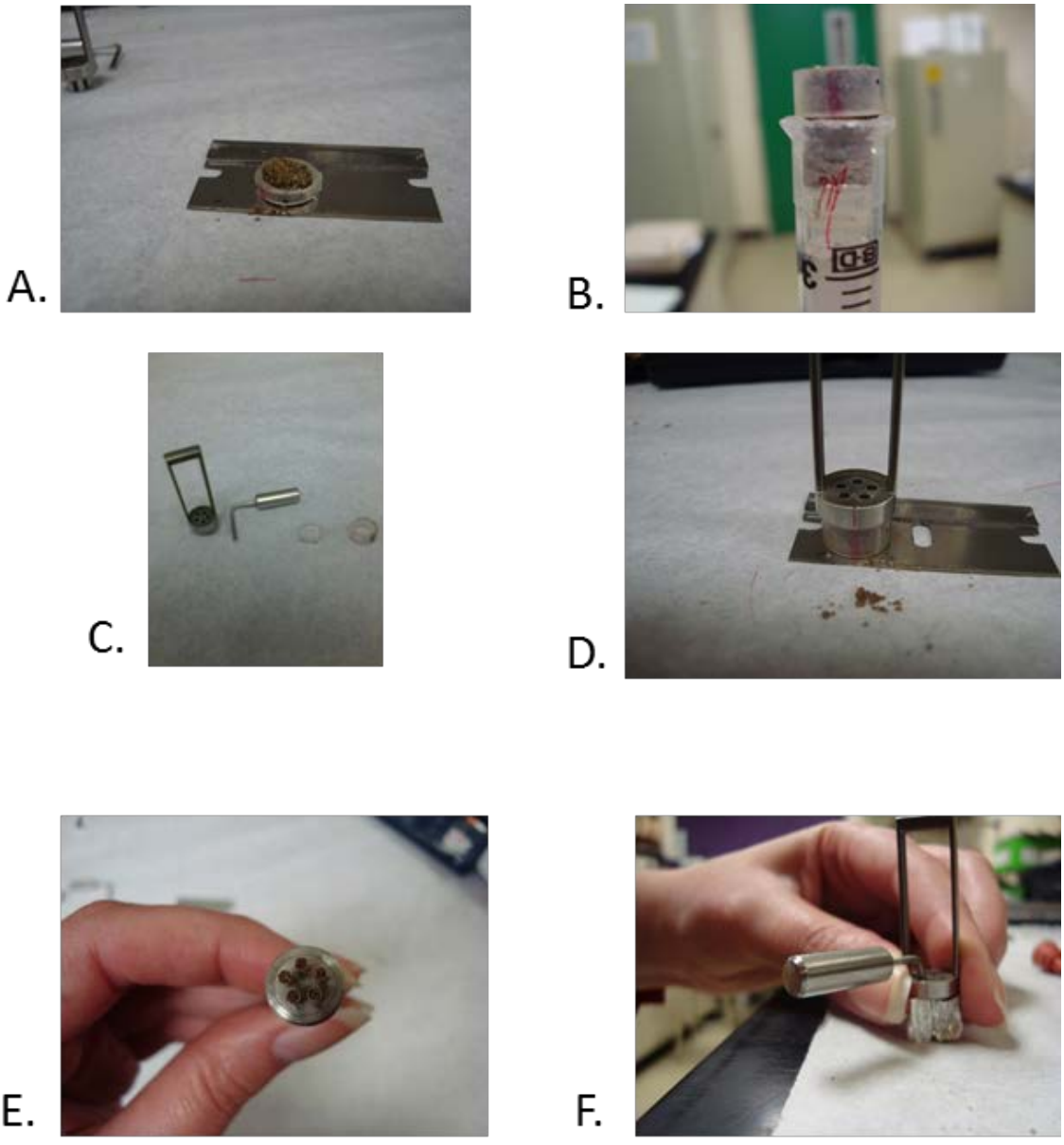

4.2.4 Collection of μCT images

Images were obtained on the bending magnet beam line, station 13-BM-D of the GeoSoilEnvironCARS (GSECARS) at the Advanced Photon Source (APS), Argonne National Laboratory (ANL), IL. Images were collected with the Si (111) double crystal monochromator

tuned to 28 keV incident energy, the distance from sample to source was approximately 55 m, and the X-ray dose is estimated to be 1 kGy. Two-dimensional projections were taken at 0.25° rotation angle steps with a one second exposure and combined into a three-dimensional image consisting of 1198 slices with 1920 by 1920 pixels per slice for Pre scans. This resulted in a voxel size of 4.2 μm. Post scans had 1200 slices of 1920 by 1920 pixels and resulted in a voxel size of 4.3 μm. The data were pre-processed by correcting for dark current and flat field and reconstructed using the GridRec fast Fourier transform reconstruction algorithm (Rivers, 2012).

The indicator kriging method was utilized for segmentation of pore/solid in the images using 3DMA-Rock software (Oh and Lindquist, 1999; Wang et al, 2011). Total image porosity (pores > 4 μm in diameter), and the size distribution of > 4 μm diameter pores were collected from each sampled section. The total image porosity was calculated as the percent of pore voxels within the sample voxels. Size distribution of image identified pores was determined using the burn number distribution approach in 3DMA-Rock (Lindquist et al, 2000; Ananyeva et al, 2013). Briefly, the burn number represents the shortest distance from the pore medial axis to the pore wall. For clarity, burn numbers have been converted into pore diameters. I specifically focused the data analyses on the pores of the following four diameter size ranges: 4-15 μm, 15-40 μm, 40-90 μm, and >90 μm. These pore sizes were chosen to match pore sizes previously studied in macro-aggregates that have demonstrated strong associations with carbon in the studied soil (Wang et al, 2012, 2013; Ananyeva et al, 2013; Kravchenko et al, 2014, 2015; Quigley et al, 2018a).

4.2.5 Incubation experimental design

Prior to incubation, water was added from the top of the cores to achieve 50% of water filled pore space. Mini-cores were sealed at the bottom and placed into 10 ml vacutainers (BD

Franklin Lakes NJ, USA) with 1 mL of de-ionized water added to the bottom to maintain high humidity and consistent moisture levels. Samples were then incubated at 22.4±0.1°C for 21 days. Emission of CO_2 and $\delta^{13}C$ measurements were taken at day 1, 3, 7, 14, and 21. An LI-820 CO_2 infrared gas analyzer (Lincoln, Nebraska, USA) was used to take CO_2 measurements. After each CO_2 and $\delta^{13}C$ sampling, the headspace was flushed using CO_2 free air. One sample from conventional tillage intact-structure with root exclusion was lost and was not used in the analysis.

4.2.6 Total C and $\delta^{13}C$ analyses

Soil, rye roots and shoots, and gas samples were analyzed for $\delta^{13}C$ and total C at the Stable Isotope Facility at the University of California Davis. Soil samples were analyzed using an Elementar Vario EL Cube or Micro Cube elemental analyzer (Elementar Analysensysteme GmbH, Hanau, Germany) interfaced to a PDZ Europa 20-20 isotope ratio mass spectrometer (Sercon Ltd., Cheshire, UK). Rye roots and shoots were analyzed using a PDZ Europa ANCA-GSL elemental analyzer interfaced to a PDZ Europa 20-20 isotope ratio mass spectrometer (Sercon Ltd., Cheshire, UK). Gas samples were analyzed using a ThermoScientific GasBench system interfaced to a ThermoScientific Delta V Plus isotope ratio mass spectrometer (ThermoScientific, Bremen, Germany).

The carbon isotopes are reported relative to Vienna PeeDee Belemnite (VPDB) with a 0.1‰ standard deviation for all samples.

4.2.7 Determination of POM and root presence

Both the amount of particulate organic matter (POM) and amount of roots were determined from μCT images, specifically from each image corresponding to the 2 mm sections sampled for $\delta^{13}C$. A piece of organic material was visually identified by grayscale value, shape,

and size. Once designated organic material was identified, it was then classified as POM or root. Organic matter was designated as POM pieces if they were non-root shaped or, if root shaped, did not extend for more than a few hundred microns in any direction. In order to determine the true influence of roots on the sampled soil due to root exudation, roots were counted not only in the sample, but also in a 0.5 mm radius around the sample.

4.2.8 Total N, nitrate, and ammonium

Samples collected for $\delta^{13}C$ and total carbon were too small to determine total N, nitrate, and ammonia concentrations. Due to its lower concentration in soil, measurements for total N require more soil than total C; at least 20 μg for reliable data. For total N, approximately 20-40 μg of soil was sampled from the side of the hole left by the mini-core sampling and analyzed at the Stable Isotope Facility at the University of California Davis on the same instrumentation as used for total C analysis.

Two 10 g samples for nitrate and ammonium determination were collect from the root area of each container. Nitrate and ammonium were then extracted from the soil using a 1M KCl solution. Concentrations of nitrate and ammonium were determined using a Biotek Synergy H1 microplate reader. Nitrate was determined via vanadium(III) sulfanilamide and N-(1-naphthyl)-ethylenediamine dihydrocloride (NED) solution (Doane and Horwáth, 2003), while ammonium concentration was determined by salicylate and cyanurate assay (Sinsabaugh et al, 2000).

4.2.9 Statistical analysis

Comparisons between treatments were conducted using the mixed model approach implemented in the PROC MIXED procedure of SAS Version 9.4 (SAS Inc., 2009).

The analysis of $\delta^{13}CO_2$ data collected during the incubation used the statistical model with fixed effects of management history, structure, root presence (samples next to plants and

samples from root exclusion area), day (1, 3, 7, 14, and 21), and their interactions. The model also included the random effects of containers nested within management history and structure as well as root by container interaction. Day was treated as a repeated measure in the analysis.

The statistical model for the analysis of the soil samples for pores, total carbon, and $\delta^{13}C$ consisted of the fixed effects of the management history, soil structure, root presence, incubation status (Pre and Post), and their interactions. The model included the random effects of container within management and structure as well as the interaction of root presence with container.

The normality assumption was visually assessed using normal probability plots and stem-and-leaf plots, while equal variance assumption was assessed using Levene's test. Where the equal variance assumption was violated, analysis with unequal variances was conducted (Milliken and Johnson, 2009). Significant differences are reported at α=0.05.

Regression analyses between pore characteristics and $\delta^{13}C$ were conducted using the ANCOVA approach in the PROC MIXED procedure in SAS Version 9.4 (SAS Inc., 2009). Three data points from the biologically based Pre interaction were excluded from the analysis due to the high $\delta^{13}C$ values, which were driven by the presence of root material within the samples. The regressions slopes significant at the 0.05 level were reported. Multiple regression analysis was performed with the PROC REG procedure in SAS Version 9.4 (SAS Inc., 2009) and adjusted R^2 selection was used to determine the best model.

4.3. Results

4.3.1 Soil and plant characteristics

Prior to rye planting, the only observed differences between soil characteristics were due to soil management history (Table 4.1). Soil from biologically based treatment had higher total C

and N levels and more depleted $\delta^{13}C$ than soil from conventional management. The two soils did not differ in their bulk density.

Table 4.1: Bulk density in g/cm^3 (n=8), $\delta^{13}C$ (n=12), total C (n=12), and total N (n=12) from the soil before rye planting. Shown are means and standard errors (in parenthesis). Letters indicate significant differences within each column at α=0.05.

Management	Structure	Bulk Density	$\delta^{13}C$	Total C (%C)	Total N (%N)
Biological	Intact	1.49(0.05)a	-23.2(0.6)a	0.86(0.01)a	0.085(0.005)a
Biological	Destroyed	1.46(0.05)a	-23.9(0.2)a	0.84(0.09)a	0.094(0.002)a
Conventional	Intact	1.37(0.05)a	-22.3(0.6)b	0.59(0.02)b	0.066(0.005)b
Conventional	Destroyed	1.46(0.05)a	-21.9(0.2)b	0.60(0.02)b	0.062(0.002)b

The chemical characteristics of the rye roots grown in intact- and destroyed-structure soils were similar, except $\delta^{15}N$, which was more depleted in intact-structure soils (Table 4.2). The enrichment of the rye roots was uniform for all treatments and structures.

Table 4.2: Means of the chemical characteristics of pulse labeled rye roots (n=43). Standard errors are shown in parenthesis. Letters indicate significant differences within each column at α=0.05.

Structure	$\delta^{13}C$	Total C (%C)	$\delta^{15}N$	Total N (%N)
Intact	571(103)a	28(1)a	4.5(0.5)b	1.2(0.1)a
Destroyed	521(103)a	25(2)a	1.7(0.5)a	0.9(0.1)a

There were no observed differences between ammonia and nitrate concentrations in the soils after 3 months of rye growth (Table 4.3). Total nitrogen was higher in biologically based management history samples. Intact-structure with roots in conventional management was lower than the other conventional management history treatments. Intact-structure conventional with roots was the only treatment to not gain nitrogen during rye growth. After 3 months of rye growth, total carbon was higher in the biologically based management with roots, but not without roots compared to the conventional management.

Table 4.3: Total C (n=40), Total N (n=40), ammonia (n=16), and nitrate (n=16) means from the soil after rye growth. Standard errors are shown in parenthesis. Letters indicate significant differences within each column at α=0.05.

Management	Structure	Root	Total N (%N)	Total C (%C)	Ammonia (ppm)	Nitrate (ppm)
Biological	Intact	Root	0.094(0.007)a	1.00(0.06)a	0.13(0.03)a	0.19(0.02)a
Biological	Intact	No Root	0.108(0.006)a	0.88(0.05)ad		
Biological	Destroyed	Root	0.101(0.004)a	0.97(0.02)a	0.15(0.03)a	0.14(0.02)a
Biological	Destroyed	No Root	0.094(0.004)a	0.89(0.06)ad		
Conventional	Intact	Root	0.067(0.006)c	0.64(0.04)ab	0.13(0.03)a	0.14(0.02)a
Conventional	Intact	No Root	0.088(0.007)ab	0.79(0.08)bd		
Conventional	Destroyed	Root	0.074(0.004)bc	0.77(0.04)b	0.13(0.03)a	0.13(0.02)a
Conventional	Destroyed	No Root	0.072(0.004)bc	0.71(0.02)bd		

Root presence decreased the amount of POM in all managements and structures (Table 4.4). Biologically based management history had significantly more POM than conventional. The amount of roots did not vary significantly between any studied treatments.

Table 4.4: Mean of POM (n=16) and roots (n=8) in samples identified and counted from μCT images. Standard errors are shown in parenthesis. Letters indicate significant differences within each column at α=0.05.

Management	Structure	Root	POM	Roots
Biological	Intact	Root	19.1(1.5)ab	6.7(4.0)a
Biological	Intact	No Root	30.4(3.1)c	
Biological	Destroyed	Root	21.9(1.5)a	16.1(4.3)a
Biological	Destroyed	No Root	44.2(3.1)d	
Conventional	Intact	Root	7.1(0.9)e	19(4.2)a
Conventional	Intact	No Root	15.2(1.5)bd	
Conventional	Destroyed	Root	7.9(0.9)e	12(4.0)a
Conventional	Destroyed	No Root	14.5(1.5)d	

4.3.2 Pore characteristics

Total image porosity of the soil cores ranged from 12 to 32%. Differences between structure and Pre and Post were observed in the 4-15, 15-40, and 90+ μm pores (Figure 4.3).

Increases in 4-15 µm pores Post were observed for both structures with increases greater in destroyed-structure soils. Both 15-40 and 90+ µm pores had differences between the structures, but where 90+ µm pores saw an increased presence in intact soils, 15-40 µm pores saw a decreased presence.

Figure 4.3: Relative abundances of 4–15, 15–40, 40–90, and >90 µm pores by incubation and management. Relative pore abundance refers to the percent of medial axes per total soil volume as determined from 3DMA-Rock software. Bars represent standard errors. Letters indicate significant differences at a = 0.05.

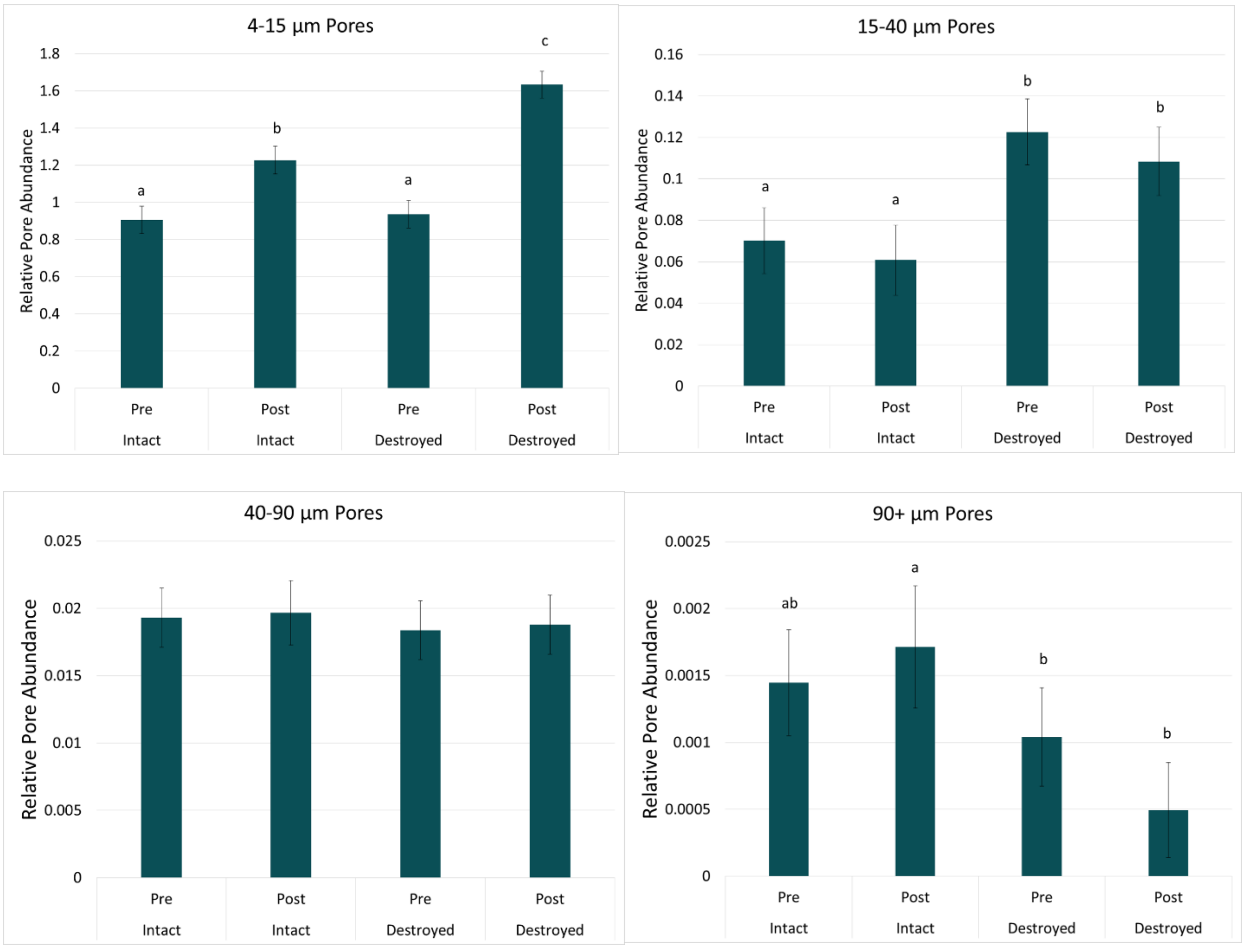

4.3.3 Associations between pores and new carbon

Significant positive correlations between new carbon and pores were only observed in soils prior to incubation and under the influence of roots. Structure was the main driver of observed associations. In intact-structure soils, increases in new carbon were significant in

relation to all observed pore sizes (Figure 4.4). On the other hand, destroyed-structure soils saw significant increases in new carbon only in conjunction with 15-40 and 40-90 µm pores (Figure 4.5).

Figure 4.4: Relationship between $\delta^{13}C$ and relative abundances of 4–15µm pores **(A)**, 15-40 µm pores **(B)**, 40-90 µm pores **(C)**, and >90 µm pores **(D)** for the intact-structure with root for both Pre and Post. Relative pore abundances refer to the percent of medial axes per total soil volume as determined from 3DMA-Rock software. Outliers removed from analysis are circled in orange. Stars next to the end of the lines indicate significant slopes at α=0.05. Gray area indicates 95% confidence interval.

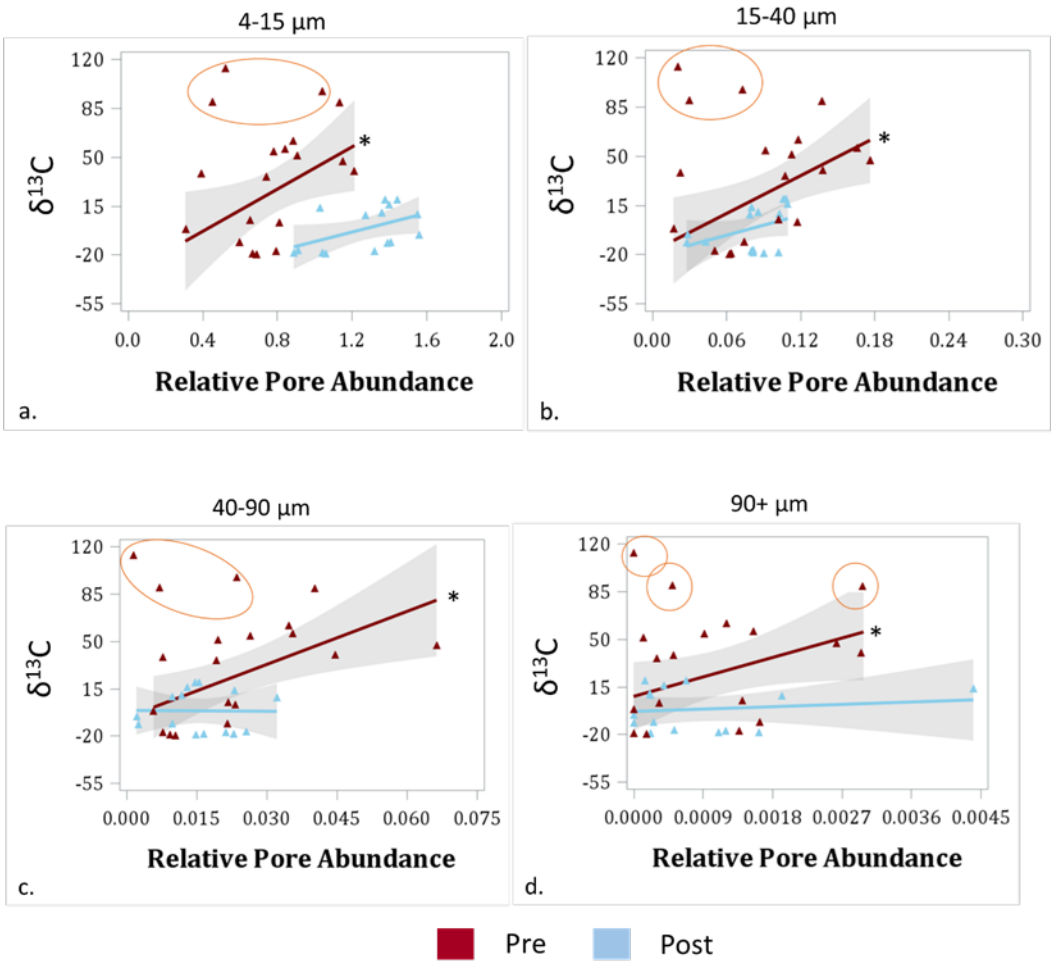

Figure 4.5: Correlations between $\delta^{13}C$ and relative abundances of 4–15µm pores **(A)**, 15-40 µm pores **(B)**, 40-90 µm pores **(C)**, and >90 µm pores **(D)** for destroyed-structure soils when roots are present during both Pre and Post. Relative pore abundances refer to the percent of medial axes per total soil volume as determined from 3DMA-Rock software. Stars next to the end of the lines indicate significant slopes at α=0.05. Gray area indicates 95% confidence interval.

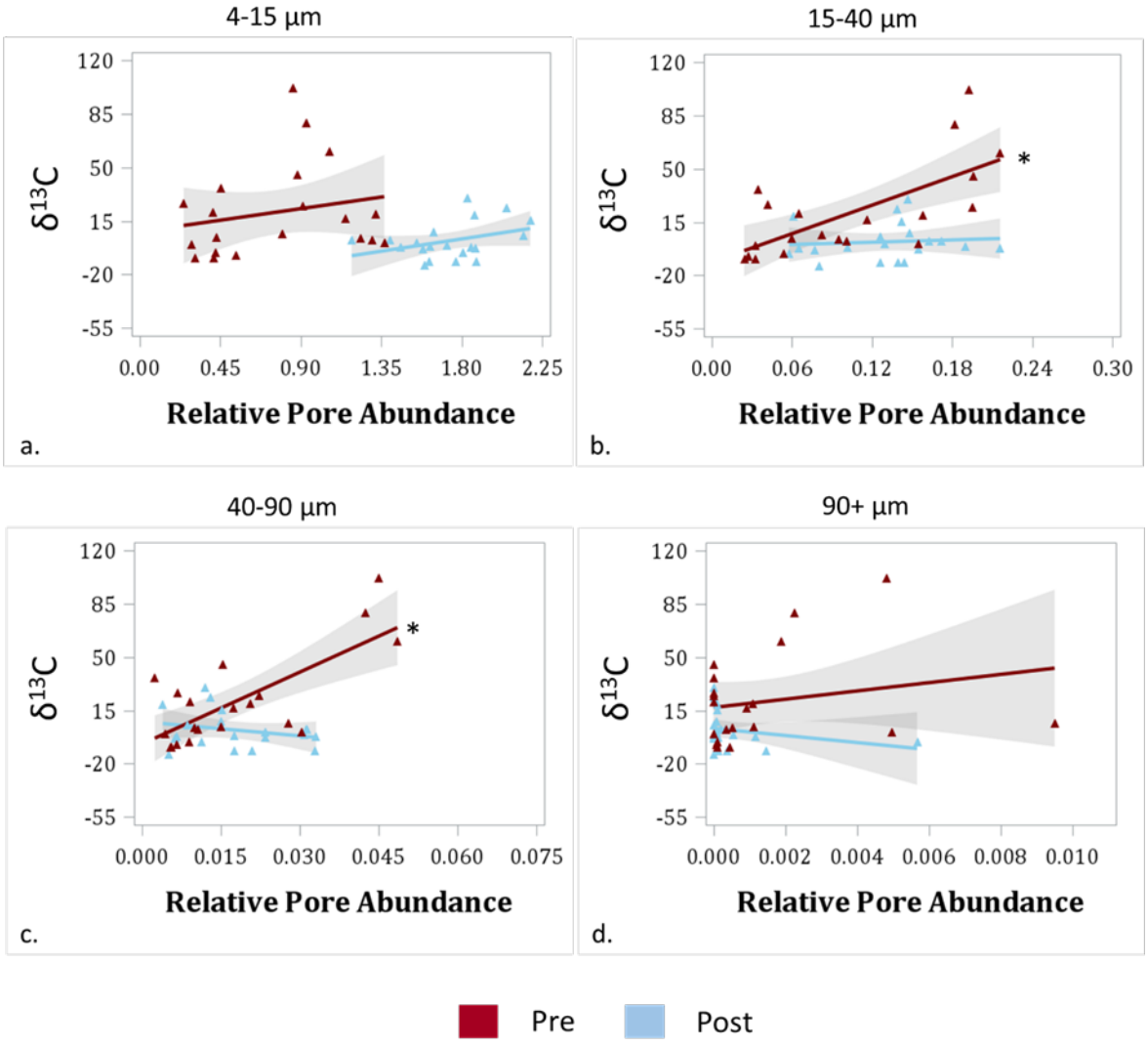

After incubation, intact-structure soils lost substantial amounts of new carbon from the two largest pore sizes, but reduced losses were observed in the two smallest pore sizes. In contrast, destroyed-structure soils lost considerable amounts of new carbon from both 15-40 and 40-90 µm pores.

Multiple regression indicated that the model explaining the most variation for the relationship between $\delta^{13}C$ and pore size distribution for intact-structure soil prior to incubation was the single regression between $\delta^{13}C$ and 40-90 μm pores. The equation for this model was:

$$y=1306 * (40\text{-}90) - 6.54 \quad (4.3)$$

This only had an R^2 of 0.39, indicating that this did not model well the variation in $\delta^{13}C$ values. For destroyed-structure soil, the model that explained the most variation included 4-15, 15-40, and 40-90 μm pores. The equation for this model was:

$$y=886 * (40\text{-}90) + 321 * (15\text{-}40) - 40 * (4\text{-}15) + 2.7 \quad (4.4)$$

This model had an R^2 of 0.68 indicating that this model explained most of the variation in $\delta^{13}C$ values. Both 4-15 and 15-40 μm pores were drivers of this model (P-value of 0.02 and 0.03, respectively).

4.3.4 Utilization of carbon during incubation

Prior to the incubation of the soil cores, the only significant factor in regards to amount of new carbon added to the soil by rye was whether roots were present or not. This indicates that root presence was the main contributor to new carbon incorporation into the soil during rye growth. After incubation, while root presence was still a significant factor, management history and structure played a larger role in whether new carbon was utilized within each soil by microorganisms during the incubation. For example, the conventional management history with intact-structure and roots exhibited a minimal loss of new carbon, while biologically based intact-structure with roots lost a substantial portion of its new carbon (Figure 4.6a). In the destroyed-structure, biologically based management history lost an insubstantial amount of new carbon, while the conventional lost a noteworthy amount of new carbon. The amount of new

carbon added during rye growth without roots was not significantly different from zero (Table 4.5).

Figure 4.6: µg of new carbon in the soil Pre and Post **(A)** and released as CO_2 during incubation **(B)**. Bars indicate standard errors. Stars indicate significant differences between Pre and Post for soil carbon and intact- and destroyed-structure for CO_2 at α=0.05.

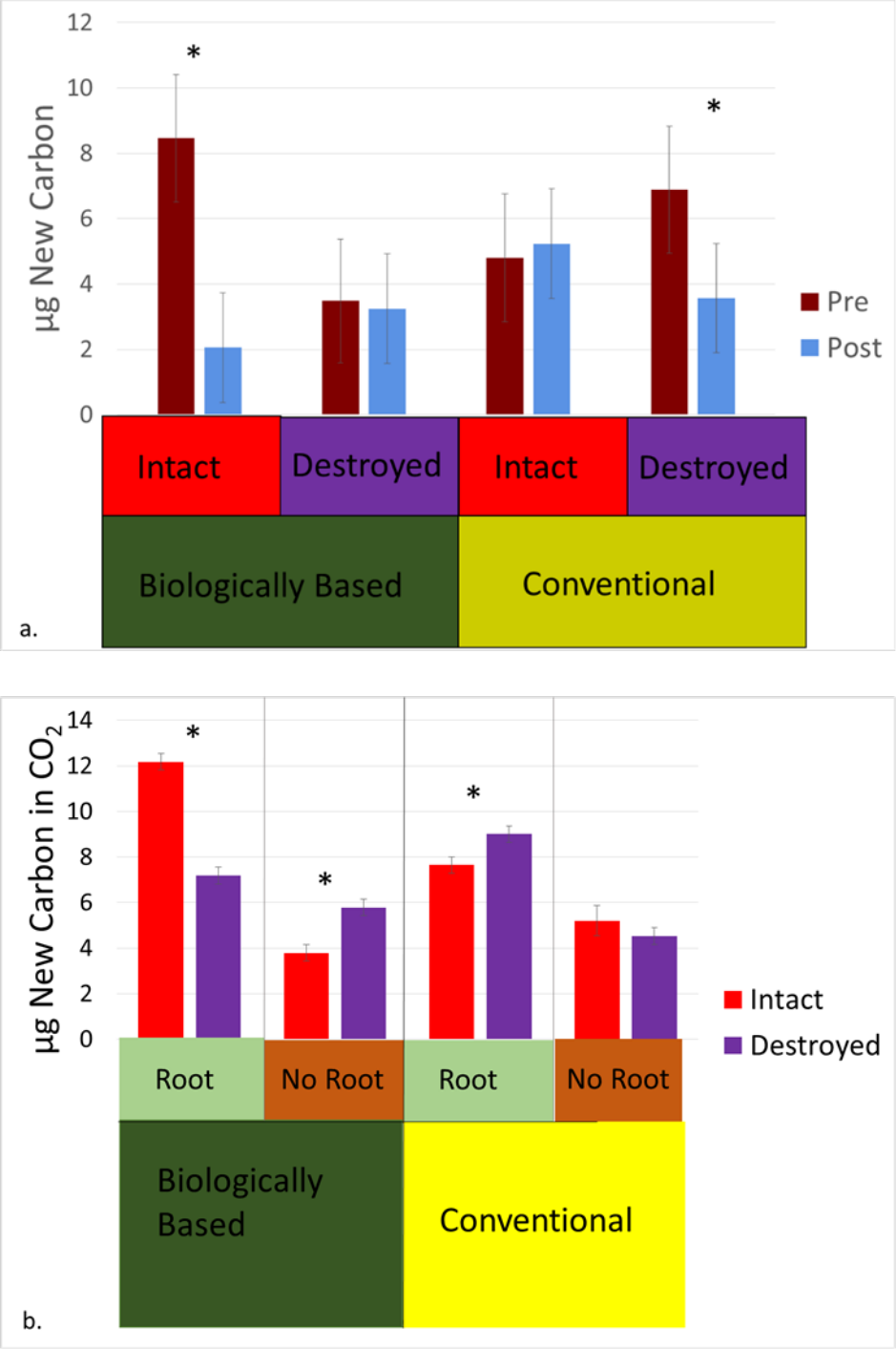

Table 4.5: Mean µg of new carbon in the soil without roots Pre and Post incubation. Standard errors are shown in parenthesis. No statistical differences were found.

Management	Structure	Incubation	µg New Carbon
Biological	Intact	Pre	1.1(1.9)
Biological	Intact	Post	0.5(1.7)
Biological	Destroyed	Pre	0.6(1.8)
Biological	Destroyed	Post	0.9(1.7)
Conventional	Intact	Pre	1.6(1.9)
Conventional	Intact	Post	-0.9(2.0)
Conventional	Destroyed	Pre	1.3(1.9)
Conventional	Destroyed	Post	1.0(1.7)

During the incubation, intact-structure biologically based management history with roots lost the most new carbon, while destroyed-structure biologically based without roots lost the least new carbon (Figure 4.6b). An interesting pattern emerged between the two management histories. Biologically based, with roots present, lost more new carbon in intact-structure soils, while conventional with roots lost the most new carbon in destroyed-structure. However, when roots were not present, biologically based soil lost more new carbon in destroyed treatments, while conventional soil saw no differences between structures.

4.4. Discussion

In intact-structure soil, that is, in soil with legacy root channels, additions of new carbon were equally associated with all studied pore sizes. However, in destroyed-structure soils, where older root channels were not present, new carbon was positively associated only with the 15-90 µm pores. This preferential addition signal was lost after incubation, indicating that greater losses of new carbon occurred in those same pores where it was initially preferentially added.

4.4.1 Carbon addition during rye growth

In intact-structure soil new carbon was positively associated with all studied pore sizes (Figure 4.4). However, multiple regression indicated that the association with presence of 40-90 µm pores was the strongest (Equation 4.3). Plant roots are >40 µm diameter in size and it has

been shown that they can only enter pores of this size or greater (Wiersum, 1957; Cannell, 1977). Therefore, a direct contribution of rye plant roots likely occurred within the 40-90 μm or >90 μm pores. Previous work also has shown these pores to be associated with new carbon additions (Quigley et al, 2018a). However, the R^2 value is low, which indicates substantial contribution of other factors to the observed variation in $\delta^{13}C$ values.

One of such confounding factors is preferential root growth into already established pores of old root channels (Rasse and Smucker, 1998). If the growth of roots of specific size are a controlling factors in new carbon addition, but the roots grow through pores of larger size, this would uncouple root size and pore size, potentially dismissing pore size limitations on new root carbon additions. This preferential root growth may also explain the association of new carbon with >90 μm pores in these soils.

Fungal growth and transport is another factor that may explain the increases in new carbon associated with the 15-40 μm pores (Figure 4.4b, 4.5b). These pores are too small for plant roots to enter, but fungal mycelia can enter these pores and they have been known to push aside silt particles to create 20-30 μm pores (Dorioz et al, 1993; Bearden, 2001; Emerson and McGarry, 2003). In intact-structure soil of this study, this relationship would be associated with carbon transport through an existing fungal network. Fungi are known to be able to transport carbon great distances (Godbold et al, 2006) and some are reliant on plants for lipids and other building materials (Luginbuehl et al, 2017). This means that a well-established fungal network can and does transport new carbon throughout its hyphae network. In destroyed-structure soils, on the other hand, the fungal network was broken by sieving and, therefore, the associations with new carbon and 15-40 μm pores is more likely related to the re-establishment of the fungal network rather than transport through the fungal network.

Unlike intact-structure soil, the multiple regression model that explained the most variation in destroyed-structure soils included 4-15, 15-40, and 40-90 μm pores with 4-15 and 15-40 μm pores contributing the most to the model (Equation 4.4). While 15-40 and 40-90 μm pores were positively associated with new carbon, 4-15 μm pores were negatively associated with new carbon. This indicates that new carbon was unable to enter 4-15 μm pores. Roots would not be able to penetrate 4-15 μm pores and, while fungal mycelia can partially enter these pores, the destruction of the fungal network would limit the extent that fungi could deposit new carbon into these pores. Additionally, these pores would be potential reservoirs of protected carbon due to the prevalence of anaerobic conditions, potentially decreasing new carbon preservation in destroyed soils, which was seen in the conventional management soils (Figure 4.6). Keiluweit et al (2017) found that anaerobic micro-sites in upland soils can retard decomposition by 10-fold, effectively protecting carbon. Pores of 4-15 μm would be mostly water filled as pores of 10 μm are permanently water filled at field conditions, resulting in anaerobic conditions (Schurgers et al, 2006). The creation of new root pores, instead of using older root channels, may have also retarded the transport of new carbon from roots to the surrounding soil. Quigley et al (2018a) found increased grayscale values in the vicinity of root pores in destroyed-structure soils. This was believed to be due to compaction as the root grew. This compacted soil around the root would restrict flow of carbon from new roots to the rest of the soil and, therefore, prevent the spread of new carbon to smaller pores.

4.4.2 Carbon utilization during incubation

The observed positive relationships between pores and carbon were lost after incubation (Figure 4.4, 4.5). This indicates that either gains of new carbon were lost as CO_2 or that they were distributed more evenly through the soil. Due to the significant loss of new carbon observed

in soil from biologically based management with intact-structure and in soil from conventional management with destroyed-structure (Figure 4.6), the loss as CO_2 is more likely the explanation. On the other hand, the relative lack of carbon loss in biologically based destroyed-structure and conventional management intact-structure (Figure 4.6) indicates redistribution in the soil. The difference in biologically based management may relate to availability of older carbon. Soil from biologically based management had higher POM as compared to conventional (Table 4.4). However, this POM would mostly likely be physically protected and inaccessible to decomposers in intact-structure soils, while fresh roots would be more easily available, increasing new carbon usage. In destroyed-soils, POM would have lost its physical protection and therefore, was more available for decomposition. This could result in preferential decomposition of POM over fresh roots in these soils, resulting in less new carbon losses.

In soils from conventional management, POM is sparse (Table 4.4) and, therefore, could not explain the difference between new carbon utilization in intact-structure and destroyed-structure soils. With little available POM, new material would preferentially be used in both structures. However, the compaction around roots in destroyed-structure soil would restrict carbon flow out of the 40-90 μm pores, which are known to have increased microbial activities (Chenu et al, 2001; Strong et al, 2004; Ruamps et al, 2011). This restriction to pores with increased microbial activities would promote complete oxidation of root material to CO_2 over preservation of the intermediates. However, in intact-structure soil, roots preferentially grew in old root channels, which Quigley et al (2018b) showed did not have adjacent soil compaction. This would not restrict carbon to 40-90 μm pores, allowing for transport to pores where preservation was more likely to occur.

While both intact-structure and destroyed-structure lost new carbon from soil pores during incubation, intact-structure lost substantial amount of new carbon, specifically from 40-90 and >90 μm pores, resulting in a flat non-significant association with these pores (Figure 4.4). However, 4-15 and 15-40 μm pores were still positively related, potentially indicating preferential new carbon preservation in these pores. Both Quigley et al (2018a) and Ananyeva et al (2013) found increased carbon in association with 15-40 μm pores, which may support this postulate of preferential carbon preservation in soils with intact-structure within these pores. Destroyed-structured soil preferentially lost new carbon from both 15-40 and 40-90 μm pores after incubation (Figure 4.5), which is consistent with previous investigations of destroyed-structure soils (Quigley et al, 2018a).

4.4.3 POM, roots, and nitrogen

The numbers of POM fragments in the studied soil revealed an interesting pattern (Table 4.4). Consistent with previous reports, POM was approximately twice as abundant in biologically based management compared to conventional (Kravchenko et al, 2014). However, the difference between the treatments with and without roots was consistent with the concept of priming. Priming is the addition of new carbon stimulating the decomposition of older carbon (Kuzyakov et al, 2000; Fontaine et al, 2004; Schimel and Schaeffer, 2012; Blagodatskaya et al, 2014). POM in the treatments without roots were approximately twice as prevalent as treatments with roots, indicating priming took place during rye growth (Table 4.4).

The finding of similar nitrate and ammonium concentrations were unexpected (Table 4.3). Total soil nitrogen was lower in the conventional management prior to rye planting (Table 4.1). This would indicate less sources of nitrogen available as nitrate and ammonium to the plants, since no fertilizer was added to the soil during rye growth. Additionally, sieving the soil

would have exposed protected organic matter and, therefore, potentially increased soil nitrogen mineralization (Fukumasu and Shaw, 2017). However, rye is known as an efficient nitrogen scavenger (Staver and Brinsfield, 1990; Strock et al, 2004) and, therefore, may have been responsible for the similar nitrate and ammonium concentrations present after its growth.

The pattern of total nitrogen was as predicted in the conventional intact-structure soils (Table 4.1, 4.3). Rye growth, due to its efficiency as a nitrogen scavenger, was expected to lower nitrogen levels in the soil. This was observed in the conventional intact-structure soil. However, the increases in total nitrogen in the biologically based management soils and destroyed-structure conventional management soils during rye growth was unanticipated. I hypothesize that free living nitrogen fixing bacteria in the soil are responsible for this increase. Increases were more prevalent in the biologically based management. While activity of free living nitrogen fixing bacteria has not been measured in these soils, overall microbial activity is known to be increased in the biologically based management (Xue et al, 2013). This would result in more nitrogen fixation occurring in this management.

4.4.4 Soil aggregates vs. intact soil cores

Prior to the use of μCT images, research on soil carbon was limited to measuring the distribution of soil aggregates (Six et al, 2000). While useful as an indicator of soil carbon addition (Six et al, 1999; Denef et al, 2004; 2007), underlying mechanisms were unknown as the relationship between pores and aggregates, while theoretically inversely related, was ambiguous (Six and Paustian, 2014). Furthermore, it was unknown if soil pores have the same function in aggregates of different size fractions and, therefore, it is unclear if aggregate data can be extrapolated to the intact soil (Young and Ritz, 2000; Young et al, 2001).

This study, along with Quigley et al (2018a), and Ananyeva et al (2013), may help bridge the gap between soil pore studies based on μCT images and aggregate studies. The results from all three studies are consistent in the relationships between pores and carbon, however, Ananyeva et al (2013) used strict aggregates, Quigley et al (2018) used soil fragments, and this study used intact mini-cores. Consistent results obtained in all three studies suggest that pores behave the same, in regards to carbon, regardless of whether located in aggregates or intact soil. Furthermore, the behavior of pores was independent of management. This indicates that aggregate distributions, if they can be connect to pore distributions, would be useful as a proxy, at least for carbon.

4.5 Conclusion

Distributions of new soil carbon in relation to pores was different before and after incubations. Prior to incubation, the disturbace level of soil structure was the major regulator of new soil carbon additions. In intact-structure soils, new carbon addition was associated with all studied pore sizes, potentially directed by the influence of legacy root channels and fungal activities with 40-90 μm pores being important new carbon sources. In destroyed-structure soils, new carbon addition was related to 4-15, 15-40, and 40-90 μm pores, with 15-40 and 40-90 μm pores having a positive association while 4-15 μm pores having a negative association with new carbon. This indicates that new carbon is unable to reach the 4-15 μm pores in destroyed-structure soils. Overall, pores play a large role in new carbon addition but can be masked when legacy root channels are present.

After incubation, no associations between new carbon and pore sizes were observed. Management history, seemed to play a larger role in whether new carbon was utilized or not. Biologically based management with intact-structure and conventional with destroyed-structure

both lost significant amounts of new carbon during the incubation. Biologically based with destroyed-structure and conventional with intact-structure lost negligible amounts of new carbon. These patterns may relate to POM availability and root carbon mobility. Losses of carbon were most visible in relation to 40-90 μm pores implicating these pores as both important for carbon addition and carbon loss. This association was independent of management, indicating a universal mechanism for these pores.

Funding

Support for this research was provided in part by the USDA-NIFA, Award No. 2016-67011-24726 “Using stable isotopes and computer tomography to determine mechanisms of soil carbon protection in cover crop based agricultural systems” and by the US National Science Foundation Long-Term Ecological Research Program (DEB 1027253) at the Kellogg Biological Station and by Michigan State University AgBioResearch. Portions of this work were performed at GeoSoilEnviroCARS (The University of Chicago, Sector 13), Advanced Photon Source (APS), Argonne National Laboratory. GeoSoilEnviroCARS is supported by the National Science Foundation - Earth Sciences (EAR - 1634415) and Department of Energy- GeoSciences (DE-FG02-94ER14466). This research used resources of the Advanced Photon Source, a U.S. Department of Energy (DOE) Office of Science User Facility operated for the DOE Office of Science by Argonne National Laboratory under Contract No. DE-AC02-06CH11357.

REFERENCES

REFERENCES

Abraha, M., Hamilton, S. K., Chen, J., and Robertson, G. P. (2018). Ecosystem carbon exchange on conversion of Conservation Reserve Program grasslands to annual and perennial cropping systems. *Agric For Meteorol.* 253-254, 151-160. doi: 10.1016/j.agrformet.2018.02.016

Ananyeva, K., Wang, W., Smucker, A. J. M., Rivers, M. L., and Kravchenko, A. N. (2013). Can intra-aggregate pore structures affect the aggregate's effectiveness in protecting carbon? *Soil Biol. Biochem.* 57, 868-875. doi: 10.1016/j.soilbio.2012.10.019

Austin, E. E., Wickings, K., McDaniel, M. D., Robertson, G. P., and Grandy, S. (20I7). Cover crop root contributions to soil carbon in a no-till corn bioenergy cropping system. *GCB Bioenergy* 9, 1252-1263. doi: 10.1111/gcbb.12428

Bailey, V. L., Smith, A. P., Tfaily, M., Fansler, S. J., and Bond-Lamberty, B. (2017). Differences in soluble organic carbon chemistry in pore waters sampled from different pore size domains. *Soil Biol. Biochem.* 107, 133-143. doi: 10.1016/j.soilbio.2016.11.025

Barber, D. and Martin, J. (1976). Release of organic substances by cereal roots into soil. *New Phytol.* 76, 69-80. doi: 10.1111/j.1469-8137.1976.tb01439.x

Bauer, A. and Black, A. L. (1994). Quantification of the effect of soil organic matter content on soil productivity. *Soil Sci. Soc. Am. J.* 58, 185-193. doi: 10.2136/sssaj1994.03615995005800010027x

Bearden, B. N. (2001). Influence of arbuscular mycorrhizal fungi on soil structure and soil water characteristics of vertisols. *Plant Soil* 229, 245– 258. doi: 10.1023/A:1004835328943

Bengough, A. G., Bransby, M. F., Hans, J., McKenna, S. J., Roberts, T. J., and Valentine, T. A. (2006). Root responses to soil physical conditions; growth dynamics from field to cell. *J. Exp. Bot.* 57, 437-447. doi: 10.1093/jxb/erj003

Bird, J. A., van Kessel, C., and Horwath, W. R. (2003). Stabilization of ^{13}C-carbon and immobilization of ^{15}N-nitrogen from rice straw in humic fractions. *Soil Sci. Soc. Am. J.* 67, 806-816. doi: 10.2136/sssaj2003.0806

Blagodatskaya, E., Khomyakov, N., Myachina, O., Bogomolova, I., Blagodatsky, S., and Kuzyakov, Y. (2014). Microbial interactions affect sources of priming induced by cellulose. *Soil Biol. Biochem.* 74, 39-49. doi: 10.1016/j.soilbio.2014.02.017

Bowen, H. D. (1981). "Alleviating mechanical impedance", in *Modifying the Root Environment to Reduce Crop Stress*, eds. G. F. Arkin and H. M. Taylor (St. Joseph, MI: Am. Soc. Agric. Engineers) 21-57.

Brimecombe, M. J., de Leij, F., and Lynch, J. M. (2001). "The effect of root exudates on rhizosphere microbial populations," in *The rhizosphere: biochemistry and organic substances at*

the soil-plant interface, eds. R. Pinton, Z. Varanini and P. Nannipieri. (New York, New York, USA: Marcel Dekker), 95–140.

Cannell, R. Q. (1977). Soil aeration and compaction in relation to root growth and soil management. *Appl. Biol*. 2, 1-86.

Chenu, C., Hassink, J., and Bloem, J. (2001). Short-term changes in the spatial distribution of microorganisms in soil aggregates as affected by glucose addition. *Biol. Fertil. Soils* 34, 349-356. doi: 10.1007/s003740100419

Chimento, C., Almagro, M., and Amaducci, S. (2016). Carbon sequestration potential in perennial bioenergy crops: the importance of organic matter inputs and its physical protection. *GCB Bioenergy* 8, 111-121. doi: 10.1111/gcbb.12232

Crum, J. R. and Collins, H. P. (1995). KBS Soils [Online]. W. K. Kellogg Biological Station Long-Term Ecological Research Project, Michigan State University, Hickory Corners, MI. http://www.lter.kbs.msu.edu/soil/characterization.

Davidson, E. A. and Janssens, I. A. (2006). Temperature sensitivity of soil carbon decomposition and feedbacks to climate change. *Nature* 440, 165-173. doi: 10.1038/nature04514

Denef, K., Six, J., Merckx, R., and Paustian, K. (2004). Carbon sequestration in micro-aggregates of no-tillage soils with different clay mineralogy. *Soil Sci. Soc. Am. J.* 68, 1935-1944. doi: 10.2136/sssaj2004.1935

Denef, K., Zotarelli, L., Boddey, R. M., and Six, J. (2007). Microaggregate-associated C as a diagnostic fraction for management-induced changes in soil organic carbon in two Oxisols. *Soil Biol. Biochem*. 39, 1165-1172. doi: 10.1016/j.soilbio.2006.12.024

Dexter, A. R. (1987). Compression of soil around roots. *Plant Soil* 97, 401-406. doi: 10.1007/BF02378351

Doane, T. A. and Horwáth, W. R. (2003). Spectroscopic determination of nitrate with a single reagent. *Anal. Lett.* 36, 2713-2722. doi: 10.1081/AL-120024647

Dorioz, J. M., Robert, M., and Chenu, C. (1993). The role of roots, fungi and bacteria on clay particle organization. An experimental approach. *Geoderma* 56, 179– 194. doi:10.1016/0016-7061(93)90109-X

Dungait, J. A. J., Hopkins, D. W., Gregory, A. S., and Whitmore, A. P. (2012). Soil organic matter turnover is governed by accessibility not recalcitrance. *Global Change Biol.* 18, 1781-1796. doi: 10.1111/j.1365-2486.2012.02665.x

Ekschmitt, K., Kandeler, E., Poll, C., Brune, A., Buscot, F., Friedrich, M., et al. (2008). Soil-carbon preservation through habitat constraints and biological limitations on decomposer activity. *J. Plant Nutr. Soil Sci.* 171, 27-35. doi: 10.1002/jpln.200700051

Ekschmitt, K., Liu, M., Vetter, S., Fox, O., and Wolters, V. (2005). Strategies used by soil biota to overcome soil organic matter stability – why is dead organic matter left over in soil? *Geoderma* 128, 167-176. doi: 10.1016/j.geoderma.2004.12.024

Emerson, W. W. and McGarry, D. (2003). Organic carbon and soil porosity. *Aust. J. Soil Res.* 41, 107–118. doi: 10.1071/SR01064

Falconer, R. E., Battaia, G., Schmidt, S., Baveye, P., Chenu, C., and Otten, W. (2015). Microscale heterogeneity explains experimental variability and non-linearity in soil organic matter mineralization. *PloS One*. 10: e0123774. doi: 10.1371/journal.pone.0123774

Falkowski, P., Scholes, R. J., Boyle, E., Canadell, J., Canfield, D., Elser, J., et al. (2000). The global carbon cycle: a test of our knowledge of Earth as a system. *Science*. 290, 291-296. doi: 10.1073/pnas.0811302106

Fontaine, S., Bardoux, G., Abbadie, L., and Mariotti, A. (2004). Carbon input to soil may decrease soil carbon content. *Ecol Lett* 7, 314-320. doi: 10.1111/j.1461-0248.2004.00579.x

Fukumasu, J. and Shaw, L. (2017). The role of macro-aggregation in regulating enzymatic depolymerization of soil organic nitrogen. *Soil Bio. Biochem.* 115, 100-108. doi: 10.1016/j.soilbio.2017.08.008

Gaillard, V., Chenu, C., and Recous, S. (2003). Carbon mineralization in soil adjacent to plant residues of contrasting biochemical quality. *Soil Biol. Biochem.* 35, 93-99. doi: 10.1016/S0038-0717(02)00241-9

Gaillard, V., Chenu, C., Recous, S., and Richard, G. (1999). Carbon, nitrogen and microbial gradients induced by plant residues decomposing in soil. *Eur. J. Soil Sci.* 50, 567-578. doi: 10.1046/j.1365-2389.1999.00266.x

Gale, W. J., Cambardell, C. A., and Bailey, T. B. (2000). Surface residue- and root-derived organic matter under simulated no-till. *Soil Sci. Soc. Am. J.* 64, 196-201. doi: 10.2136/sssaj2000.641196x

Garten, C. T. and Wullschleger, S. D. (1999). Soil carbon inventories under a bioenergy crop (switchgrass): measurement limitations. *J Environ. Qual* 28, 1359-1365. doi: 10.1016/j.biombioe.2010.08.013

Godbold, D. L., Hoosbeek, M. R., Lukac, M., Cotrufo, M. F., Janssens, I. A., Ceulemas, R., et al. (2006). Mycorrhizal hyphal turnover as a dominant process for carbon input into soil organic matter. *Plant Soil* 281, 15-24. doi: 10.1007/s11104-005-3701-6

Graecen, E. L., Farrell, D. A., and Cockroft, B. (1968). Soil resistance to metal probes and plant roots. *9th International Congress of Soil Science*, Angus and Roberton, Adelaide. 769-779.

Grandy, A. S. and Neff, J. C. (2008). Molecular C dynamics downstream: the biochemical decomposition sequence and its impact on soil organic matter structure and function. *Sci Total Environ* 404, 297-307. doi: 10.1016/j.scitotenv.2007.11.013

Grandy, A. S. and Robertson, G. P. (2007). Land-use intensity effects on soil organic carbon accumulation rates and mechanisms. *Ecosystems* 10, 58-73. doi: 10.1007/s10021-006-9010-y

Jackson, R. B., Lajtha, K., Crow, S. E., Hugelius, G., Kramer, M. G., and Piñeiro, G. (2017). The ecology of soil carbon: pools, vulnerabilities, and biotic and abiotic controls. *Annu Rev Ecol Evol Syst*. 48, 419-445. doi: 10.1146/annurev-ecolsys-112414-054234

Kallenbach, C. M., Frey, S. D., and Grandy, A. S. (2016). Direct evidence for microbial-derived soil organic matter formation and its ecophysiological controls. *Nat. Commun.* 7:13630. doi: 10.1038/ncomms13630

Kallenbach, C. M., Grandy, A. S., Frey, S. D., and Diefendorf, A. F. (2015). Microbial physiology and necromass regulate agricultural soil carbon accumulation. *Soil Biol. Biochem* 9, 279-290. doi: 10.1016/j.soilbio.2015.09.005

Keel, S. G., Liefeld, J., Mayer, J., Taghizadeh-Toosi, A., and Olesen, J. E. (2017). Large uncertainty in soil carbon modelling related to method of calculation of plant carbon input in agricultural systems. *Eur. J. Soil Sci.* 68, 953-963. doi: 10.1111/ejss.12454

Keiluweit, M., Wanzek, T., Kleber, M., Nico, P., and Fendorf, S. (2017). Anaerobic microsites have an unaccounted role in soil carbon stabilization. *Nat. Commun.* 8: 1771. doi: 10.1038/s41467-017-01406-6

Kell, D. B. (2012). Large-scale sequestration of atmospheric carbon via plant roots in natural and agricultural ecosystems: why and how. *Philos T R Soc B.* 367, 1589-1597. doi: 10.1098/rstb.2011.0244

Kong, A. Y. Y. and Six, J. (2010). Tracing root vs. residue carbon into soils from conventional and alternative cropping systems. *Soil Sci. Soc. Am. J.* 74, 1201-1210. doi: 10.2136/sssaj2009.0346

Kravchenko, A. N., and Guber, A. K. (2017). Soil pores and their contributions to soil carbon processes. *Geoderma* 287, 31-39. doi: 10.1016/j.geoderma.2016.06.027

Kravchenko, A. N., Negassa, W. C., Guber, A. K., Hildebrandt, B., Marsh, T. L., and Rivers, M. L. (2014). Intra-aggregate pore structure influences phylogenetic composition of bacterial community in macroaggregates. *Soil Sci. Soc. Am. J.* 78, 1924-1939. doi: 10.2136/sssaj2014.07.0308

Kravchenko, A. N., Negassa, W. C., Guber, A. K., and Rivers, M. L. (2015). Protection of soil carbon within macro-aggregates depends on intra-aggregate pore characteristics. *Sci. Rep.* 5:16261. doi: 10.1038/srep16261

Kuzyakov, Y., and Blagodatskaya, E. (2015). Microbial hotspots and hot moments in soil: concept & review. *Soil Biol. Biochem.* 83, 184-199. doi: 10.1016/j.soilbio.2015.01.025

Kuzyakov, Y., Friedel, J. K., and Stahr, K. (2000). Review of mechanisms and quantification of priming effects. *Soil Biol. Biochem.* 32, 1485-1498. doi: 10.1016/S0038-0717(00)00084-5

Kuzyakov, Y., Leinweber, P., Sapronov, D., and Eckhardt, K. U. (2008). Qualitative assessment of rhizodeposits in non-sterile soil by analytical pyrolysis. *J. Plant Nutr.* 166, 719-723. doi: 10.1002/jpln.200320363

Lal, R. (1999). Soil management and restoration for carbon sequestration to mitigate the accelerated greenhouse effect. *Prog. Env. Sci.* 1, 307-326. doi: 10.1055/s-2008-1072270

Lal, R. (2006). Enhancing crop yields in the developing countries through restoration of the soil organic carbon pool through restoration of the soil organic carbon pool in agricultural lands. *Land Degrad. Develop.* 17, 197-209. doi: 10.1002/ldr.696

Lal, R. (2011). Sequestering carbon in soils of agro-ecosystems. *Food Policy.* 36, S33-S39. doi: 10.1016/j.foodpol.2010.12.001

Lindquist, W. B., Venkatarangan, A., Dunsmuir, J., and Wong, T. (2000). Pore and throat size distributions measured from synchrotron X-ray tomographic images of Fontainebleau sandstornes. *J. Geophys. Res.* 105, 21,509-21,527. doi: 10.1029/2000JB900208

Luehmann, M. D., Peter, B. G., Connallon, C. B., Schaetzl, R. J., Smidt, S. J., Liu, W., et al. (2016). Loamy, two-storied soils on the outwash plains of southwestern lower Michigan: Pedoturbation of loess and the underlying sand. *Ann Am Assoc Geogr.* 106, 551-572. doi: 10.1080/00045608.2015.1115388

Luginbuehl, L. H., Menard, G. N., Kurup, S., Van Erp, H., Radhakrishnan, G. V., Breakspear, A., et al. (2017). Fatty acids in arbuscular mycorrhizal fungi are synthesized by the host plant. *Science*. 356, 1175-1178. doi: 10.1126/science.aan0081

Mazzilli, S. R., Kemanian, A. R., Ernst, O. R., Jackson, R. B., and Piñero, G. (2015). Greater humification of belowground than aboveground biomass carbon into particulate soil organic matter in no-till corn and soybean crops. *Soil Bio. Biochem.* 85, 22-30. doi: 10.1016/j.soilbio.2015.02.014

Meharg, A. A. and Killham, K. (1991). A novel method of quantifying root exudation in the presence of soil microflora. *Plant Soil* 113, 111-116. doi: 10.1007/BF00010488

Melsted, S. W. (1954). New concepts of management of corn belt soils. *Adv. Agron.* 6, 121-142. doi: 10.1016/S0065-2113(08)60383-1

Milliken, G .A. and Johnson, D. E. (2009). Analysis of Messy Data Volume I: Designed Experiments, second ed. Boca Raton, FL: CRC Press.

Necpálová, M., Anex Jr., R. P., Kravchenko, A. N., Abendroth, L. J., Del Grosso, S. J., Dick, W. A., et al. (2014). What does it take to detect a change in soil carbon stock? A regional comparison of minimum detectable difference and experiment duration in the north central United States. *J Soil Water Conserv.* 69, 517-531. doi: 10.2489/jswc.69.6.517

Oechel, W. C. and Vourlitis, G. L. (1994). The effects of climate change on land-atmosphere feedbacks in arctic tundra regions. *Trends Ecol Evol*. 9, 324-329. doi: 10.1016/0169-5347(94)90152-X

Oh, W., and Lindquist, W. B. (1999). Image thresholding by indicator kriging. *IEEE Trans. Pattern Anal. Mach. Intell.* 21, 590-602. doi: 10.1109/34.777370

Park, E. J., Sul, W. J., and Smucker, A. J. M. (2007). Glucose additions to aggregates subjected to drying and wetting cycles promote carbon sequestration and aggregate stability. *Soil Biol. Biochem.* 39, 2758-2768. doi: 10.1016/j.soilbio.2007.06.007

Paustian, K., Lehmann, J., Ogle, S., Reay, D., Robertson, G. P., and Smith, P. (2016). Climate-smart soils. *Nature* 532, 49-57. doi: 10.1038/nature17174

Quigley, M. Y., Negassa, W. C., Guber, A. K., Rivers, M. L., and Kravchenko, A. N. (2018a). Influence of pore characteristics on the fate and distribution of newly added carbon. *Front. Environ. Sci.* 6:51. doi: 10.3389/fenvs.2018.00051

Quigley, M. Y., Rivers, M. L., and Kravchenko, A. N. (2018b). Patterns and sources of spatial heterogeneity in soil matrix from contrasting long term management practices. *Front. Environ. Sci.* 6:28 doi: 10.3389/fenvs.2018.00028

Raun, L. and Robertson, G. P. (2013). Initial nitrous oxide, carbon dioxide, and methane costs of converting Conservation Reserve Program grassland to row crops under no-till vs. conventional tillage. *Global Change Biol.* 19, 2478-2489. doi: 10.1111/gcb.12216

Rabot, E., Wiesmeier, M., Schlüter, S., and Vogel, H.-J. (2018). Soil structure as an indicator of soil functions: a review. *Geoderma* 314, 122-137. doi:10.1016/j.geoderma.2017.11.009

Rasse, D. P., Rumpel, C. and Dignac, M.-F. (2005). Is soil carbon mostly root carbon? Mechanisms for a specific stablisation. *Plant Soil* 269, 341-356. doi: 10.1007/s11104-004-0907-y

Rasse, D. P. and Smucker, A. J. M. (1998). Root recolonization of previous root channels in corn and alfalfa rotations. *Plant Soil* 204, 203-212. doi: 10.1023/A:1004343122448

Rivers, M. L. (2012). tomoRecon: High-speed tomography reconstruction on workstations using multi-threading. *Proc. SPIE* 8505:OU. doi:10.1117/12.930022

Rorick, J. D. and Kladivko, E. J. (2017). Cereal rye cover crop effects on soil carbon and physical properties in southeastern Indiana. *J Soil Water Conserv.* 72, 260-265. doi: 10.2489/jswc.72.3.260

Ruamps, L. S., Nunan, N., and Chenu, C. (2011). Microbial biogeography at the soil pore scale. *Soil Biol. Biochem.* 43, 280-286. doi: 10.1016/j.soilbio.2010.10.010

SAS Inc. (2009). *SAS user's guide. Verssion 9.2*. Cary, NC: SAS Inst.

Schimel, J. P. and Schaeffer, S. M. (2012). Microbial control over carbon cycling in soil. *Front. Microbial* 3:348. doi: 10.3389/fmicb.2012.00348

Schurgers, G., Dörsch, P., Bakken, L., Leffelarr, P., and Haugen, L. E. (2006). Modelling soil anaerobiosis from water retention characteristics and soil respiration. *Soil Biol. Biochem.* 38, 2637-2644. doi: 10.1016/j.soilbio.2006.04.016

Senthilkumar, S., Basso, B., Kravchenko, A. N., and Robertson, G. P. (2009). Contemporary evidence of soil carbon loss in the U.S. corn belt. *Soil Sci. Soc. Am. J.* 73, 2078-2086. doi: 10.2136/sssaj2009.0044

Sinsabaugh, R. I., Reynolds, H., and Long, T. M. (2000). Rapid assay for amidohydrolase (urease) activity in environmental samples. *Soil Biol. Biochem.* 32, 2095-2097. doi: 10.1016/S0038-0717(00)00102-4

Six, J., Elliot, E. T., and Paustian, K. (1999). Aggregate and soil organic matter dynamics under conventional and no-tillage systems. *Soil Sci. Soc. Am. J.* 63, 1350-1358. doi: 10.2136/sssaj1999.6351350x

Six, J., Elliott, E. T., and Paustian, K. (2000). Soil macroaggregate turnover and microaggregate formation: a mechanism for C sequestration under no-tillage agriculture. *Soil Biol. Biochem.* 32, 2099-2103. doi: 10.1016/S0038-0717(00)00179-6

Six, J. and Paustian, K. (2014). Aggregate-associated soil organic matter as an ecosystem property and measurement tool. *Soil Biol. Biochem* 68, A4-A9. doi: 10.1016/j.soilbio.2013.06.014

Smet, S., Beckers, E., Plougonven, E., Léonard, A., and Degré, A. (2018). Can the pore scale geometry explain soil sample scale hydrodynamic properties? *Front. Environ. Sci.* 6:20. doi: 10.3389/fenvs.2018.00020

Sprunger C. D. and Robertson, G. P. (2018). Early accumulation of active fraction soil carbon in newly established cellulosic biofuel systems. *Geoderma* 318, 42-51. doi: 10.1016/j.geoderma.2017.11.040

Staver, K. W. and Brinsdield, R. B. (1990). Patterns of soil nitrate availability in corn production systems: Implications for reducing ground water contamination. *J. Soil Water Conserv.* 53, 230-240.

Strock, J. S., Porter, P. M., and Russelle, M. P. (2004). Cover cropping to reduce nitrate loss through subsurface drainage in the northern U.S. Corn Belt. *J. Environ Qual* 33, 1010-1016. doi: 10.2134/jeq2004.1010

Strong, D. T., De Wever, H., Merckx, R., and Recous, S. (2004). Spatial location of carbon decomposition in the soil pore system. *Eur. J. Soil Sci.* 55, 739-750. doi: 10.1111/j.1365-2389.2004.00639.x

Swift, R. S. (2001). Sequestration of carbon by soil. *Soil Sci.* 166, 858-871. doi: 10.1097/00010694-200111000-00010

Syswerda, S. P., Corbin, A. T., Mokma, D. L., Kravchenko, A. N., and Robertson, G. P. (2011). Agricultural management and soil carbon storage in surface vs. deep layers. *Soil Sci. Soc. Am. J.* 75, 92-101. doi: 10.2136/sssaj2009.0414

Toosi, E. R., Kravchenko, A. N., Guber, A. K., and Rivers, M. L. (2017). Pore characteristics regulate priming and fate of carbon from plant residue. *Soil Biol. Biochem.* 113, 219-230. doi: 10.1016/j.soilbio.2017.06.014

Wang, W., Kravchenko, A. N., Johnson, T., Srinivasan, S., Ananyeva, K. A., Smucker, A. J. M., et al. (2013). Intra-aggregate pore structures and *Escherichia coli* distribution by water flow within and movement out of soil macroaggregates. *Vadose Zone J.* 12:4. doi: 10.2136/vzj2013.01.0012

Wang, W., Kravchenko, A. N., Smucker, A. J. M., Liang, W., and Rivers, M. L. (2012). Intra-aggregate pore characteristics: X-ray computed microtomography analysis. *Soil Sci. Soc. Am. J.* 76, 1159-1171. doi: 10.2136/sssaj2011.0281

Wang, W., Kravchenko, A. N., Smucker, A. J. M., and Rivers, M. L. (2011). Comparison of image segmentation methods in simulated 2D and 3D microtomographic images of soil aggregates. *Geoderma*. 162, 231-241. doi: 10.1016/j.geoderma.2011.01.006

Wickings, K. and Grandy, A. S. (2013). Management intensity interacts with litter chemistry and climate to drive temporal patterns in arthropod communities during decomposition. *Pedobiologia* 56, 105-112. doi: 10.1016/j.pedobi.2013.01.001

Wieder, W. R., Grandy, A. S., Kallenback, C. M., and Bonan, G. B. (2014). Integrating microbial physiology and physiochemical principles in soils with MIcorbial-MIneral carbon stabilization (MIMICS) model. *Biogeosci. Discuss.* 11, 1147-1185. doi:10.5194/bgd-11-1147-2014

Wiersum, L. K. (1957). The relationship of the size and structural rigidity of pores to their penetration by roots. *Plant Soil* 9, 75-85. doi: 10.1007/BF01343483

Williams, M. A., Myrold, D. D., and Bottomley, P. J. (2006). Distribution and fate of 13C-labeled root and straw residues from ryegrass and crimson clover in soil under western Oregon field conditions. *Biol. Fertil. Soils* 42, 523-531. doi: 10.1007/s00374-005-0046-5

Xue, K., Wu, L., Deng, Y., He, Z., Nostrand, J.V., Robertson, G. P., et al. (2013). Functional gene differences in soil microbial communities from conventional, low-input, and organic farmlands. *Appl. Environ. Microbiol.* 79, 1284-1292. doi: 10.1128/AEM.03393-12

Young, I. M., Crawford, J. W., and Rappoldt, C. (2001). New methods and models for characterizing structural heterogeneity of soil. *Soil Tillage Res.* 61, 33-45. doi: 10.1016/S0167-1987(01)00188-X

Young, I. M. and Ritz, K. (2000). Tillage, habitat space and function of soil microbes. *Soil Till Res.* 53, 201-213. doi: 10.1016/S0167-1987(99)00106-3

Chapter 5: Conclusion

Improving soil carbon stocks is important to mitigating global climate change as well as increasing crop yields and improving sustainability in agriculture. However, the microscale dynamics of soil carbon preservation, the scale at which soil carbon preservation takes place, are poorly understood. This has resulted in general guidelines for the improvement of soil carbon that fail to perform as predicted in several cases. This study sought to elucidate some of these microscale mechanisms in relation to specific soil pore sizes and pore origins for a better understanding of microscale soil carbon dynamics.

Spatial variability of the soil matrix of conservation managements, specifically biologically based and early successional managements, was greater than in conventional tillage. It is believed this variability was the result of variability in soil carbon distributions within the matrix. Root pores were found to increase carbon concentrations for 123 μm, while non-root pores were found to decrease carbon concentrations for 30 μm. A mixture of root and non-root pores would result in areas of high and low carbon, possibly creating the variability in biologically based and early successional managements. Conventional management, which has less root pores, would be more uniform in soil carbon distributions, resulting in less spatial variability. Increasing the spatial variability of soil carbon would result in more diverse microenvironments, a potential driver of soil carbon dynamics.

Pores of 15-40 μm size were associated with increased amounts of carbon. The association found in this study was nearly identical to previously reported results, despite being from two different agricultural managements collected at different times of the year from two different fields. This indicates a universal mechanism for carbon preservation in these soils in

association with 15-40 μm pores, possibly through fungal activity, but further research would be necessary to confirm this.

Pores of 40-90 μm size were found to be places where carbon was easily gained, but also easily lost. Both natural abundance and enriched isotopes showed that new carbon was preferentially associated with pores of these sizes prior to incubation, but this association was lost during subsequent incubations. This is thought to be connected to root growth in these soils, as 40-90 μm pores would contain very fine plant roots.

The findings of this study improve the understanding of microscale carbon dynamics within soil. Increased amounts of root pores lead to higher spatial variability of soil carbon in soil aggregates due to a larger influence on the surrounding soil matrix. Soil carbon preservation is believed to occur through organo-mineral interactions in this matrix. Larger amounts of 15-40 μm pores were associated with soil carbon gains from a possibly universal mechanism, however, further research would be needed to determine the source of this mechanism. Higher amounts of 40-90 μm pores were associated with fast gains and losses in soil. This might be related to root growth dynamics, but further research is necessary to confirm this. These studies, when combined, show that pores behave similarly regardless of management, indicating that if a pore distribution is known, carbon dynamics may be predictable and may help bridge the gap between currently used aggregate distributions and a more pore centric approach; however, determining if pores behave the same in different soil types would be necessary. While this study improves knowledge of micro-scale carbon dynamics, further research is necessary for full comprehension.

APPENDIX

Table A.1: Slopes calculated by ANCOVA for the relationship between the amount of pores of the specified size and $\delta^{13}C$ of the soil. Slopes significant at $\alpha=0.05$ are denoted in bold.

Pore Size	Structure	Root	Pre	Post
4-15 μm	Intact	Root	**75.5084**	26.9310
	Intact	Control	8.9397	11.3010
	Destroyed	Root	16.7750	6.8059
	Destroyed	Control	7.6211	3.5835
15-40 μm	Intact	Root	**447.68**	231.00
	Intact	Control	-113.90	-80.5010
	Destroyed	Root	**312.14**	31.8726
	Destroyed	Control	131.04	22.7433
40-90 μm	Intact	Root	**1306.00**	-590.72
	Intact	Control	-330.48	-153.21
	Destroyed	Root	**1573.15**	-112.06
	Destroyed	Control	98.0046	79.6818
90+ μm	Intact	Root	**15853**	-5965.45
	Intact	Control	-1432.11	-192.13
	Destroyed	Root	2715.94	-3518.71
	Destroyed	Control	-737.93	2359.21